



UiT The Arctic University of Norway

Analysis of xyloglucan-modifying genes and enzymes at graft-junctions of tomato plants

Herman Lundblad

Faculty of Biosciences, Fishery and Economics, Department of Arctic and Marine Biology

Master thesis in Biology Bio-3950 May 2020

(This page is intentionally left blank)

**Analysis of xyloglucan-modifying genes and enzymes
at graft-junctions of tomato plants**

Herman Lundblad
May 2020

Supervisors
Prof. Kirsten Krause
Dr. Stian Olsen
University of Tromsø
Faculty of Biosciences, Fishery and Economics
Department of Arctic and Marine Biology

(This page is intentionally left blank)

Table of contents

Acknowledgements	v
Abbreviations	vi
Abstract	1
1 Introduction	4
1.1 Grafting.....	4
1.1.1 History of grafting	6
1.1.2 Importance of grafting.....	7
1.2 Cellular and molecular aspects of the graft interface	9
1.2.1 Formation of vascular connections in grafts	9
1.2.2 Signaling and graft crosstalk	10
1.2.3 Parasitic plants: Natural grafters	12
1.2.4 Cell wall and xyloglucan modifying enzymes	13
1.3 Hypothesis and aims	15
2 Methods.....	16
2.1 Plant material.....	16
2.2 Grafting.....	16
2.3 Xyloglucan endo-transglycosylation activity assay	17
2.3.1 Vibratome sectioning	17
2.3.2 Fluorescence labeling of XET activity.....	18
2.3.3 Microscopy.....	19
2.4 Gene expression analysis.....	19
2.4.1 Plant tissue harvesting.....	19
2.4.2 RNA extraction	20
2.4.3 DNase treatment.....	20
2.4.4 Gel electrophoresis.....	20
2.4.5 cDNA Synthesis	21
2.4.6 Primer Design.....	22

2.4.7	RT-qPCR.....	24
2.5	Data processing.....	25
2.6	Statistical analysis.....	26
3	Results.....	27
3.1	Grafting.....	27
3.2	Xyloglucan Endo-transglycosylase (XET) activity assay.....	31
3.3	Gene Expression.....	39
3.3.1	Sequence alignment.....	39
3.3.2	Profiling of <i>SIXTH1</i> , <i>SIXTH4</i> and <i>SIXTH12</i>	40
3.3.3	Cambium related gene expression (<i>WOX4</i>).....	43
4	Discussion.....	44
4.1	<i>S. pennellii</i> 's low graft success.....	44
4.2	Correlation between graft success and XET activity (or lack thereof).....	45
4.3	XET activity in grafts compared to <i>Cuscuta</i>	46
4.4	<i>SIXTH1</i> plays a minor role in grafting.....	47
4.5	The effect of the Scion.....	48
4.6	Increased gene expression in younger cells.....	49
4.7	XET activity in specific to the graft union.....	50
4.8	Relevance of cambium in grafts.....	51
4.9	Choice of methods.....	51
4.10	Conclusion.....	52
4.11	Outlook.....	52
5	References.....	53
Appendix	I
Grafting	I
Grafting clips	I
NanoDrop measurements	II

Primer melt data and standard curves from qPCR	VI
qPCR product amplification and melt data	VII
Gel electrophoresis	VIII
DNase treated RNA.....	VIII
PCR products.....	IX
Gene expression included Moneymaker Scion Stem.....	X
Supplemental XET activity images.....	X
ImageJ Fiji script.....	XI
RNA extraction protocol	XII

(This page is intentionally left blank)

Acknowledgements

I would like to thank my supervisors, Prof. Kirsten Krause and Dr. Stian Olsen for providing absolute fantastic guidance and patience. You have both helped me improve academically for the duration of this thesis by providing expert advices, and I am so very grateful for the help you have given me.

I would also like to thank the lab employees for always being helpful and bringing joy to the hallways and labs, and a special thanks to Anne Grethe for expert knowledge and assistance in anything microscopy related.

The great people in the parasitic plants research group do indeed deserve acknowledgement for their research enthusiasm which provided me with great inspiration throughout my own studies.

Thank you to my fellow master students for being the best lunch mates and making the study day more enjoyable. Lastly, I want to thank my family for always believing in me, and always being there for me no matter what.

Abbreviations

- μg – Microgram
- μl – Microliter
- μM – Micro molar
- μm – Micrometer
- ANOVA – Analysis of Variance
- cDNA – Complementary deoxyribonucleic acid
- Cos33 - *SIXTH1* co-suppression transgenic line of *Solanum lycopersicum* cv. MoneyMaker
- Cq – Cycle quantification
- DAG – Day(s) after grafting.
- DNA – deoxyribonucleic acid
- dNTP – Deoxynucleoside triphosphate
- DTT – Dithiothreitol
- EIF4a-2 – Eukaryotic initiation factor 4a-2
- GAPDH - Glyceraldehyde 3-phosphate dehydrogenase
- Kb – Kilo basepair
- M - Molar
- M82 – *Solanum lycopersicum* introgression line
- mM – milli molar
- MM – *Solanum lycopersicum* cv. MoneyMaker
- Na – Sodium
- NaCl – Sodium Chloride
- nm – Nanometer
- NO-RT – No reverse transcriptase
- Oex13 - *SIXTH1* over-expression transgenic line of *Solanum lycopersicum* cv. MoneyMaker
- Oligo(dT)₁₂₋₁₈ – Oligo deoxythymine
- PCR – Polymerase chain reaction.
- RNA – Ribonucleic acid
- RT-qPCR – Reverse transcription quantitative polymerase chain reaction.
- SuperScriptTM II RT – SuperScriptTM II Reverse transcriptase

- V – Volt
- XEH – Xyloglucan endo-hydrolase activity.
- XET – Xyloglucan endo-transglycosylase activity.
- XTH – Xyloglucan endo-transglycosylase/hydrolase
- XyGO-SR – Sulforhodamine labeled xyloglucan oligosaccharides

(This page is intentionally left blank)

Abstract

Grafting is a widely used technique for propagation of plants in both agriculture and horticulture worldwide and involves combining two or more plants into one chimeric plant, ultimately with a shared vascular system. Benefits of grafting such as pathogen resistance, increase in fruit yield and abiotic stress tolerance have long been known, but the biological mechanisms of how plants graft are still not fully understood. The process of graft development is interestingly similar to that of the host infection process of parasitic plants. This knowledge has contributed to viewing the parasitic plants as a blueprint for optimal graft development, as the parasites can bypass a taxonomic barrier that seem to exist for conventional grafting. Previous research has revealed interesting knowledge on the involvement of xyloglucan endo-transglycosylase/hydrolase (XTH) enzymes, a group of enzymes involved in loosening and tightening the plant cell wall through the modification of xyloglucan. Specifically, the gene *Cr-XTH-1* in *Cuscuta reflexa* has been revealed to play a role in the infection process.

The aim of this thesis was to investigate similarities between the graft formation in tomato plants and the infection of *Cuscuta* with respect to xyloglucan-associated activities. Graft success rates between the tomato lines *Solanum lycopersicum* cv. Moneymaker and M82, *Solanum pennellii* and two transgenic lines were assessed. The importance of a specific *XTH* gene in grafting was investigated using the two transgenic tomato lines, one over-expressing *SIXTH1*, the other suppressing *SIXTH1* expression. Xyloglucan endo-transglycosylation activity (XET) was assessed using an *in vivo* activity assay on sectioned graft sites. The gene *SIXTH1* was chosen along with its close homolog, *SIXTH4*, and a tomato *XTH* similar to *Cr-XTH-1*: *SIXTH12*, to investigate the gene expression of specific *XTHs* at the graft sites using RT-qPCR. The gene expression revealed no clear pattern between the three *XTHs* in relation to grafting. XET activity was observed to be graft specific based on this study design, with little difference between the genotypes. Several genotypes of tomato all showed XET activity at, or in cells with close proximity to the graft union, indicating that *XTHs* are involved in the grafting process. The findings of this thesis are proposed to be used as preliminary data and encourage further investigation of the effect of *XTHs* and XET activity at the graft interface.

Keywords: Grafting, XTH, XET, tomato, *Cuscuta*

(This page is intentionally left blank)

1 Introduction

1.1 Grafting

Grafting is the procedure when one plant is attached to another in such a way that the two plants grow together and share their vascular tissue. This can be done in several ways, and the number of grafting methods are plenty. A few ways of grafting are illustrated in Figure 1, and as shown, the shoot (termed scion) can be attached to a root system (termed rootstock or stock) of another plant (A, C, D and E), or the stems can be attached together (B). This unlocks a myriad of ways to combine plants for several different purposes, some of which will be explained later on.

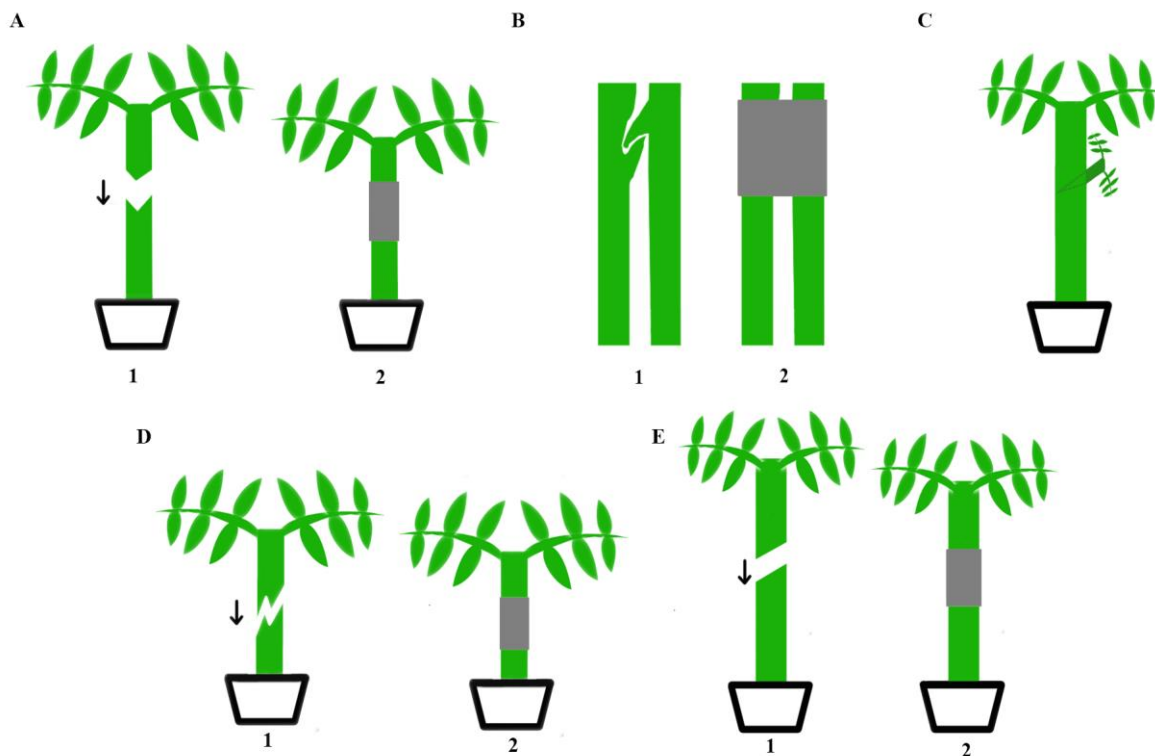


Figure 1 Illustration of five different grafting techniques. A) Cleft graft, also called wedge graft. B) Tongue graft. C) Hole insertion graft, D) Whip-and-tongue graft, and E) Splice graft, also called tube graft. The gray square in A, B, D and E two represents a way of attaching the scion to the stock, for example with a clip or thread.

What is common for all these methods of grafting are the alignment of the vascular cambium, to ensure possible xylem (transport of water) and phloem (transport of photosynthates) connections. The tissue needs to be mechanically kept together for optimal graft success (Pina and Errea, 2005; Crang, Lyons-Sobaski and Wise p.500, 2018), a process usually done by applying grafting tape, or a clip at, or around the graft site (represented in Figure 1 as gray squares on the plants). High levels of humidity would also be an advantage due to the scion having no vascular connections to the soil for water until some days after the grafting

procedure (Melnik, 2017). Some grafters apply wax to their grafts to reduce water loss in the plant, while others simply bag their plants.

Vascular re-connection is crucial for long-term graft survival, as the scion usually has no direct root connections at the point of grafting, and therefore no water uptake via roots. Although vascular continuity is crucial, it has been shown to occur also in unsuccessful grafts (Moore, 1984a), and was therefore shown to not necessarily be an indication of a successful graft. Both herbaceous and woody plants can graft, either by human input or naturally, but one seeming trend is that monocotyledons cannot graft (in most cases). Poor alignment of the disorganized vascular bundles in monocotyledons (monocots) (see Figure 2A) is likely a reason why this group of plants are in most cases unable to graft. The regenerative ability of the vascular cambium (see Figure 2B) is one important factor for vascular attachment in grafts, and in monocot, the vascular cambium is not present, or have poor regenerative ability, resulting in even unsuccessful autografts (Turnbull, 2010). The monocotyledons have, as illustrated in Figure 2A, scattered vascular bundles, and the possible alignment of these during a graft would in most cases be up to chance. Additionally, the vascular veins from leaves in monocots are arranged in parallel, in contrast to the branched veins of eudicots. These parallel veins meet up at internodes in the stem. Eudicotyledonous (eudicots) plants, on the other hand, have the vascular bundles arranged in a circular pattern (Figure 2B), making alignment of vascular tissue, and the active growth zone in the vascular bundles (the cambium), possible. It has been reported that monocots can only be grafted at the internodes, and only internode grafts resulted in successful grafts, although with very low success rate of 3% (Melnik and Meyerowitz, 2015).

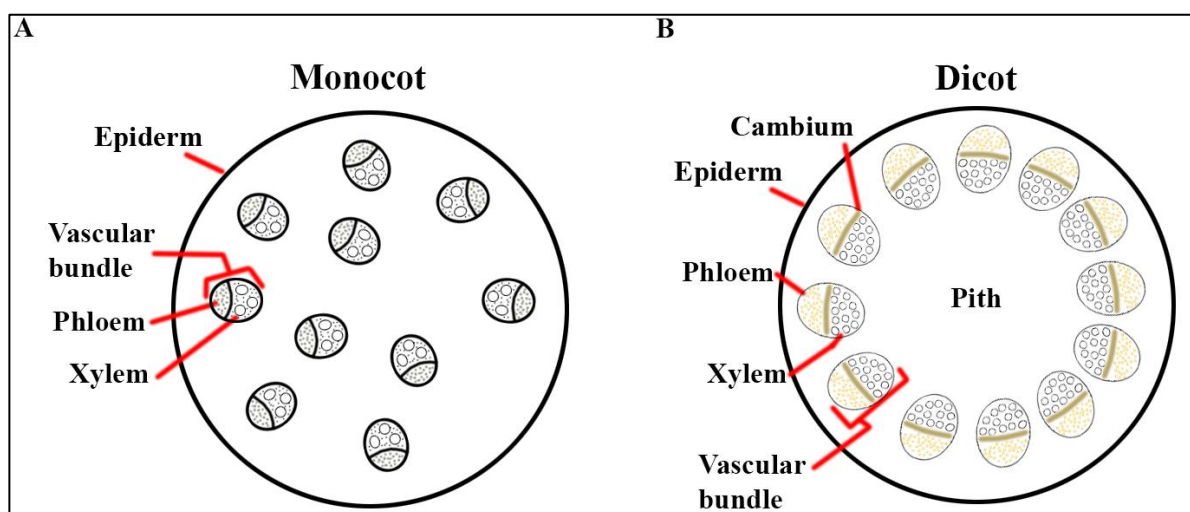


Figure 2 Simplified illustration of monocot and eudicot stem anatomy. The vascular bundles of monocots have no specific arrangement, while the eudicots have. Important cell structures have been labeled in the illustration.

The biggest problem with grafting is the compatibility and success of the grafted plants. It has been proven that closely related species have a higher graft success than more distant relatives. Intraspecific (within the same species) grafts, like autografts (the same individual) will most often form compatible grafts, homografts (same species, different individual) as well. Interspecific (between species) heterografts (graft of two different species) are more limited. Intrafamilial (within family) grafts may succeed, while interfamilial (between families) grafts rarely succeed (Mudge *et al.*, 2009). The plant family *Solanaceae* (order *Solanales*) proves to be an exception from the taxonomic affinity, due to the fact that several different species within family are able to form successful grafts with other species not necessarily in the same genus, for example the genus *Solanum* and genus *Nicotiana* (Turnbull, 2010). A great example of an intrafamilial graft would be the TomTato[®] (from Thompson & Morgan), a potato (*Solanum tuberosum*) - tomato (*Solanum lycopersicum*) chimera. This results in a plant that can produce potatoes as well as tomatoes, while taking up less physical space.

1.1.1 History of grafting

The origin of grafting is not precisely known, but texts and literature throughout the history have either directly described the process of grafting, or indirectly described a process like grafting dating several hundreds if not thousands of years back (Juniper and Mabblerley, 2006; Mudge *et al.*, 2009). Throughout the history of humans, plants have been used as food as well as ornamental objects. The Persian kingdom was famous for their gardens and skilled gardeners, who likely knew about the benefits of grafting, most likely by observing the effects in natural grafts (Juniper and Mabblerley, 2006). Grape grafting is referenced in the religious texts of the Hebrew and Christian Bible (Hartmann *et al.* 1997, as cited in Lee and Oda, 2003; Mudge *et al.*, 2009), and the Greeks and Romans likely grafted trees in their orchards (Juniper and Mabblerley, 2006), both of which is a common practice today. In the late nineteenth century, the wine industry of Europe was devastated by the insect *Phylloxera vastatrix*, which originated from America. This incident was named the Great French Wine Blight, due to most wine production being located in France. The solution to this was to graft the European wine cultivars shoots system onto *Phylloxera* resistant American root system (Gale, 2011). This resulted in most wine grapes today being grafted plants.

In the twentieth century, grafting of vegetables came into focus. By the end of the century, a majority of greenhouse vegetables in Japan and Korea were grafted plants (Lee and Oda, 2003). Data from the first decade of the 2000's show that several other regions and nations also have a significant amount of grafted vegetables (Lee *et al.*, 2010). With modern times comes modern technology, and scientists have started tinkering with automatic grafting by the means of machines, which certainly have the potential to enhance the grafting industry. Grafting machines have been developed with a success rate as high as 95% for vegetables (Chen, Chiu and Chang, 2010). Although human input is necessary for these machines (i.e. plantlets, graft clips etc.) these machines are of great use for mass production of grafts, with rates of several hundreds of grafts an hour. This advance in grafting technology makes grafting a viable method of improving agri- and horticulture.

1.1.2 Importance of grafting

1.1.2.1 Resistance to soilborne pathogens

More and more effort is dedicated towards understanding the biology of grafting. Although much is still unknown about the mechanisms, there are documented effects of grafting (Lee, 1994). Soilborne pathogens, like the one that caused the Great French Wine Blight (the insect *P. vestatrix*) are one of the more common problems for agriculture today. The mechanism of *Phylloxera* resistance is thought to be morphological alterations in the roots, being toxic to the insect, or being unattractive for the initial feeding by the insect (Granett *et al.*, 2001). Pest resistant rootstocks are therefore of great use in agriculture and horticulture to overcome the threat exerted by these pathogens. They can replace chemical fumigation of the soil (a former common practice to prevent pests from feasting on the roots of plants, that was restricted due to environmental policies around the globe). Schneider *et al.* (1995) found that a certain cultivar of roses served as a resistant rootstock to nematodes, a common problem in horticulture, which helped against the nematode problem without affecting the quality of the rose flowers. Suchoff, Louws and Gunter (2019) showed that grafting tomato onto three different rootstocks, all provided resistance to bacterial wilt caused by *Ralstonia solanacearum*, serving as a good option for farmers with infected fields.

1.1.2.2 Abiotic stress tolerance

In addition to biotic factors, abiotic factors influence growth of plants. It has been estimated that close to 10% of all land-surface has salt affected soils (Pessarkli and Szabolcs, 1999; Munns, 2005), although much is natural, there is an increase in salinity especially in irrigated

land which stands for one third of the global food production (Munns, 2005). Salt challenges the plant on two fronts: the osmotic, and ionic (Rivero, Ruiz and Romero, 2003; Munns, 2005). High concentrations of salt in the soil often lead to lowered water potential in the soil, ultimately resulting in water stress in the plant (Rivero, Ruiz and Romero, 2003). This acts as the osmotic component. The other component is the ionic, which is the internal ion concentration in the plant cells which reaches toxic levels. Such ions can be Na^+ and Cl^- , which will accumulate in the vacuoles of the cells, or if the vacuole has reached its capacity, in the cytosol. This can ultimately lead to inhibited growth, for example due to the plant using extra resources on channeling the toxic amount of ions into different pathways to reduce the concentration of ions to a non-toxic concentration (Rivero, Ruiz and Romero, 2003).

In agriculture one solution to this can be grafting productive scions on salt resistant rootstocks. Martinez-Rodriguez *et al.*, (2008) observed that one cultivar of tomato (Radja) reduced transport of saline ions to the shoot, when acting as a rootstock. In an earlier study Estañ *et al* (2005) found the same effect of the Radja cultivar, while another cultivar (Pera) adjusted the uptake of saline ions depending on the soil-salt concentration. For both studies, the trait of salt excluder and includer was of interest to enhance the plant system to resist saline conditions. Grafting plants with these traits is of great agronomical benefit based on the concentrations of salt at the given location and being able to graft a productive scion to a rootstock with the suiting trait for saline soil would enhance the food production where saline soil is a problem.

1.1.2.3 Crop yield

Enhancing the uptake of nutrients is an important goal of agrobiotechnology in the quest to increase the yield of food crops. Grafting a scion onto an already well established and vigorous rootstock was shown to improve the fruit yield in watermelons (Lee, 1994), although it can be argued that increase in fruit yield is a combined result from various stress tolerances, and not just the scion itself being productive (Ruiz *et al.*, 1997). Pear and apple scions are commonly grafted onto already established rootstocks to boost the scion production. Having an already established root system reduces growth time of the shoot, which has a big impact on slow growing trees like fruit trees. Although some cultivars cannot be grafted onto each other, grafting a third plant in between sometimes solves this. The process is called double-working (Mudge *et al.*, 2009) and involves grafting a compatible interstock in between the rootstock and scion (illustrated in Figure 3). The interstock, of course, is compatible with both

scion and stock. Some pear cultivars are often grafted onto a quince rootstock to induce dwarfing of the plant. Dwarfing is a wanted trait for area efficiency of planting the trees, and a common grafting trait for fruit trees. In one case, however, it was shown that quince produces a secondary metabolite, which in the pear scion can be converted into cyanide (Gur et al 1968 as cited by Moore, 1986). This resulted in the death of the scion, and an incompatibility of the graft. Interestingly enough, one pear cultivar was compatible to both the scion and stock and served as an interstock that did not produce harmful secondary metabolites, nor converted the secondary metabolite of the quince to cyanide. The final result of this double-working was a successful graft of three plants, and a dwarfing effect on the wanted pear scion. (Musacchi et al 2002 as cited by Francescatto *et al.*, 2010)

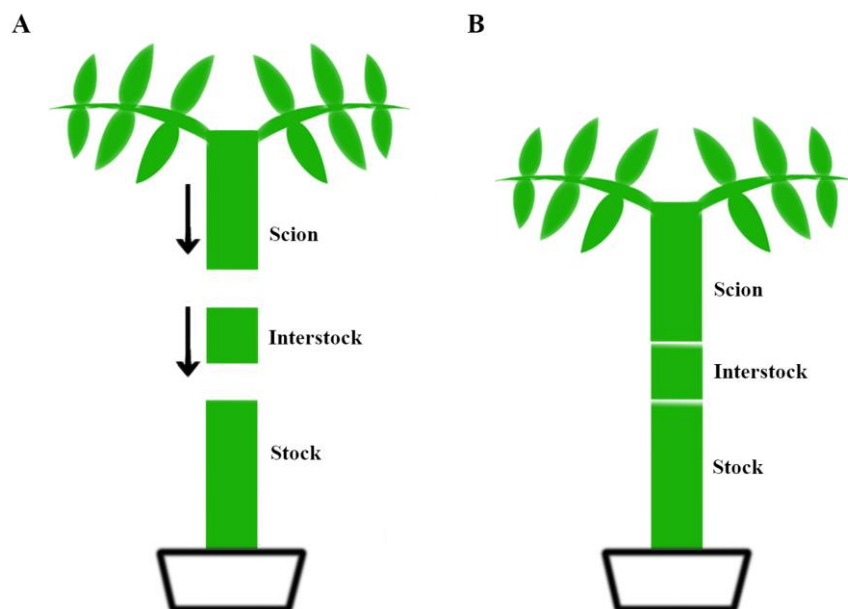


Figure 3 Simplified illustration of double-working (interstock grafting). The interstock is a third plant put in between the scion and stock. This is then tightly kept together like any other graft, and a chimeric plant with a continuous vascular system are ultimately the result. Interstock grafts can be homografts or heterografts.

1.2 Cellular and molecular aspects of the graft interface

1.2.1 Formation of vascular connections in grafts

As mentioned, it is the ability to form vascular connections between the scion and the stock that makes a graft survive in the long run, however scion survival has been shown for longer periods of time without xylem and / or phloem connections in woody species (Asante and Barnett, 1997). On the other hand, it has also been shown that woody species can grow for years after grafting, then die off due to graft incompatibility, which is an indication that also incompatible grafts can have vascular connections (Mosse, 1962; Hartmann et al., 1997 as cited by Pina and Errea, 2005). Although the mechanisms of how these connections occur are

still not fully understood, great progress has been made in recent years. Shortly after grafting, a necrotic layer forms from the cut of tissue in the scion and stock, and pectins are secreted at the graft union (Nanda and Melnyk, 2018). Cell differentiation starts in the vascular bundles, as well as the endodermis and cortex (Melnyk, 2017). After some days when the cambial regions of both parts (the stock and scion) are in close proximity of each other, parenchymatous cells proliferate, and a callus (undifferentiated cells) bridge creates cellular contact between the two parts, which enables transport of water and nutrients without any continuous vascular system (Pina, Errea and Martens, 2012), through the apoplast and likely also through the symplast *via* plasmodesmata. The necrotic layer starts to fragment and disappears (Melnyk, 2017). The space between both scion and stock fills up with callus, and from the callus, new cambial cells differentiate, creating a cambial connection between the scion and stock. From here (a week or more after grafting) new vascular tissue differentiates, of which phloem tissue has been shown to differentiate before xylem tissue (Melnyk *et al.*, 2015).

1.2.2 Signaling and graft crosstalk

The cellular connection between the stock and scion enables transport of molecules from shoot to root and vice versa. Phytohormones have lately been shown to play an important role in vascular regeneration, with emphasis on the graft union. In *Arabidopsis* grafts, the auxin related genes aberrant lateral root formation (*ALF4*) and auxin-resistant 1 (*AXRI*) have been shown to be necessary in the stock for phloem reconnection in the graft (Melnyk *et al.*, 2015). Further, two auxin inducible xyloglucan endo-transglycosylases/hydrolases (*XTHs*) (*XTH19* and *XTH20*) genes have been shown to be regulated by the transcription factor ANAC071 in *Arabidopsis* (Pitaksaringkarn *et al.*, 2014). A transcriptomic analysis in *Arabidopsis* grafts showed that *WOX4* and *PXY* (both related to cambium) were induced by grafting (Melnyk *et al.*, 2018).

The phytohormone brassinosteroid (BR) is known to promote xylem formation, although little graft specific knowledge is available for this phytohormone, experiments in BR transport have shown that BR mutants can graft successfully, and the phytohormone might therefore not be important for grafting, which also seems to be the case based on current knowledge for ethylene, jasmonic acid, strigalactones, and cytokinins, as nicely reviewed by Nanda and Melnyk, (2018)

Phytohormones mostly travel in the apoplast and need active transporters to travel across the plasma membrane, with a few exceptions like the volatile phytohormone ethylene, ABA, and auxin which have been shown to diffuse across the plasma membrane (Park *et al.*, 2017). In grafts, it has been proposed that cell-cell connection *via* plasmodesma can enable a cell recognition mechanism (Jeffree and Yeoman, 1983), which could be a determining factor for graft compatibility. The thought that cells communicate and recognize each other is indeed interesting, but the specific molecular mechanism behind this potential communication is yet unknown.

The formation of plasmodesma in the graft site gives rise to symplastic transport and is thought to be happening in the callus bridge. These plasmodesmata connections are proposed to arise *de novo*, indicating that these are secondary plasmodesmata that makes channels through already established cell walls (Kollmann and Glockmann, 1985).

In contrast to primary plasmodesma, that are made by endoplasmic reticulum (ER) entrapments in the middle lamella during cell division, secondary plasmodesmata seem to be a coordinated invagination of cell walls, which results in ER bridging the cytoplasm of both cells. Researchers have observed that this formation of secondary plasmodesmata formation seems to be special for the graft union, as mechanistic pressure did not seem to initiate formation of secondary plasmodesmata (Kollmann and Glockmann, 1991). The mechanism known so far for the creation of secondary plasmodesmata seem to be that the cell walls of both cells are thinned, and an invagination meets up at the middle, forming passages between cells cytoplasm (plasmodesmata) (Kollmann and Glockmann, 1991; Pina, Errea and Martens, 2012)

When it comes to graft compatibility, a growing collection of evidence is supporting the hypothesis that the amount of plasmodesmata connections at the graft union is a key factor for determining graft compatibility - incompatibility (Pina, Errea and Martens, 2012). Pina *et al* (2012) observed in their experiments that incompatible graft unions accumulated phenolic compounds, while finding the same trend, Zarrouk *et al.*, (2010) also observed higher levels of peroxidases in incompatible graft pairs, which earlier was proposed by Gulen *et al.*, (2002). This has been one proposed mechanism of graft incompatibility, yet the mechanism for this process is still a mystery.

1.2.3 Parasitic plants: Natural grafters

An example of organisms that have mastered the form of cellular connections are parasitic plants. These plants live on other plants by connecting to their hosts tissue with a specialized organ called “haustorium” (see Figure 4), and some species have adapted their lifestyle to be fully dependent on parasitism (holoparasites), while others may survive without a host, and produce energy *via* photosynthesis (hemiparasites). The process of infection for the parasite have similarities to that of conventional grafting. With the genus *Cuscuta* as an example, there is an initial adherence stage, where pectins, among other molecules, are secreted, as with grafts (see Formation of vascular connections in grafts). After adherence, there is another stage where the haustorium penetrates into the host, and searching hyphae seek out xylem and phloem and a connection through secondary plasmodesmata is established between the host and parasite (Albert *et al.*, 2008). This process is similar to the bridging process that occurs in the graft union between stock and scion (as described in subsection 1.2.1 Formation of vascular connections in grafts, and 1.2.2 Signaling and graft crosstalk) and the parasite actually ends up developing a vascular bridge, connecting both plants vascular tissue.

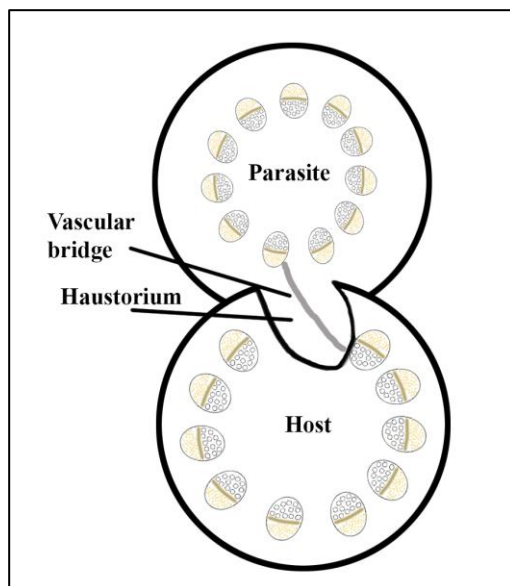


Figure 4 Simplified illustration of the parasite-host interface, visualizing the infection organ of the parasite termed the haustorium, and a vascular bridge forming between the two plants.

In essence, this lifestyle can be seen as natural grafting. What is even more interesting is that most parasitic plants infect inter-familial hosts, in contrast to conventional grafting and the taxonomic barrier that seems to restrict compatible grafts across families (see section 1.1 Grafting). Many parasitic plants are only able to establish xylem connections, but there are examples of parasitic plants that also establish phloem connections. One example is the widely spread genus *Cuscuta* that encompasses about 200 species of exclusively shoot-parasitizing plants (Heide-Jørgensen, 2008).

In addition, few parasitic plants parasitize on monocot shoots, which is yet another similarity to conventional grafting.

In this regard, parasitic plants are expert grafters that have solved the main issue of a taxonomic barrier in conventional grafting, which makes parasitic plants an interesting system to study for increased knowledge in grafting. As pointed out by Melnyk (2016) the

haustorium/host interface can be regarded as a natural blueprint for the optimal graft union. Therefore, their strategy of infection and the hosts responses (or the lack thereof) have been in focus the recent years, and researchers have found that XTHs seem to play an important role in the establishment of the parasite-host interface (Olsen *et al.*, 2016; Olsen, 2017). In fact, *Cuscuta reflexa* *Cr-XTH1* and *Cr-XTH2* was found to be upregulated on the onset of haustoriogenesis (Olsen *et al.*, 2016). Since this corroborates the reports on the induction of *XTH* genes at the graft interface, these enzymes and their target, the plant cell wall, shall be illuminated in the next chapter.

1.2.4 Cell wall and xyloglucan modifying enzymes

The cell walls of plants are responsible for the structural integrity of the plants. The primary cell wall itself is a complex matrix of the polysaccharides cellulose, hemicellulose and pectin (Cosgrove, 2005). Cellulose acts as the main backbone of the cell wall, forming microfibrils (with impressive tensile strength of ~100 Giga pascal) which have been an inspiration for nanomaterials with extraordinary strength used in modern engineering (Höfte and Voxeur, 2017). Pectins are involved in the middle lamella, which acts as a glue between adjacent cell walls in an organism, that tightly keeps plant cells together (Cosgrove, 2005). The hemicelluloses (xyloglucans, xylans and mannans), together with pectins (homogalacturonan and rhamnogalacturonan I & II), interact in between the cellulose microfibrils, and act as cross-linkers, as well as separators of the cellulose microfibrils (Höfte and Voxeur, 2017) as illustrated in Figure 5.

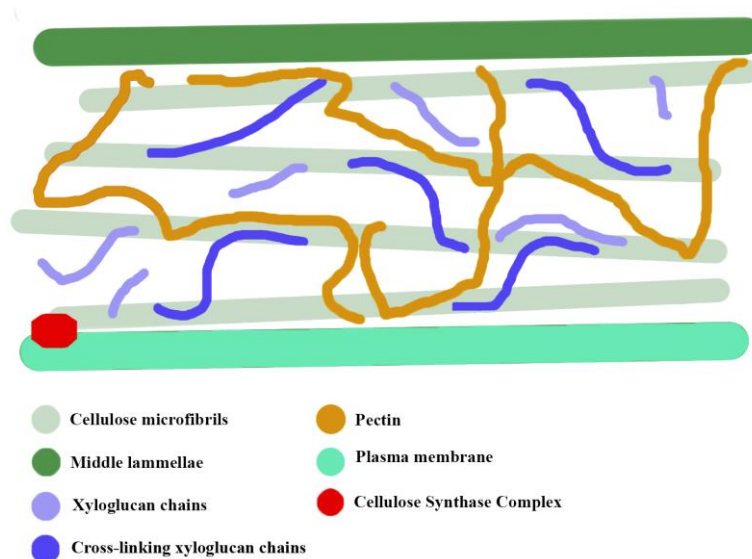


Figure 5 Simplified illustration of the composition of the primary cell wall in plants (eudicot). The hemicelluloses are represented by xyloglucan, as this is the most abundant hemicellulose in eudicots. The illustration is simplified, and structural proteins are not represented.

Structural proteins are also involved in the plant cell wall, but with a minor role (Höfte and Voxeur, 2017). Among the hemicelluloses, xyloglucans play an important role as a tension-bearing structure (Catala *et al.*, 2001), and is the most abundant hemicellulose in eudicotyledonous plants (Pauly *et al.*, 1999; Scheller and Ulvskov, 2010). Xyloglucans (together with pectins (Höfte and Voxeur, 2017)) have the ability to engage in hydrogen bonds with cellulose microfibrils and cross-link them (see dark blue lines in Figure 5), while the enzymatic cleavage of the xyloglucans results in cell wall loosening (Fry *et al.*, 1992).

Evidence has been presented that xyloglucans can be cut and pasted onto other xyloglucan molecules through the xyloglucan endo-transglycosylation activity (XET) of XTHs (Fry *et al.*, 1992). This reaction can be described as follows: XTH cuts the xyloglucan chain, and the cut chain is covalently bonded with XTH. The XTH-xyloglucan complex is broken up, and the xyloglucan chain binds with the acceptor which is the nonreducing end of another xyloglucan chain (Eklöf and Brumer, 2010) (see Figure 6 for illustration). XET activity seems to be the most common enzymatic process for XTHs, although some XTHs have been shown to use water as an acceptor and thereby catalyze hydrolysis, a process that has been dubbed xyloglucan endo-hydrolysis (XEH) (Rose *et al.*, 2002) (Figure 6).

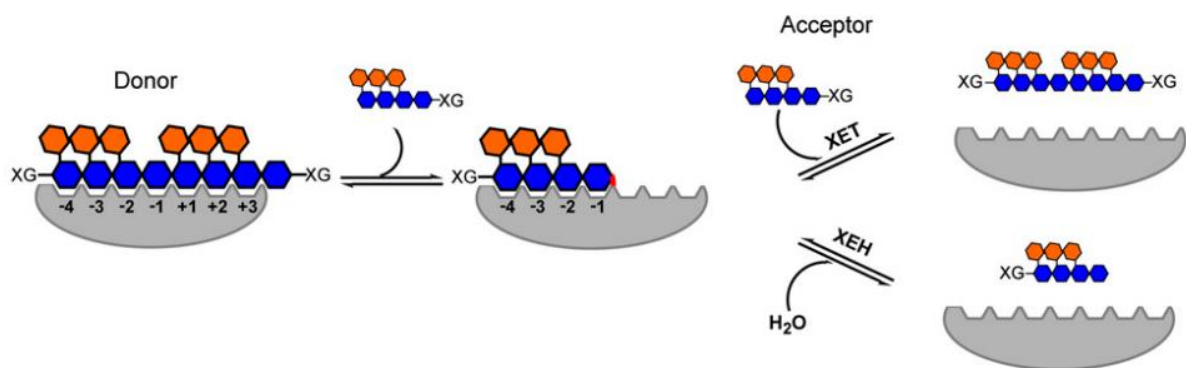


Figure 6 Illustration of XET and XEH activity of XTHs. Grey figure is the enzyme. Blue and orange is the xyloglucan chain and donor substrate. XET acceptor is another xyloglucan chain, while XEH acceptor is water. Reference: Figure 3 in Eklöf and Brumer, (2010).

1.3 Hypothesis and aims

Little previous research has been done on the involvement of xyloglucan endotransglucosylase/hydrolase activity in grafting. Given that XTHs play a role at the parasite-host interface, and that the parasite-host interface shares several similarities with conventional grafting, it is possible that XTHs also serve a function at the graft union. The tomato plant serves as a popular grafted plant in horticulture, and in addition, the tomato is a well-studied host for parasitism, and the interface between tomato and the parasite *Cuscuta*, and the involvement of XTHs has previously been investigated (Krause *et al.*, 2018) as well as in other eudicots (Olsen *et al.*, 2016; Olsen, Popper and Krause, 2016; Olsen, 2017; Olsen and Krause, 2017).

This current knowledge, and the lack of knowledge about XTH in relation to grafting provides the foundation of the hypothesis for this thesis:

“Since XTHs have proven to be an important factor in parasite-host interface, and this interface being similar to the formation of the graft union, it is hypothesized that there is a similar role of XTHs in conventional grafts in tomato”

The aims of this thesis is therefore to investigate three tomato XTHs, *SIXTH1*, *SIXTH4*, and *SIXTH12* with respect to their gene expression, their effect of grafting success and their *in situ* activity in graft junctions. This will be achieved by, utilizing two transgenic tomato lines, one over- expressing *SIXTH1*, the other suppressing *SIXTH1*, which will help shed light on the role of *SIXTH1* in the conventional graft. With the *Cuscuta* resistant tomato introgression line M82 the potential link between grafting and *Cuscuta* will be investigated with graft success, whereas the same accounts for the *Cuscuta* receptive wild tomato *Solanum pennellii*. To further investigate the XET activity at the graft sites the *in vivo* enzyme activity assay described by Vissenberg *et al.* (2000) will serve as an interesting technique resulting in fluorescence images that visualize the co-localizing of XET activity and the endogenous donor substrate in the plant cell wall. Finally, expression analysis will be done using reverse transcriptase polymerase chain reaction (RT-qPCR) in comparison to reference genes.

2 Methods

2.1 Plant material

Plant material was sown and grown in the greenhouse at the Phytotron of the University of Tromsø, Norway (N7732152.56 E651887.25) under 24h light conditions ($150\text{-}250\ \mu\text{mol}\cdot\text{m}^{-2}\cdot\text{s}^{-1}$), and $18\text{-}24^{\circ}\text{C}$. Several different lines of tomato were used in this thesis: The cultivated *S. lycopersicum* cv. Moneymaker (MM) (obtained from local plant store), the *S. lycopersicum* introgression line M82, and the uncultivated wild tomato (*Solanum pennellii*) (Both obtained from the Tomato Genetic Resource Center (TGRC) (<https://tgrc.ucdavis.edu>). In addition, two transgenic lines, one overexpressing (named Oex13) and one co-suppressing (named Cos33)



Figure 7 sowing tray covered with a thin layer of vermiculite. Metal rods provide structural support when the tray is covered with plastic.

the *XTH* gene *SIXTH1* (Miedes *et al.*, 2011), (which were both donated kindly as a gift by Prof. Ester Pérez Lorences, University of Valencia), with *Solanum lycopersicum* cv. MM as the background was investigated. All lines of tomato were sown in 50:50 peat:perlite soil. The soil was covered with a thin layer vermiculite (Figure 7). *S. pennellii* was sown

one week earlier than *S. lycopersicum* to compensate for slower growth. Sowing trays were then wrapped in transparent plastic supported by metal rods to create a moisture chamber. The plastic was removed when the seeds had germinated, and seedlings were repotted to 10 cm pots after 2-3 weeks based on plant size and growth. After 4 weeks the plants were of appropriate size for grafting, with 2-3 true leaves and a stem diameter of approximately 6 mm.

2.2 Grafting

Grafting was performed by hand using a scalpel rinsed in 70% ethanol to cut the plant material. Plants were cut as cleft grafts (Figure 1A) and cutting occurred either close to the cotyledons, or in the hypocotyl region as specified where relevant in the Results chapter. The scalpel blade was changed frequently to ensure a sharp edge for all cuts. It was rinsed in ethanol between each plant and dried with a paper towel. After the plants were cut, the scions were transferred reciprocally to the stock, and the two parts were held together with a plastic clip (unknown provider, clips from old stock at the greenhouse). A total of two different plastic clips were used throughout the grafting processes, where one was discontinued early on (termed clip 1 in the appendix) due to small size and improper physical support of the

grafted plant (See Figure 28 and Figure 29 in the appendix p. I for details). The preferred clip had a height of approximately 1.3 cm, where the discontinued clip had a height of approximately 1.1 cm. The preferred clip also had a stronger grip than the discontinued clip and a curvature of the clip surface that neatly fitted around the stems of the plants (with a stem diameter of approximately 6 mm) to improve support.



A wooden stick was placed close to the grafts to give structural support. The grafted plants were then moved to transparent plastic bags, sprayed with water, and sealed by pulling the bag up and twisting the end, sealing it with a plastic clip. Metal bows and/or wooden sticks were used to make sure the plastic bags did not collapse on the plants as shown in Figure 8.

All the bagged grafts were incubated in a growth chamber at 18°C in 24h darkness for three days, then moved to 24h light ($150\text{-}250\ \mu\text{mol}\cdot\text{m}^{-2}\cdot\text{s}^{-1}$) at the same temperature. Grafts were checked to make sure the bags kept a high relative humidity. If there were signs that the bags had lost humidity relative to the starting humidity, the bags were opened and water was sprayed into the bags, then they were resealed. After three to five days, small holes were cut in the plastic to start acclimatization of the

Figure 8 Photograph of an example for a bagged graft directly after finished grafting

grafts. Three to four days after this, the bags were fully opened and kept opened, and one to three days later the bags were completely removed. Two to three weeks after grafting the plants were analyzed (see Methods chapters 3. Xyloglucan endo-transglycosylation activity assay and 4. Gene expression analysis).

2.3 Xyloglucan endo-transglycosylation activity assay

2.3.1 Vibratome sectioning

Sections used for the enzyme activity assay were cut with the Leica Vibratome VT1000E (Leica Biosystems). A series of test cuts were done to find the thickness yielding the most intact sections. The vibratome uses a vibrating blade to cut the samples, which often torn the fragile graft sites apart. Sections were cut at 100 μm thickness, with vibratome frequency settings at 2-3. The blade used to cut was exchanged whenever it seemed dull to prevent

damaging the samples. Cross-sections were cut using a standard mount supplied with the vibratome. The plant tissue samples were cut to an approximate length of 2 cm. Samples for cross-sections were mounted vertically, and graft sites were extracted so that the graft site was the top part of the sample and rootstock the bottom of the same sample to ensure a stable mounting of the sample (Figure 9A).

Longitudinal samples were mounted in a modified mount. The modifications included adding potato segments as holdfasts between the plastic mount and the plant sample. Staples were pressed through the potato segments so that small tips went through the potato and into the plant sample (Figure 9B). Due to the samples being mounted horizontally on the mount, the staples were necessary to secure the sample and prevent it from slipping out. The sample was placed so that no tissue needed for analysis was destroyed by the staples. To further fix the sample to the mount, a rubber band was tied around the mount and the sample-staple-potato segment. A series of photographs of the customized mounting solutions are shown in Figure 9 below.

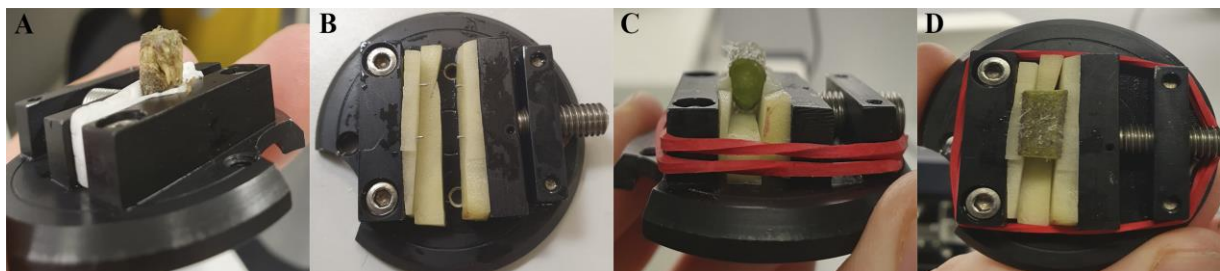


Figure 9 Pictures of the vibratome mounting for cross-sections (A) and longitudinal sections (B-D). (A) Small pieces of Styrofoam were used to add structural integrity to the samples for cross-sectioning. The Styrofoam also prevented the sample from being mechanically crushed by the metal mount. (B) The metal mount with potato slices used for longitudinal sectioning. The staple tips are visible in the middle area of the mount, coming out of the potato segments. (C and D) The longitudinal mounting system with a sample mounted. The potato segments are as shown in B. The staple tips are locking the plant sample in place, and the rubber band is locking the potato segments in place.

2.3.2 Fluorescence labeling of XET activity

To investigate the role of XTHs in the graft interface, an XET activity assay described by Vissenberg *et al.* (2000) was done. The vibratome sections, both cross-sections and longitudinal sections, were incubated in a solution of sulforhodamine labeled xyloglucan oligosaccharides (XyGO-SRs) (kindly provided by Dr. Stian Olsen, UiT, Norway) and a Na-acetate - NaCl buffer (50mM Na-acetate pH5.5, 300mM NaCl) for 1 hour in darkness (as described by Olsen and Krause, (2017)), covered with aluminum foil and placed in a cabinet. Control samples were incubated in the buffer only, also in darkness. After the incubation, the samples were washed in a 15:1:4 ethanol:formic acid:water solution for 10 minutes followed

by overnight washing in 5% formic acid. Samples were kept in darkness whenever they were not analyzed further by microscopy.

2.3.3 Microscopy

Microscopy was done using the SteREO Lumar V12 stereomicroscope (Carl Zeiss) The fluorescence from the XyGO-SRs were detectable using the CY3 filter (Carl Zeiss Filter cube 43, wide band pass filter, Excitation spectrum: 545 +/- 25 nm, Beam splitter: 570 nm, Emission spectrum: 605 +/- 70 nm), visualizing the fluorescence as red - orange. Samples were suspended in a water droplet on a microscope slide. Where the plant material was not too thick, a microscope cover slide was used. Pictures of the samples were taken using the SteREO Lumar V12 integrated AxioCam MRc5 camera. Same digital settings were used for all fluorescence images (saved presets).

2.4 Gene expression analysis

2.4.1 Plant tissue harvesting

Sample harvesting for RNA extraction was done from one biological replicate of all the graft combination, plus an un-grafted plant of each Cos33 and Oex13. At this time the grafts were 29 days old. The tissue samples collected were approximately 0.5 – 1 cm in size. The samples were cut into small pieces with a 70% ethanol-sterilized scalpel blade. Figure 10 illustrates where on each plant the tissue was collected, with upper stem, lower stem, graft site and leaf being the different tissues collected. The cut samples were transferred to a 2 ml Eppendorf safe-lock tube and shock frozen in liquid nitrogen. Between each sample from the same plant the scalpel blade was cleaned with paper towel and 70% ethanol, and between each plant the

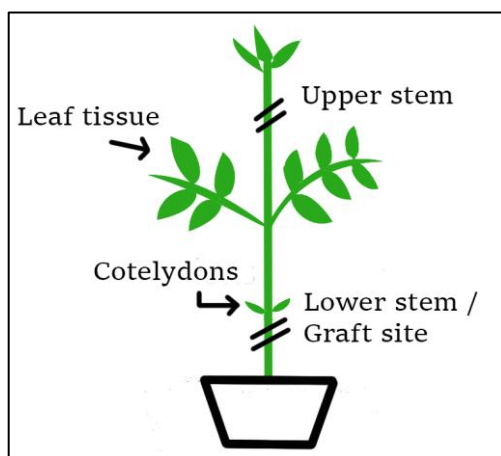


Figure 10 Illustration of where on the plants the different tissue samples were harvested for RNA extraction. Lower stem and graft site are both from the approximate same region. Lower stem accounts for the un-grafted plants.

scalpel blade was changed to a new one. The safe-lock tubes were pre-supplied with one tungsten ball to facilitate homogenization. Samples were homogenized with the TissueLyzer II (Qiagen), with pre-cooled mounts, all happening in a 7°C room to avoid thawing. Samples that were not fully homogenized with the TissueLyzer were in addition also ground up in the Eppendorf tubes with an autoclaved plastic pestle (cooled in liquid nitrogen to avoid thawing). All samples were kept frozen at -80°C until RNA extraction.

2.4.2 RNA extraction

The protocol for RNA extraction was supplied by Qiagen (RNeasy plant mini kit (Cat. No. 74104) RNeasy mini handbook 04/2006 p. 52-55, see appendix p. XII) and all steps except 12 were performed as specified there. QIAshredder and RNeasy spin columns, as well as the buffers mentioned in the protocol was supplied in the same kit. For centrifugation steps 6, 7, 8, 9 and 11, 10^4 g were used. Steps 6, 7 and 8 were centrifuged for 15 seconds. After the RNA extraction, all samples were analyzed using a NanoDrop 1000 spectrophotometer (Thermo Fischer Scientific). The concentration [$\text{ng}/\mu\text{l}$] and the purity of the RNA (OD 260/230, OD 260/280) were deduced from the absorption between 230 and 300 nm (numbers used for further calculations is summed up in NanoDrop measurements p. II-V in the appendix for more details).

2.4.3 DNase treatment

All samples were treated with DNase to remove genomic DNA. The kit DNA-freeTM (Ambion cat.no. AM1906) and the included reagents was used for this. The reaction mix was 20 μl and volumes of reagents are listed in Table 1.

Table 1 Reaction mix for the DNase treatment of total RNA.

10x DNase I Buffer	2 μl
rDNase I (2 units/μl)	1 μl
Total RNA	2 μg
Nuclease-free water	\rightarrow 20 μl

The tubes with the reaction mix were gently flicked and incubated at 37°C for 20 minutes. After the incubation, two μl of DNase Inactivation Reagent (Ambion, supplied in kit) was added to the sample tubes, and they were resuspended by brief vortexing. The samples were incubated at room temperature for two

minutes, and samples were mixed occasionally by inverting by hand. The samples were then centrifuged at 10^4 g for 1.5 minutes. The supernatant was transferred gently to a new tube. Two μl (400ng) of the DNase treated samples were run on a gel to quality control the RNA isolation process, and make sure that there was no genomic DNA carryover in the isolated RNA samples. The samples were stored at -80°C until cDNA synthesis.

2.4.4 Gel electrophoresis

Gel electrophoresis was run at several occasions as a measure of quality control of the products throughout the experiments. A 1% Agarose gel was made for all the analyses during RT-qPCR preparations. All samples used for gel electrophoresis were supplemented with a 6x

Loading dye (6x diluted to 1x with sample). The gels were added 2.5 μl Ethidium Bromide per 10 ml gel solution for band visualization, and a 1 kb GeneRuler was used as a ladder for band size reference. The gel electrophoresis was run at 50 - 100 V, for 20 - 30 minutes.

After the qPCR runs of all the genes of interest, one sample from each gene was run on a 1.5% agarose gel to check the PCR amplicon size. For this gel, Gene Ruler 50bp was used as ladder, and the gel was run for a total of 45 minutes at 70-85 V. Ethidium Bromide was used for band visualization.

2.4.5 cDNA Synthesis

cDNA synthesis was done using SuperScriptTM II RT provided by Thermo Fisher Scientific. One μg of the isolated RNA (calculated from the NanoDrop measurements) was used for the cDNA synthesis and the reagents added to each sample are found in Table 2. PCR strips with domed caps (Thermo Fisher Scientific, cat. No. strips: AB1112, and dome caps: AB0852) were used for the cDNA synthesis.

Table 2 Reagents and volumes used for cDNA synthesis.

Reagent	Volume
Oligo(dT)₁₂₋₁₈	1 μl
1 μg DNA-free RNA	X μl (see calculations below)
	$2000 \text{ ng} * \mu\text{l}^{-1}$ in 20 μl reaction \rightarrow $100 \text{ ng} * \mu\text{l}^{-1}$
	$100 \text{ ng} = 0.1 \mu\text{g}$
	$100 \text{ ng} * \mu\text{l}^{-1} * 10 = 1 \mu\text{g} \rightarrow$ used 10 μl RNA sample
1 μl dNTP Mix (10mM each) (kit)	1 μl
Deionized milli - Q water	\rightarrow 12 μl

In addition to the samples, no reverse samples lacking reverse transcriptase (NO-RT) were made for each batch of cDNA synthesis (four in total) to serve as a formal control for carryover genomic DNA. The reaction mixtures were heated to 65°C for five minutes using a

Thermal Cycler (Eppendorf) with a preset program to ensure continuity in the synthesis. The samples were briefly centrifuged with a bench microcentrifuge and further pipetting was done on ice. The following was pipetted to each tube (Table 3):

Table 3 Reagents and volumes for First strand synthesis step of cDNA synthesis.

Reagent	Volume
5x First Strand Buffer (Thermo Fisher Scientific)	4 μ l
0.1 M DTT (kit)	2 μ l
RNaseOUT™ (40 units/ μl) (Thermo Fisher Scientific)	1 μ l

Contents were mixed gently by flicking the tubes and incubated at 42°C for two minutes (using the thermal cycler). One μ l of SuperScript™ II RT was added to all tubes except the NO-RTs and mixed by gently pipetting up and down. Samples were further incubated at 42°C for 50 minutes, then 70°C for 15 minutes. Samples were stored at -18°C until further analysis by qPCR.

2.4.6 Primer Design

Primers for the reference genes: Glyceraldehyde 3-phosphate dehydrogenase (GAPDH), Eukaryotic Initiation Factor 4a-2 (EIF4- α -2) and Actin, as well as primers for *SIXTH1* was provided based on use from previous research. Primers for *SIXTH12*, *SIXTH4* and *WOX4* was designed using the Primer3 software (available at <http://frodo.wi.mit.edu/primer3/>). Gene specificity was verified using Primer-BLAST from NCBI (available at http://www.ncbi.nlm.nih.gov/tools/primer-blast/index.cgi?LINK_LOC=BlastHome). The reference genes were chosen due to low variation in expression and previous experience that these reference genes would be suitable for gene expression analysis. All primers were ordered from Sigma-Aldrich Merck.

Table 4 Primer sequences for the forward (Fwd) and reverse (Rev) primers for each target gene. Tomato XTH nomenclature as defined by Saladié *et al.*, (2006). Previous names of target gene in parenthesis.

Name	Accession number	Sequence 5' -> 3'	Amplicon size
<i>GAPDH</i>¹	NM_001279325	Fwd = CTCCCACAACCTTAACGGCAAA Rev = AAGATCGACAACGGAGACATCAG	75
<i>Actin</i>²	NM_001308447	Fwd = CCCAGAGGTACTCTTCCAACC Rev = AAGCAGTGATTTTCCTTGCTCA	188
<i>EIF4a-2</i>	XM_004253046	Fwd = CTAGGCGAAAGGTTGACTGG Rev = GCAAGGAGATCGGTTGTGAT	157
<i>SIXTH1</i> (<i>LeXTH1</i>)	NM_001246929	Fwd= TTTTTGGGGAACAGAACTGG Rev = GGAACGTCGTCCACAAAGAT	173
<i>SIXTH4</i>	NM_001247440	Fwd = TTGATGGATGTGAGGCTGTC Rev = CAGGGCCATCTAAATCTTGG	102
<i>SIXTH12</i> (<i>Br1</i>)	NM_001309868	Fwd = TATTTATGCCCAAGGCAAGG Rev = GTTGGGGTTTCCAAATGATG	101
<i>WOX4</i>	NM_001247322	Fwd = CCAGGAGGAACAAGATGGAA Rev = GTCTTTCACGGGCTTTATGG	187

All above mentioned primer sequences were analyzed by qPCR to check the amplification efficiency before analyzing the plant tissue samples. The melt curves for the initial test run of the primers were also analyzed to check for primer dimers, or other unwanted amplicons. Non-template controls were also included in this initial analysis of the primers, to ensure the primers bind to the template and nothing else in the reaction mix.

¹ GAPDH published by Solanke *et al.* (2009)

² Actin published by Suzuki *et al.* (2012)

2.4.7 RT-qPCR

The CFX96 real-time PCR Detection System C1000 Thermal cycler (BioRad) was used to run the qPCR reactions, and CFX Manager version 3.1 (BioRad) was used to analyze the results. A 10-fold dilution series (10^{-1} to 10^{-4}) of mixed cDNA from the samples were run to check for the appropriate running dilution and amplification efficiencies. The dilution series was found to be appropriate and used throughout the experiments. From the dilution series, standard curves were generated, and amplification efficiency was calculated. Melt curves were checked to ensure there were no unwanted amplifications in the samples. All standard samples were run in triplicates, and the plant samples that were not standards were run as duplicates, as a 96 well plate (BioRad cat. No. HSP9655) was used. Triplicates would be inconvenient and well-inefficient per plate, as well as duplicates being more economically viable and give a similar C_q value up till 35 cycles, and therefore considered sufficient (personal communication).

Table 5 Pipetting scheme for qPCR reactions

Reagent	Volume
SsoFast EvaGreen Supermix	10 μ l
2.5 μ M forward and reverse primers	4 μ l
cDNA (template)	→20 μ l
De-ionized milli-Q water	1 μ l

The qPCR pipetting scheme for the qPCR runs can be found in Table 5. The reaction mix had a total volume of 20 μ l, and was made by adding all reagents but the cDNA in one master mix. The mastermix was pipetted into each well, and five μ l cDNA dilution (10^{-2}) was pipetted finally. The 96-well PCR plates was sealed with a optical approved plastic film (BioRad, cat.no. MSB1001) and centrifuged briefly at 10'000x g, thereafter flicked by hand gently for mixing. One non-template control for each gene was included with water as template, as well as the no reverse transcriptase controls. Samples were so amplified by qPCR, and the protocol with cycle conditions can be found in Table 6 on the next page.

Table 6 The conditions for gene amplification and analysis through qPCR.

	Temperature	Time	Cycles
Enzyme activation	95°C	30 seconds	
Denaturation	95°C	5 seconds	40 cycles
Annealing / Extension + Plate read	61°C	5 seconds	
Melt Curve + Plate read	65-95°C (0.5°C inc.)	5 seconds per step	

2.5 Data processing

Merged images were created merging the red channel with the gray channel of CY3 and darkfield images respectively, with the ImageJ Fiji 2.0 (java 1.8.0) software (see ImageJ Fiji script p. XI in appendix for example script). Microscopy pictures were stored as .zvi files with the SteREO Lumar axiocam, and the axiovision software, and processed further with the Carl Zeiss Zen Lite Blue Edition software (version 3.0.79.00). Scalebars were calibrated using the ImageJ Fiji and Zen Lite softwares, based on saved information from the SteREO Lumar stored in the .zvi files.

Microscopy figures were compiled in Adobe[®] Photoshop 15, and same software was used to implement text and lines in the micrographs. All illustrations were also made in Photoshop 15, except Figure 6, which was borrowed from Eklöf and Brumer (2010). No manipulation of results was done with Photoshop, with the exception that some pictures have altered color levels, which are as specified. The figures for graft success and height measurements were made using Microsoft Excel (version 1908). All photographs of plants and material were taken with a Samsung Galaxy s10e smartphone, using default automatic settings with scene-optimization. Gene expression analysis was done with the CFX Manager version 3.1 (build 1517.0823), and gene expression spreadsheet was extracted from this software into Microsoft Excel for further processing and figure generation.

2.6 Statistical analysis

The height difference between heterografts and homografts were statistically compared with a one-tailed student t-test using the data analysis package in Microsoft Excel. Due to uneven amount of measurements in the heterografts compared to the homografts, the heterografts were grouped and random samples were removed to achieve an equal number of measurements in the two groups, which was required by the software to perform a t-test. The dwarfing effect in the M82 – *S. pennellii* grafts was analysed the same way, except there already were an equal number of measurements for these, so no measurements was removed.

An analysis of variance (ANOVA) where the variance was assumed equal was performed for the third set of grafts, and only this set due to the number of biological replicates being low in the first and second sets (three replicates per heterograft in set one and two, vs. 10 replicates in the third set).

3 Results

3.1 Grafting

The tensile strength of the graft unions was in most successful cases strong. An example of the established graft union in the tomato lines are shown in Figure 11. The bridging of callus is clearly shown in between the scion and stock, although at this stage in the graft development, the callus has most likely differentiated into specific cells. For some samples there were still signs of necrotic cells at the graft union, and some deformed regions in the bridge (as shown in Figure 11C). Figure 11 A-C are all successful grafts showing the morphology of the graft site as seen with the naked eye. Adventitious rooting (Figure 11D) was a problem that occurred in some graft throughout the experiment.

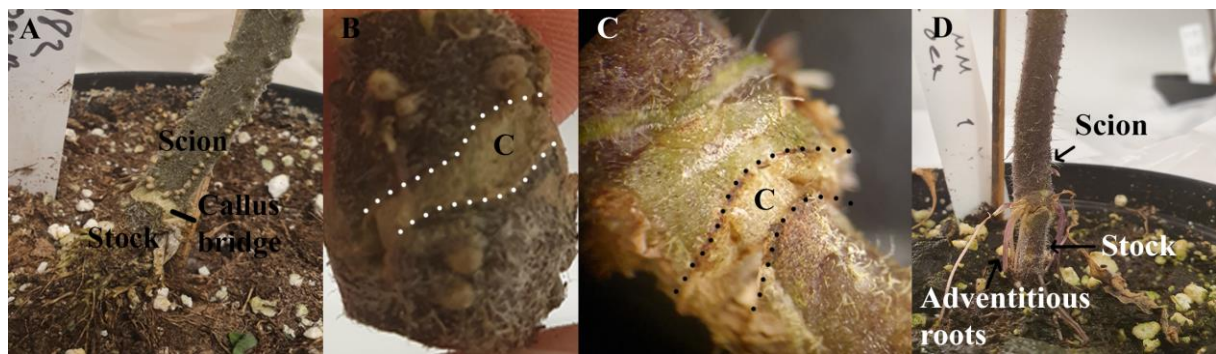


Figure 11 A) An example graft with a clear difference in tissue between the scion and stock. B) An isolated graft site visualizing where the callus fills the space between the scion and stock, marked with an “C” in figure B and C. C) A graft site showing some deformed cell growth on the sides of the stem. D) Adventitious root growth from the scion. Stippled lines indicate the end of scion and stock, and in between the stippled line the callus bridge emerge, to later differentiate into specialized cells.

The grafting was done as three separate sets. The first session included the tomato lines: *S. lycopersicum* cv. Moneymaker (MM) and M82, *S. pennellii*, and the two transgenic lines Cos33 and Oex13. During the first session, the discontinued grafting clip was used (see section 2.2 Grafting in methods or Figure 29 page I in the appendix). The total graft success for the first session is shown in Figure 12A, and the heterografts are shown in Figure 12B. The low success rate shown in Figure 12A reflect the reason for the grafting clip to be changed out. These results were done early on and acted as preliminary results for further grafting.

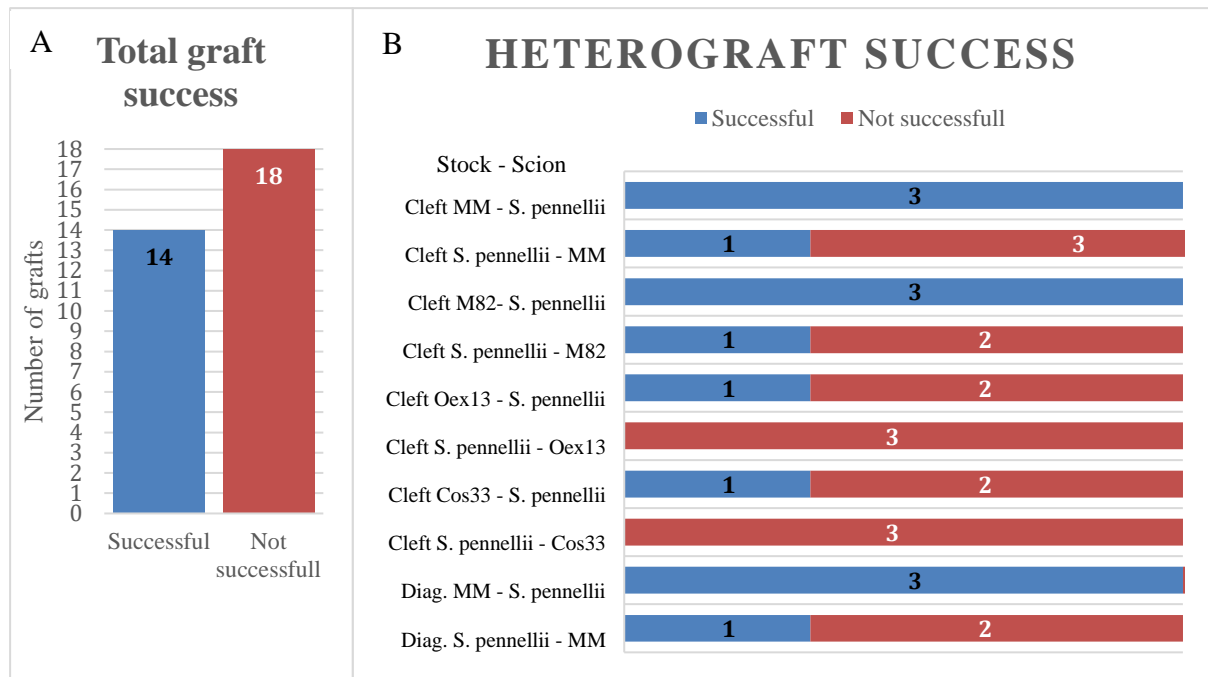


Figure 12 Results of the first session of grafting. Cleft and Diag. indicates cleft graft and diagonal cut (as shown in the tube graft in Figure 1E). Number of biological replicates (n) = 3

From the scoring of success for the first set of grafts, a trend seemed to emerge that whenever *S. pennellii* was the rootstock the grafts tended to fail (Figure 12B). The total amount of dead grafts (56%) also exceeds that of live (44%) ones for the total graft batch (Figure 12A). From Figure 12B it is also noticeable that (MM) and M82 both serve as successful rootstocks, and all grafts where they served as stock survived. As shown in the bottom part of Figure 12B, there were grafts cut diagonally (as shown in the tube graft illustrated in Figure 1E). These were discontinued as the cleft graft proved to be easier and yielded same success rates.

To further assess the possibility that *S. pennellii* was a bad stock, a second grafting set was done, with the introduction of a new grafting clip and homografts. In contrast with the first grafting set, the total success rate of grafts in this second set was high (81,5%) as shown in Figure 13A. The homografts of the tomato lines seemed to have a high success rate, except for MM with 50% success rate and *S. pennellii* with 34% success rate (Figure 13B). Again, *S. pennellii* seems to be more unsuccessful than the rest. The heterografts from grafting set two (Figure 13B) had a visibly higher success rate than set one (Figure 12B), showing that the grafting clip used had an impact on the success rate. From the same figure, one can see that the apparent trend pointing towards *S. pennellii* to be a bad rootstock was not substantiated, and all the replicates with *S. pennellii* as a rootstock survived. The MM – Cos33 graft had no successful replicates out of the total three replicates per combination, although the reciprocal

graft had all replicates successful, but one replicate was not found for scoring (Figure 13B). MM homograft had a 50% success, against expectations.

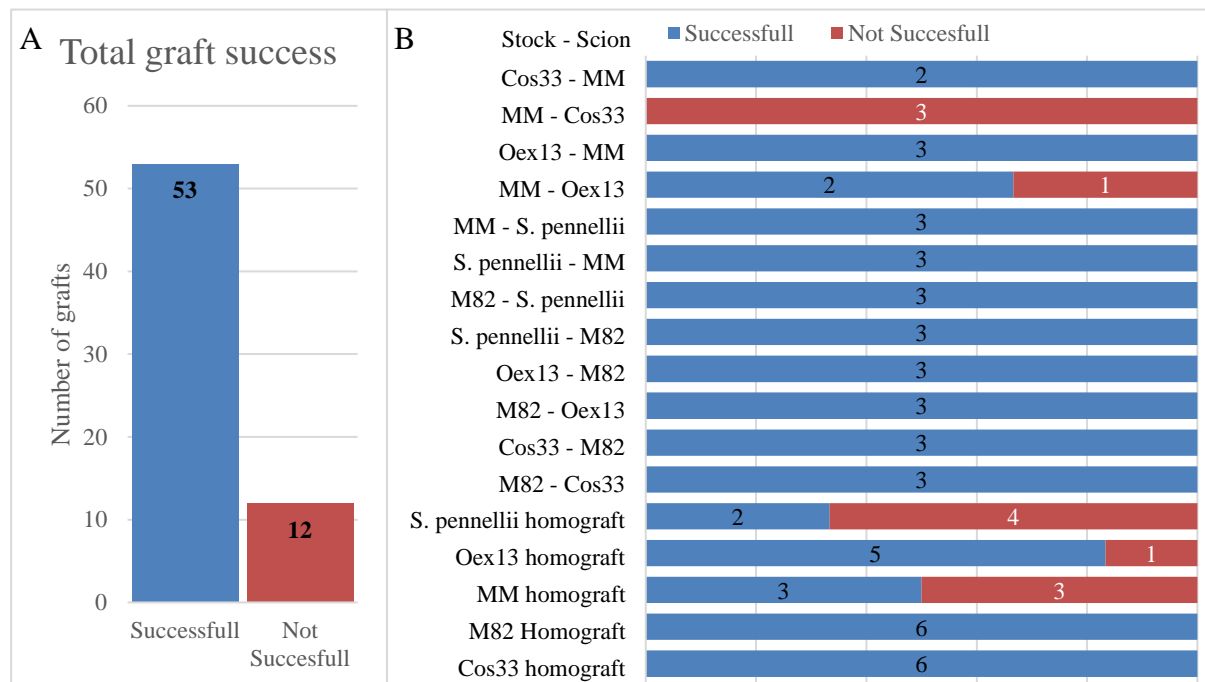


Figure 13 Scoring from the second session of grafts. A) Total graft success. B) Homografts were done to assess the self-compatibility of the grafts, in addition to a new set of *S. pennellii* grafts. Moneymaker (MM) was also included in the set, even though M82 is an introgression line of MM. Heterografts were done to further assess compatibility. Total number of biological replicates (n) =65, Homograft replicates (n) = 6 per line of tomato, Heterograft replicates (n) = 3 per line. One replicate of the Cos MM graft was not found during counting of success.

S. pennellii did seem to induce a dwarfing effect when grafted with M82 as shown in Figure 14. Based on a one-tailed student t-test there was a significant difference between M82 – *S. pennellii* graft (M = 50; SD = 2.65) and *S. pennellii* – M82 (M = 25.67; SD = 6.50) height measurements $t = (5.56)$, $p=0.015$, supporting the observation of dwarfing. Further statistical testing (ANOVA) showed that the height measurements between the homografts (M = 39.33; SD = 7.71) and the heterografts grouped (M = 38.22; SD = 9.04), were insignificant $t = (0.22)$, $p = 0.42$.

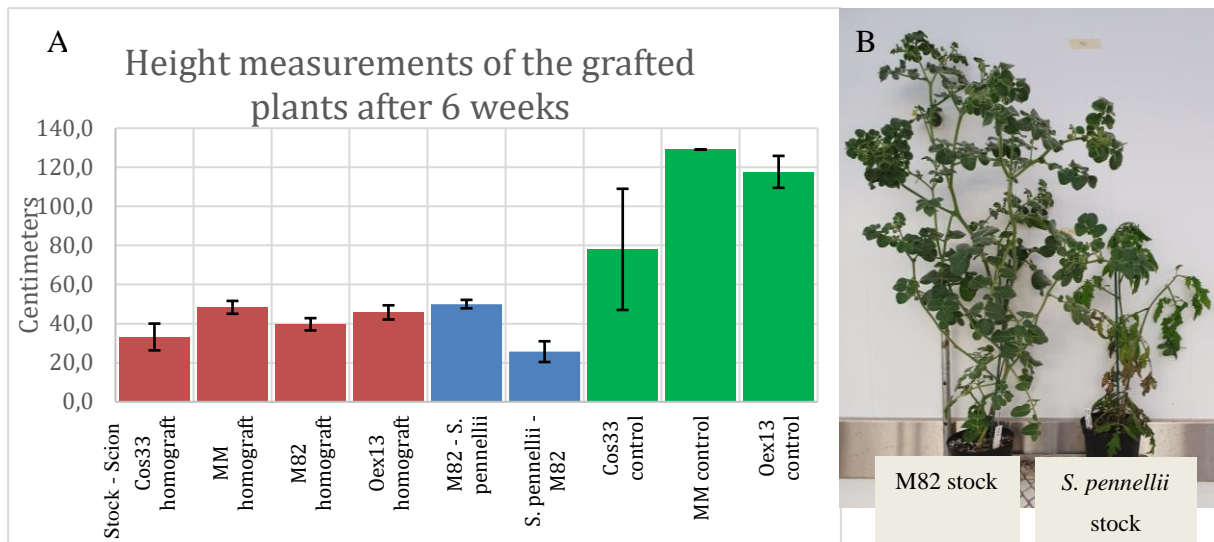


Figure 14 A) Height measurements averages of the second set of grafted plants 6 weeks after grafting. M82 and S. pennellii controls were trimmed and are therefore excluded from the measurements. B) A photograph of the dwarfing effect of S. pennellii – M82. The right plant is with a S. pennellii rootstock, while the plant to the left is with a M82 rootstock. Error bars show the standard error of the measurements for each graft combination.

The third set of grafts had an increased sample size of 10 replicates per graft pair. The total graft success rate was 60% (Figure 15A), with higher variation within the specific pairs than between, and there were no significant difference between the graft combinations ($F=[5,54]=0.63, p=0.67$) (Figure 15). In contrast to the second graft set (Figure 13B), the MM - Cos33 (incl. the reciprocal graft) grafts yielded a higher success and proved that all tested

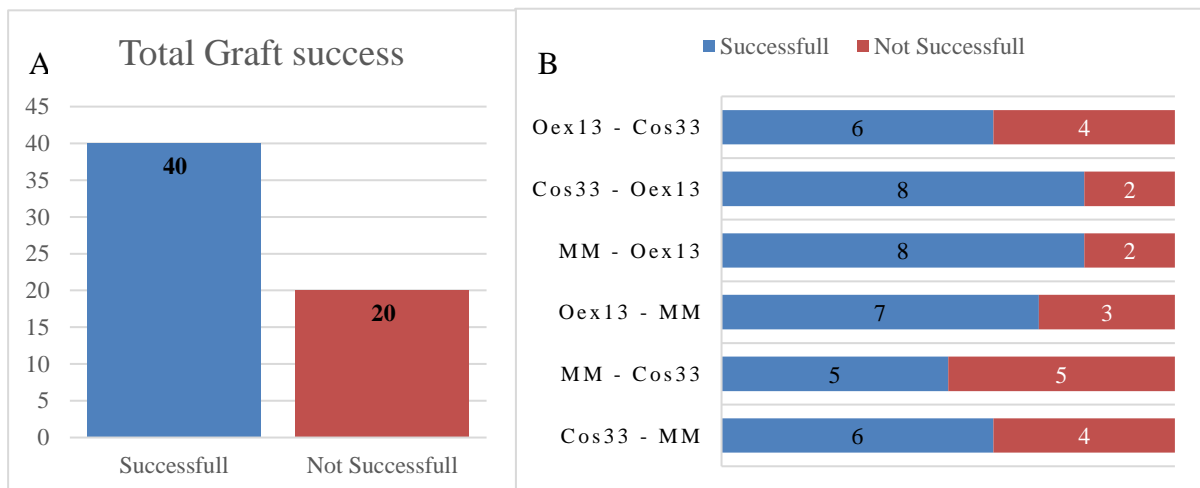


Figure 15 Third set of grafts. Focus group was the transgenic lines, and MM was used instead of M82. A) The overall graft success was 60%, but this set of grafts had a serious issue of adventitious rooting from the scion which made scoring success harder compared to previously. B) The heterografts showed no significant difference between the combinations ($F = [5,54] = 0.63, p=0.67$). Total replicates (n) = 60, Heterograft biological replicates (n) = 10.

combinations were graftable. The scoring of success for the third graft set proved difficult due to adventitious rooting from the scion, which resulted in scion survival independent of graft success (see Figure 11D). These grafts were therefore thoroughly checked for scion-stock attachment.

3.2 Xyloglucan Endo-transglycosylase (XET) activity assay

To assess the role of xyloglucan endo-transglycosylase (XET) activity in the grafted plants, an *in situ* enzyme activity assay was performed. Fluorescently labeled xyloglucan oligosaccharides were incorporated into the cell walls by XET, thereby showing the locality of active XTHs and endogenous xyloglucan donor substrate (based on the work done by Vissenberg *et al.*, 2000). The sites of enzyme activity were visualized using fluorescence microscopy, and fluorescence was visualized using Carl Zeiss filter cube 43 CY3. Typical regions that gave a high level of fluorescence were the vascular bundles, but here the fluorescence was also observed in negative controls where no activity staining was performed. These negative controls showed a weak fluorescence signal with both the GFP filter (data not shown), as well as the CY3 filter in the vasculature of some samples, although the majority of the negative controls showed no noticeable background signal with the exposure times used (Figure 16).

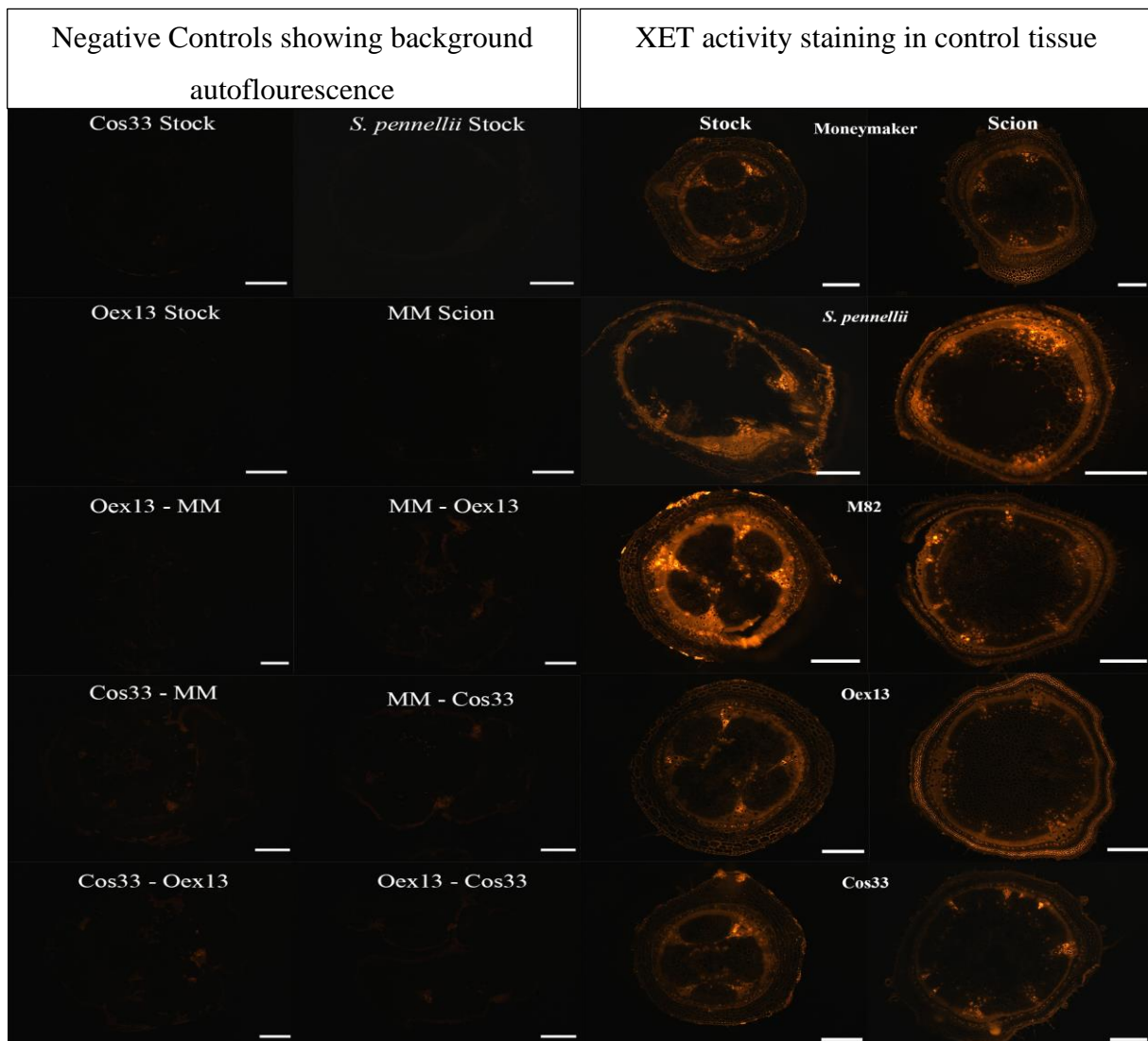


Figure 16 (on previous page). Left two columns show representative cross-sections of the negative. Only the graft sites show any clear signs of autofluorescence (red areas) in the negatives, although weakly. Right most two columns show representative cross-sections samples of fluorescently labeled of stock and scion control tissue. Filter used for detecting fluorescence was the CY3 filter. Scale bars show 1000 μm . Exposure times was 800ms.

The transgenic lines showed a difference in the level of fluorescence that was visualized best in the longitudinal sections, although weakly. The over-expresser line tended to have a higher level of fluorescence than the MoneyMaker (MM) background, and the co-suppressor had a lower level of fluorescence than MM and Oex13 (Figure 17). This pattern was not as apparent in the cross-sections.

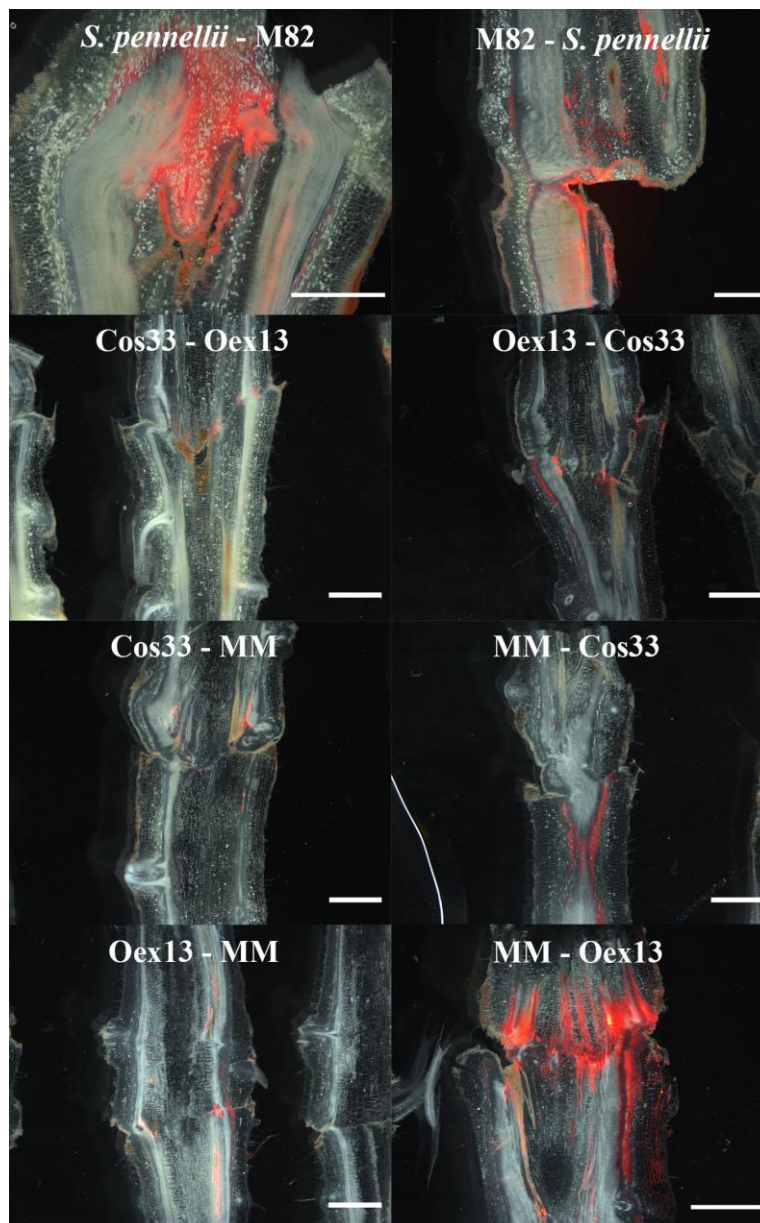


Figure 17 Longitudinal section darkfield images merged with the fluorescence images taken with the CY3 filter. The images show the fluorescence from the incorporated XyGO-SRs, visualizing (in red / orange) where XET activity has occurred. *S. pennellii* pictures had an exposure time of 200ms, the rest was 800ms. Red color is increased via software by decreasing cyan levels by 100% and increasing black levels by 100% for the purpose of overview in this specific image. All micrographs in the figure are treated equally with software. Scalebars show 2000 μm .

From the assay it was also observed that *S. pennellii* gave a weaker fluorescence than the M82 graft partner (Figure 17). Based on observations between the graft samples and the scion tissue, the fluorescence was more specific for the graft union. In scion and stock cross-sections, the fluorescence was evenly distributed across all tissue types (Figure 16 Right). This is in contrast with the graft site crosssections where the fluorescence was patchy and dispersed (Figure 18). The dispersed and patchy fluorescence was often observed at the sites where the two plants had merged, or at the vascular bundles (Figure 18).

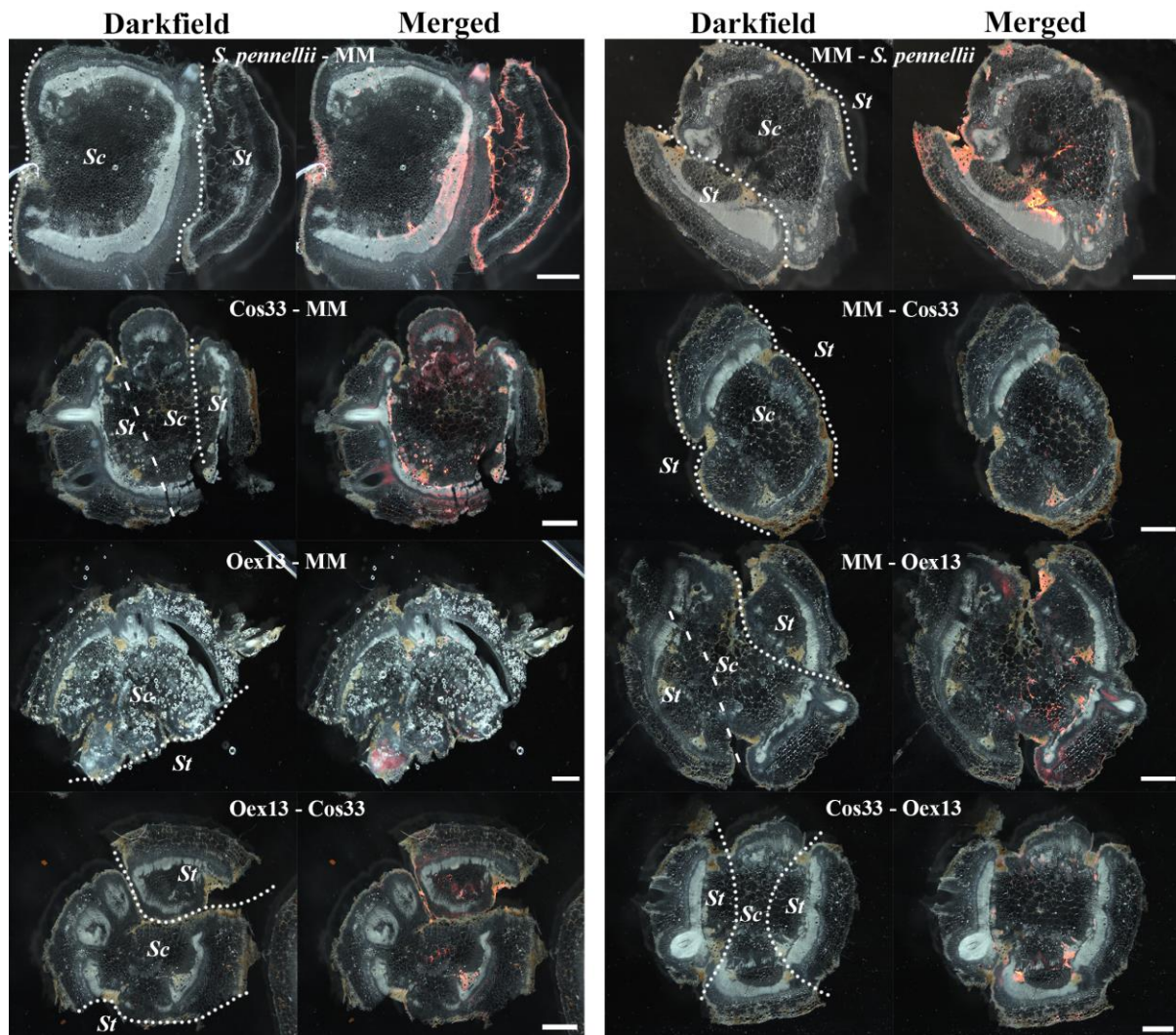


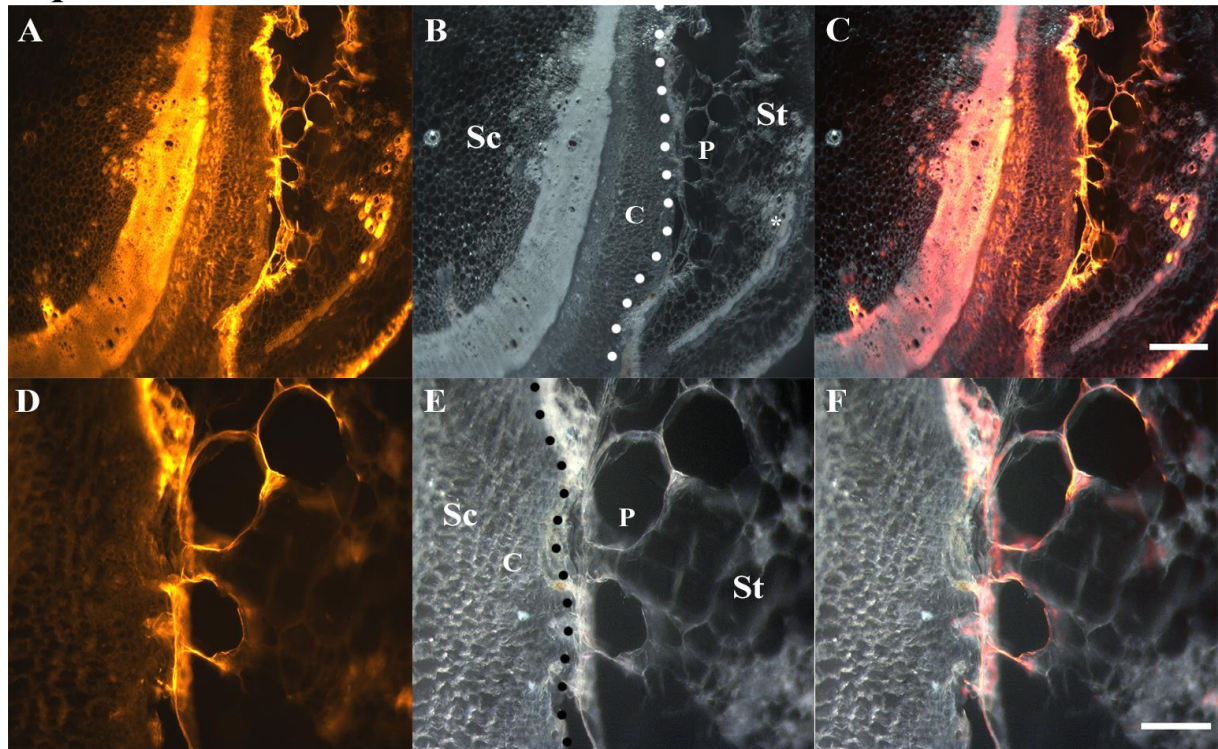
Figure 18 Crosssections of the graft sites for Oex13, Cos33, *S. pennellii*, and MM, including reciprocal grafts. Figure shows the darkfield images and merged images of the darkfield and CY3 images. The CY3 filter makes the fluorescence from the incorporated XyGO-SRs (where XET activity has occurred) visible as red / orange. Round stippled line is the graft union of the scion (Sc) and stock (St). Square stippled line is a proposed graft union, where the samples were deformed in a way that made evaluation of the specific graft union hard. Where evaluation of the location of the graft union was impossible, there is no stippled line. All crosssections have a middle scion part and stock sample originally on each side (due to the nature of the cleft graft), unfortunately was several samples destroyed during sectioning. Exposure times were 800ms, Scalebars are showing 1000 μ m.

Interestingly, a high fluorescence was observed in the *S. pennellii* – MM (reciprocal grafts incl.) grafts, as shown in Figure 19. It is noteworthy that the *S. pennellii* samples are mostly without pith cells, due to damage from cutting the sections with the Vibratome and MM are among the most intact and thickest sections. Taking a closer look at the *S. pennellii* – MM graft interface there is a clear fluorescence in the cell walls of the *S. pennellii* pith parenchymal cells, as well as MM cork cells, as shown in Figure 19 C, F and I. This same fluorescence pattern can also be seen in Oex13 – M82 samples (Figure 35 in the appendix, subchapter Supplemental XET activity images on p. X).

The reciprocal graft of *S. pennellii* – MM (MM – *S. pennellii* (Figure 19 G - L)) did not show the same connection of cells as clearly as *S. pennellii* - MM did (Figure 19A - F). Although, as shown in Figure 19 H, I, K, and L, marked with asterix' the vascular regions fluoresced relatively high. Also, some pith cells in the scion seemed to show fluorescence in linking parts of several parenchyma cells (Figure 19 K and L, marked with P). The fluorescence seen in these parenchymal cells has been seen in negatives as well (data not shown), and therefore considered less important.

If *SIXTH1* was a major factor in XET activity it would be expected to see a notable difference in fluorescence between the two mutants. As shown in Figure 20, there seemed to be little difference between the two mutants at the graft union, although the Oex13 line seem to be showing more fluorescence than the Cos33 counterpart in less magnified image of Figure 20 C, L, O and R, and Figure 17).

S. pennellii - MM



MM - *S. pennellii*

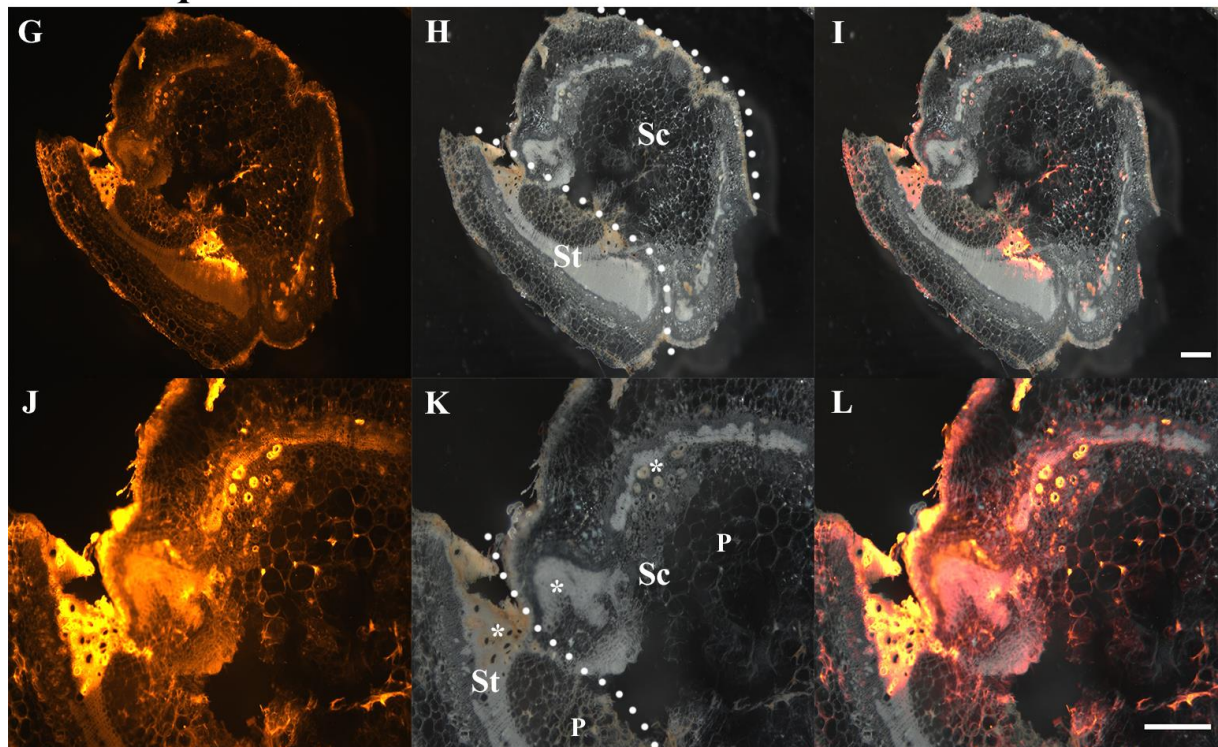
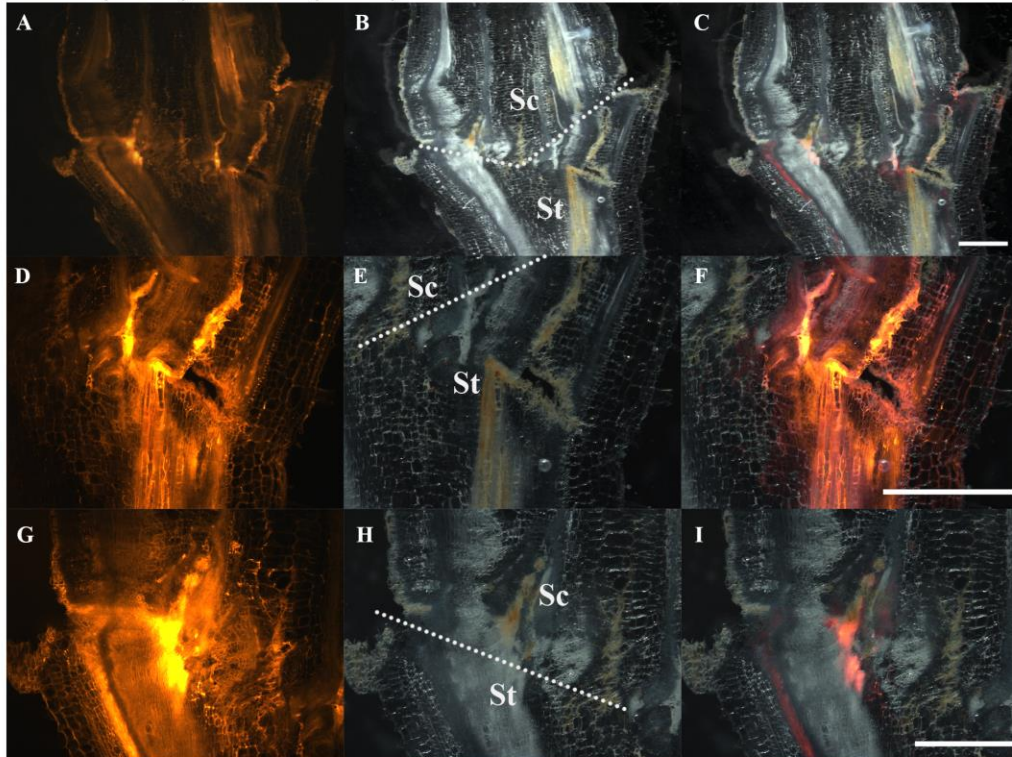


Figure 19 A – F shows cross-sections of the *S. pennellii* (stock) – Moneymaker (MM) (scion) graft interface, G- L shows the reciprocal graft. Figure shows the CY3 filter fluorescence images, darkfield images and merged images of the two latter (from left to right). The CY3 filter visualizes the fluorescence from the incorporated XyGO-SRs (where XET activity has occurred) as red / orange. Sc = Scion, St = Stock, P = parenchyma-like cells, C = cortex. Stippled line marks the graft union, where the two plants have grown together. Scalebar in C shows 500 μ m, scalebar in F shows 200 μ m. Vascular regions with XET activity marked with Asterix. Stippled line is the graft union. Scalebars in I and L show 500 μ m.

Oex13 (Stock) - Cos33 (Scion)



Cos33 (Stock) - Oex13 (Scion)

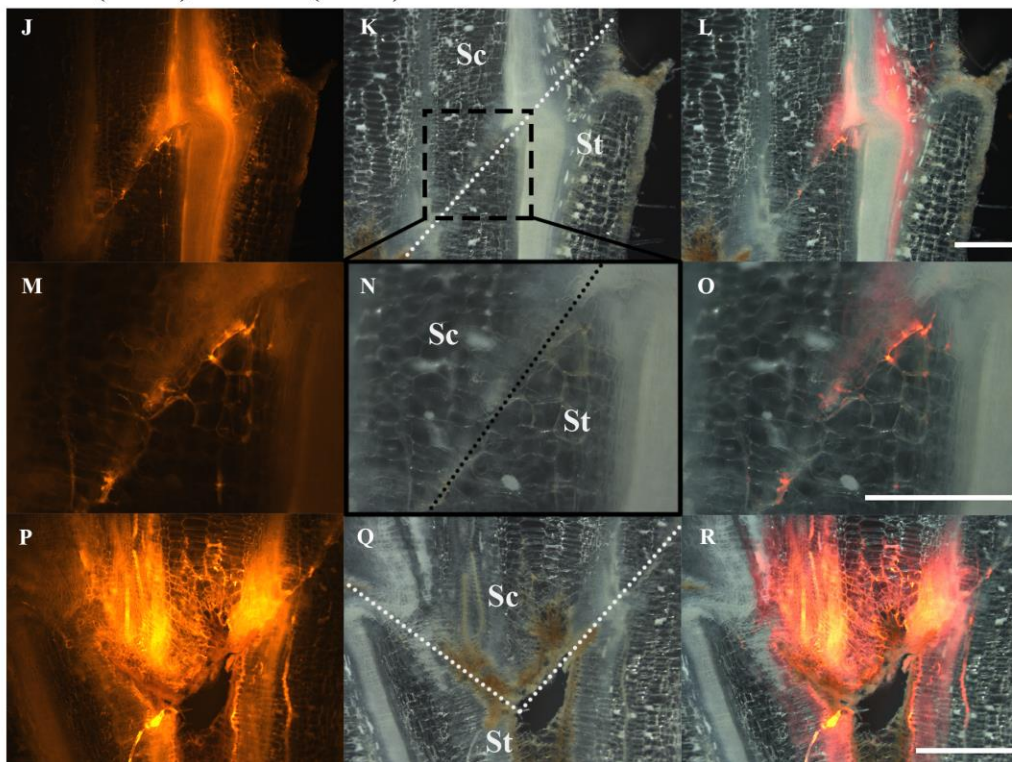


Figure 20 Longitudinal sections of Oex13 (Stock) - Cos33 (Scion) (A – I), and the reciprocal graft Cos33 (stock) – Oex13 (scion) (J – R). Figure shows the CY3 filter fluorescence images, darkfield images and merged images of the two latter (from left to right). The CY3 filter makes the fluorescence from the incorporated XyGO-SRs (where XET activity has occurred) visible as red / orange. St = Stock, Sc = Scion, stippled line marks the graft union, where the two plants have grown together. Exposure time for A, C, D, F and G were 800ms. Exposure time in I were 50ms. Cos33 (stock) – Oex13 (scion) longitudinal section of graft site exposure times were 800ms except for M-O which were 200ms due to higher magnification. All scalebars show 1000 μ m.

Differences between the Cos33 and Oex13 lines when it comes to fluorescence was not observed as clearly in the cross-sections (Figure 19, Figure 21 and Figure 22). The same accounts for the transgenic lines grafted with *S. lycopersicum* cv. M82, where there is no seeming difference between the fluorescence of the transgenic lines (Figure 22). Still the fluorescence was brightest around the vascular elements, which is clearly shown in the longitudinal sections (Figure 17, Figure 20, Figure 23), as well as in the cross-sections (Figure 18, Figure 21, Figure 22) and this seems to be the case for the cells in the closest proximity to the graft union also (Figure 19, Figure 20, Figure 21, Figure 22, Figure 23, and Figure 36 in the appendix). There also seem to be some XET activity in the pith cells, as shown in several samples (Figure 19, Figure 21, Figure 23, as well as Figure 35 and Figure 36 in the appendix) but mostly in tissue near to or related with the graft union, or at a direct wound site from the initial cutting during the grafting process. Some epidermal cells show a higher level of fluorescence (Figure 19, Figure 22) as well as endodermal cells (Figure 22 F and I), all of which seem to be in relation with wounding (from cutting) or the grafting process.

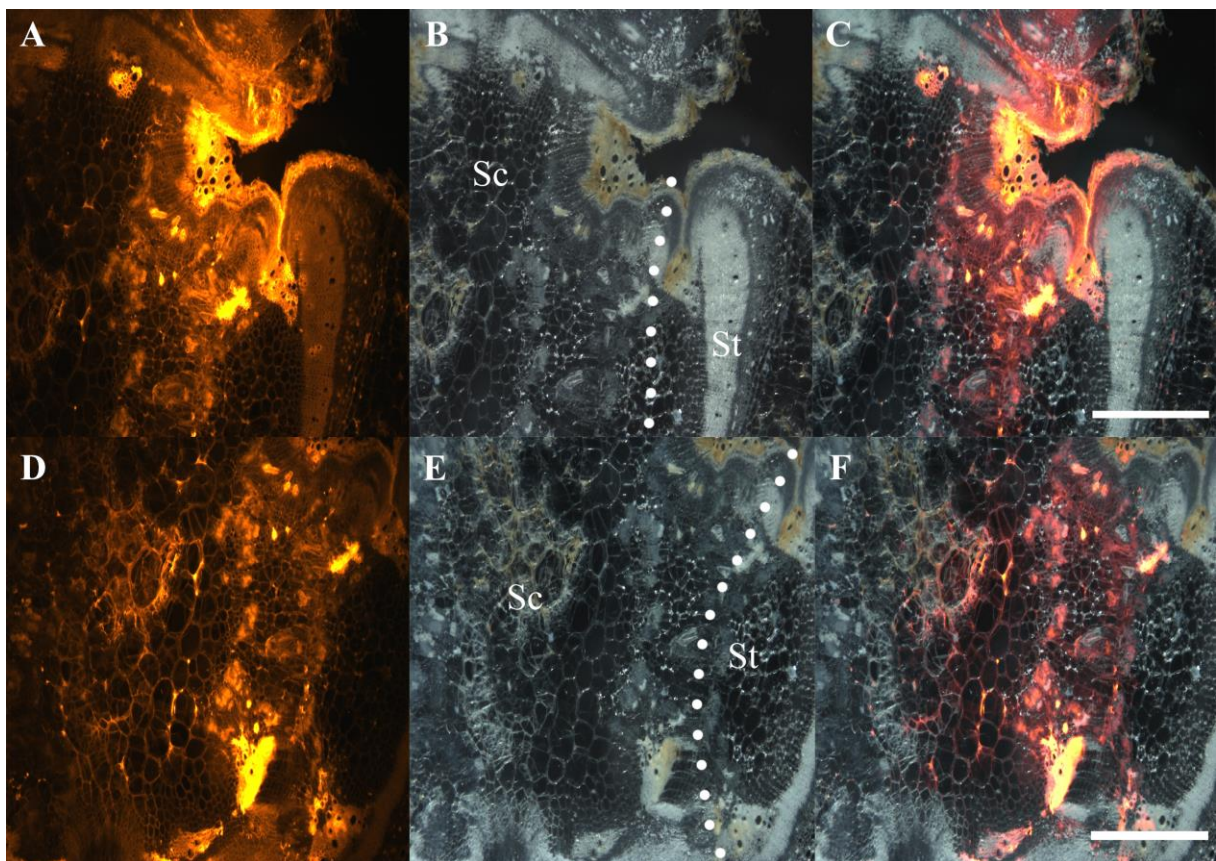


Figure 21 Cos33 (Stock) – Oex13 (Scion) graft site. Sc = Scion, St = Stock, Stippled line marks the graft union, where the two plants have grown together. Figure shows the CY3 filter fluorescence images, darkfield images and merged images of the two latter (from left to right). The CY3 filter makes the fluorescence from the incorporated XyGO-SRs (where XET activity has occurred) visible as red / orange. Exposure times were 800ms. Scalebars show 1000 μ m.

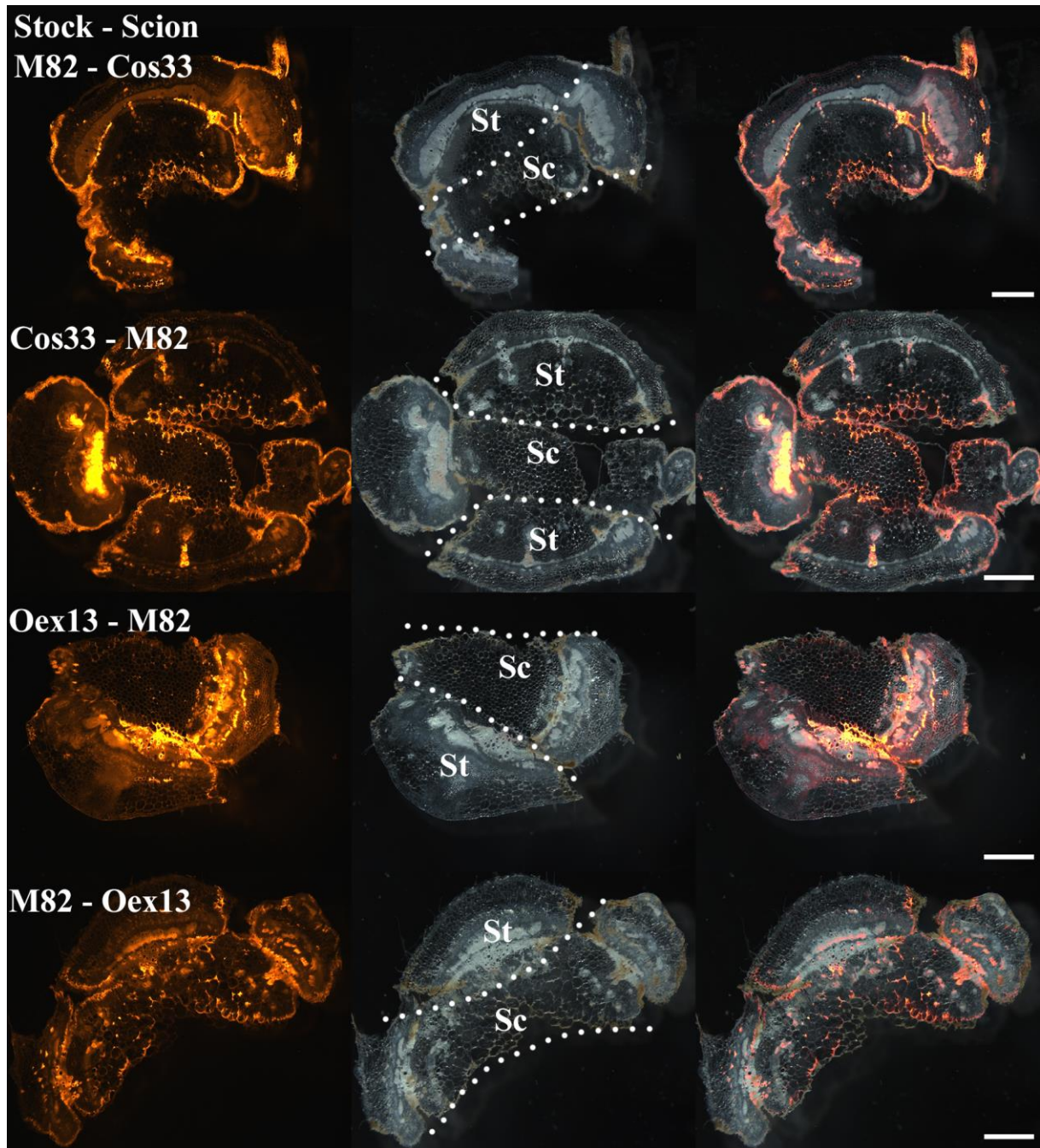


Figure 22 Transgenic lines grafted with *S. lycopersicum* cv. M82. St = Stock, Sc = Scion, stippled lines indicates graft union where the two plants have grown together. The first plant line in the name (top left in each micrograph) indicates the stock, the second plant line indicates the scion. Figure shows the CY3 filter fluorescence images, darkfield images and merged images of the two latter (from left to right). The CY3 filter makes fluorescence from the incorporated XyGO-SRs (where XET activity has occurred) visible as red / orange. Exposure times were 800ms. Scalebars show 1000 μ m.

From the darkfield images it can be seen that callus developed between the grafts, at the graft union, and vascular tissues regenerated across the union. This can be seen in the microscopy images in Figure 21 along the stippled line and in the photographs in Figure 11A-C.

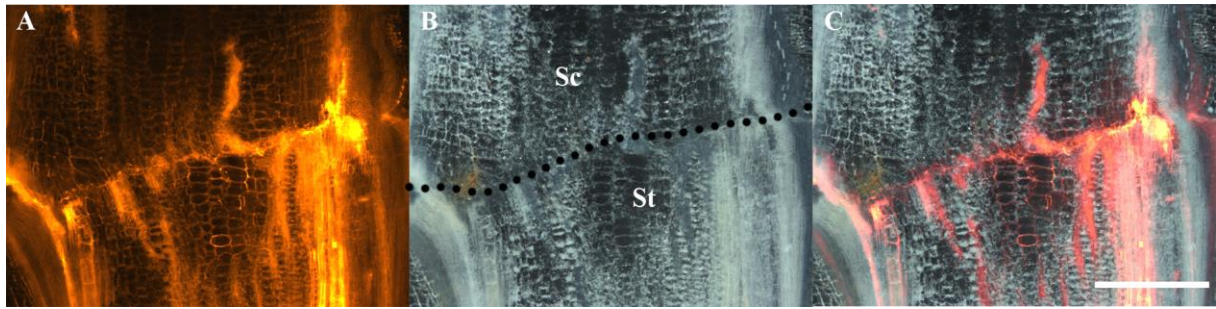


Figure 23 Oex13 (Stock) – Moneymaker (MM) (Scion) graftsite seen in the longitudinal samples. St = Stock, Sc = Scion. Stippled line marks the graft union, where the two plants have grown together. Figure shows the CY3 filter fluorescence images, darkfield images and merged images of the two latter (from left to right). The CY3 filter makes the fluorescence from the incorporated XyGO-SRs (where XET activity has occurred) visible as red / orange. Exposure times were 800ms. Scalebar show 1000 μ m.

3.3 Gene Expression

3.3.1 Sequence alignment

The amino acid sequences of *SIXTH1*, *SIXTH4* and *SIXTH12* were analyzed to ensure the relations between the tomato *XTHs*. Figure 24 shows the sequence similarities (B, and D) and shows that *SIXTH1* and *SIXTH4* are most similar, with 81% sequence similarity as shown by Saladié *et al.* (2006). *SIXTH12* (previously called BR-1) is a more distant relative as seen in the cladogram (Figure 24A) (belonging to group two *XTHs*, whereas *SIXTH1* and *SIXTH4* are members of group one (Saladié *et al.*, 2006). However, *SIXTH12* was included not because of its relation to tomato *XTHs*, but due to it being the closest relative to *Cuscuta campestris* *XTH1* (Cc015644t1). *XTH1* in *Cuscuta* has earlier been shown to play a role in the infection of hosts (a process with similarities to grafting (see subchapter 1.2.3 Parasitic plants: Natural grafters) (Olsen *et al.*, 2016). In Figure 24B the sequence DEIDFEFLG, which is considered to be a conserved region and the active site for XET (Koka *et al.*, 2000) (marked with Asterix), is shown present in all three *XTHs*, indicating that these three *XTHs* are most likely able to perform XET activity.

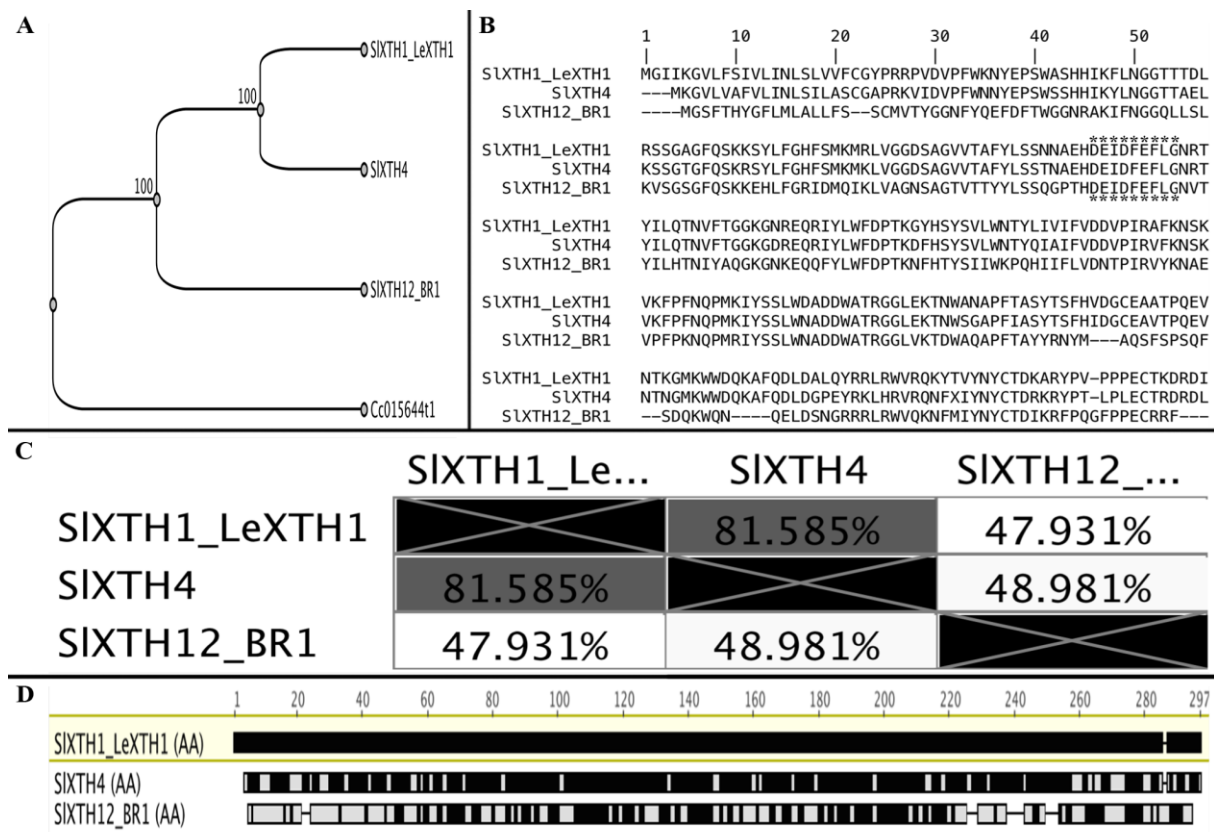


Figure 24 A) Cladogram for SIXTH1, 4 and 12, as well Cuscuta campestris XTH1 (*Cc015644t1*) as an outgroup for the cladogram. B) Amino acid sequence alignment of the three tomato XTHs. C) Overview over the similarities between the three tomato XTHs. D) Amino acid alignment depiction with SIXTH1 as the reference. Black represents similarities, gray represent dissimilarities.

3.3.2 Profiling of *SIXTH1*, *SIXTH4* and *SIXTH12*

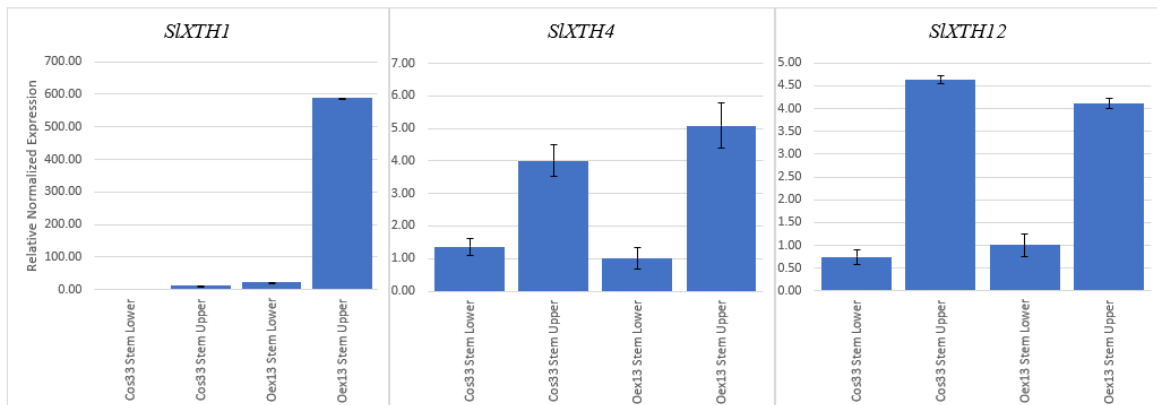
RT-qPCR was performed to assess the similarities and differences in gene expression of the three selected genes, *SIXTH1*, *SIXTH4* and *SIXTH12*. Gels were run to verify the product from cDNA synthesis and qPCR, as well as melt curve analysis to assess amplification of unwanted products. Neither NTC nor NO-RTs amplified, showing that nothing else but the template was amplified during qPCR. These results are found in the appendix (pp. VI - VII and VIII - IX). There was no unwanted amplification seen from the melt curve analysis, and gels showed clean bands at the desired sizes (see Gel electrophoresis in appendix p. VIII). No genomic carryover seemed to follow through the molecular preparations for the qPCR.

Figure 25C shows the relative expression in Oex13 leaf, Cos33 leaf and MM scion leaf. The Oex13 line over-expressed *SIXTH1* as compared to the MM sample. It was also apparent that the Cos33 line suppressed the gene. This was also observed in the stem tissue (Figure 25A), where Oex13 Upper stem tissue showed nearly a 600-fold higher expression than the Cos33 upper stem tissue. The difference in *SIXTH1* expression in the lower tissue was not as great,

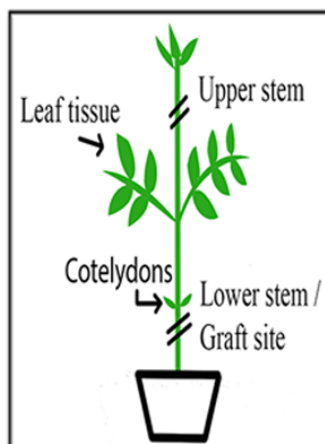
yet the Oex13 expression of *SIXTH1* in lower stem tissue was 32-fold higher than in the Cos33 line. In all the *XTHs* in Figure 25A, the upper stem tissue had a higher expression than lower stem tissue.

To further assess the *SIXTH1* suppression and over-expression, and to see if this only affect *SIXTH1*, a close homologue to *SIXTH1*, *SIXTH4* (as shown in Figure 24A-D), was analyzed, and the expression data was dissimilar to that of the *SIXTH1*. *SIXTH4* and *SIXTH12* expression showed little difference between the Oex13 and Cos33 tissues as shown in Figure 25A and C, indicating the two tomato lines modifications are specific to *SIXTH1*. Figure 25C shows that there are little to no difference in *SIXTH4* expression in leaves between the samples, while *SIXTH12* has higher expression in MM leaf than in Cos33 and Oex13 leaf. What was maybe the most noteworthy from Figure 25, was the expression differences between samples for each gene, where *SIXTH1* was as mentioned 600-fold and 32-fold for upper and lower stem tissue respectively, and such a difference was not observed in *SIXTH4* or *12*, where the highest difference was five-fold.

A



B



C

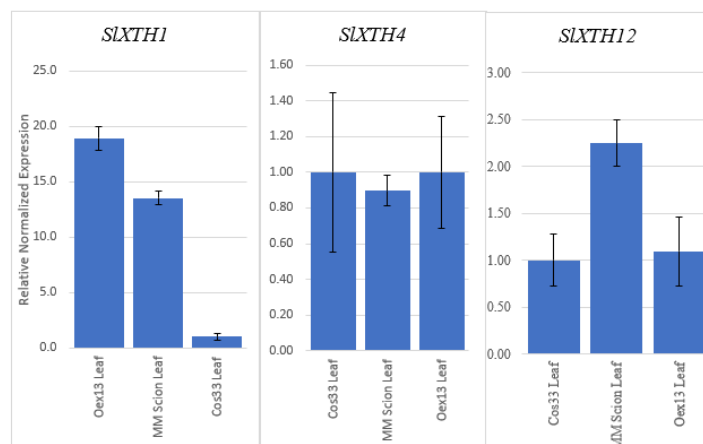


Figure 25 on previous page. Relative normalized expression, relative to Oex13 Stem Lower (A) and Cos33 Leaf (C). Control sample put to be = 1. A) The expression of SIXTH1 compared to a close relative SIXTH4, and a close relative to Cuscuta XTH, the SIXTH12. There was a visible difference in expression between the three genes, implying the over-expression and suppression of SIXTH1 in the transgenic lines. B) Illustration of the different tissue types' harvest-location on the plant. C) SIXTH1, SIXTH4 and SIXTH12 expression in the leaf tissue of the transgenic lines and Moneymaker (MM). Data based on one biological replicate and two technical replicates. Normalization = $\Delta\Delta Cq$ value of the target genes and the reference genes GAPDH, EIF4a, and Actin. Error bars show the standard error of the Cq values.

Figure 26 shows the relative gene expression of the three XTHs in the graft sites (in blue) as well as their respective scion samples (in orange). The first obvious point from the figure is the difference between gene expression in SIXTH12 at the graft sites of the two transgenic lines, Cos33 and Oex13 (Oex13 – Cos33 graftsite). This specific graft site has a 20-fold difference in expression between the graft site itself and the respective scion and reciprocal graft, something not seen in the other samples for the other XTHs. In most cases the scion had an observed higher expression than the graftsite for all the three XTHs, with an exception of SIXTH1 and SIXTH12 Oex13 – Cos33 graftsite and SIXTH1 MM – Cos33 graftsite. Several samples had a minimal or equal expression to the respective scion. For all tested XTHs, MM scions yields either a similar or higher expression compared to the Cos33 scions. The overall differences between graft tissue samples for each gene seems to be low. All gene expression data have one biological replicate and two technical replicates.

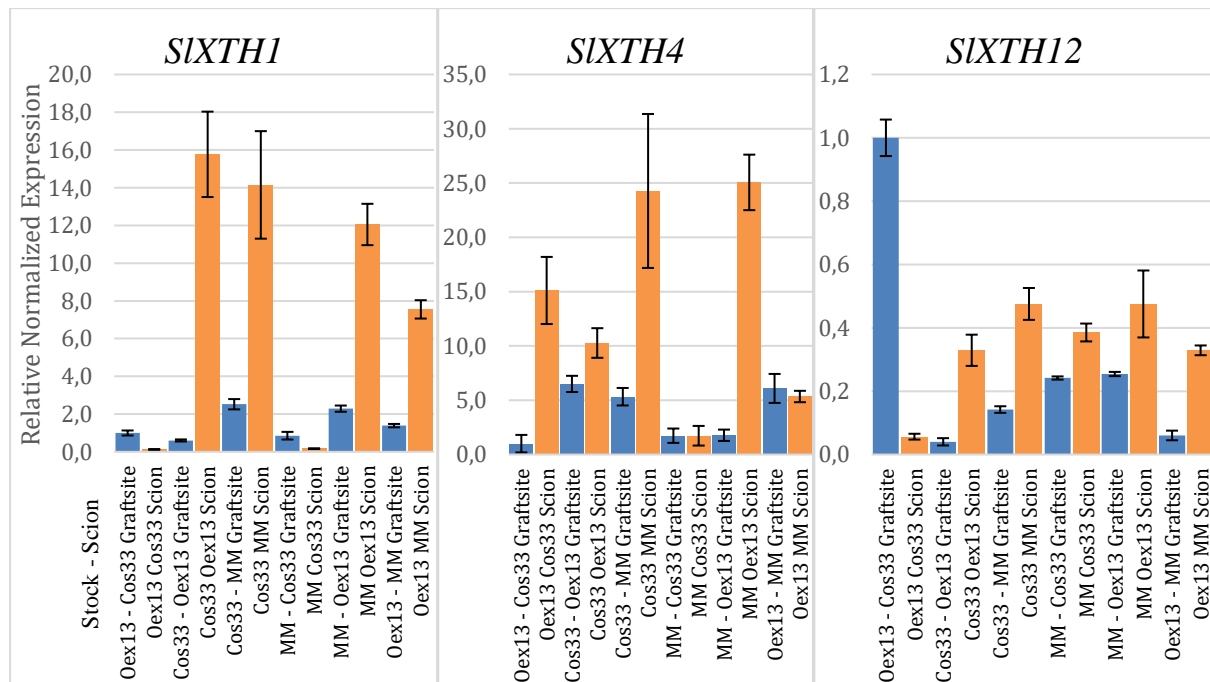


Figure 26 Normalized relative expression, relative to Oex13 - Cos33 Graft site = 1. XTH expression in the graft sites (blue) and their respective scions (Orange). Samples labeled scion is tissue from the scion of each graft, sampled above from the graft site. Normalization = $\Delta\Delta Cq$ of the target genes and reference genes GAPDH, EIF4a, and Actin. Error bars show standard error of the technical replicates Cq value. One biological replicate. Two technical replicates.

3.3.3 Cambium related gene expression (*WOX4*)

The vascular cambium plays a central role in graft development (see page 2 in the introduction) and was therefore of interest in the gene expression analysis. Additionally, Melnyk *et al.*, (2018) showed that in *Arabidopsis*, the expression of *WOX4* was high in grafted tissue and separated top (scion) tissue 10 days after grafting.

Figure 27 shows the relative gene expression of *WOX4* in all tomato samples, and there was a clear difference in the expression between stem and leaf. The un-grafted lower stem tissue of the Cos33 and Oex13 lines seem to have a lower expression of *WOX4* than the upper stem samples. The expression in graft tissue (yellow bars) show little difference from the un-grafted lower stem samples (blue bars) (which is the approximate same region on the plant for tissue harvesting (See Figure 10 in Plant tissue harvesting p. 19 or Figure 25B), with exception of the Cos33 – MM graft site which is seems to be four times lower expressed than the reciprocal graft tissue. There was a peak in expression in the MM – Oex13 scion sample, which was approximately four times more than the reciprocal sample.

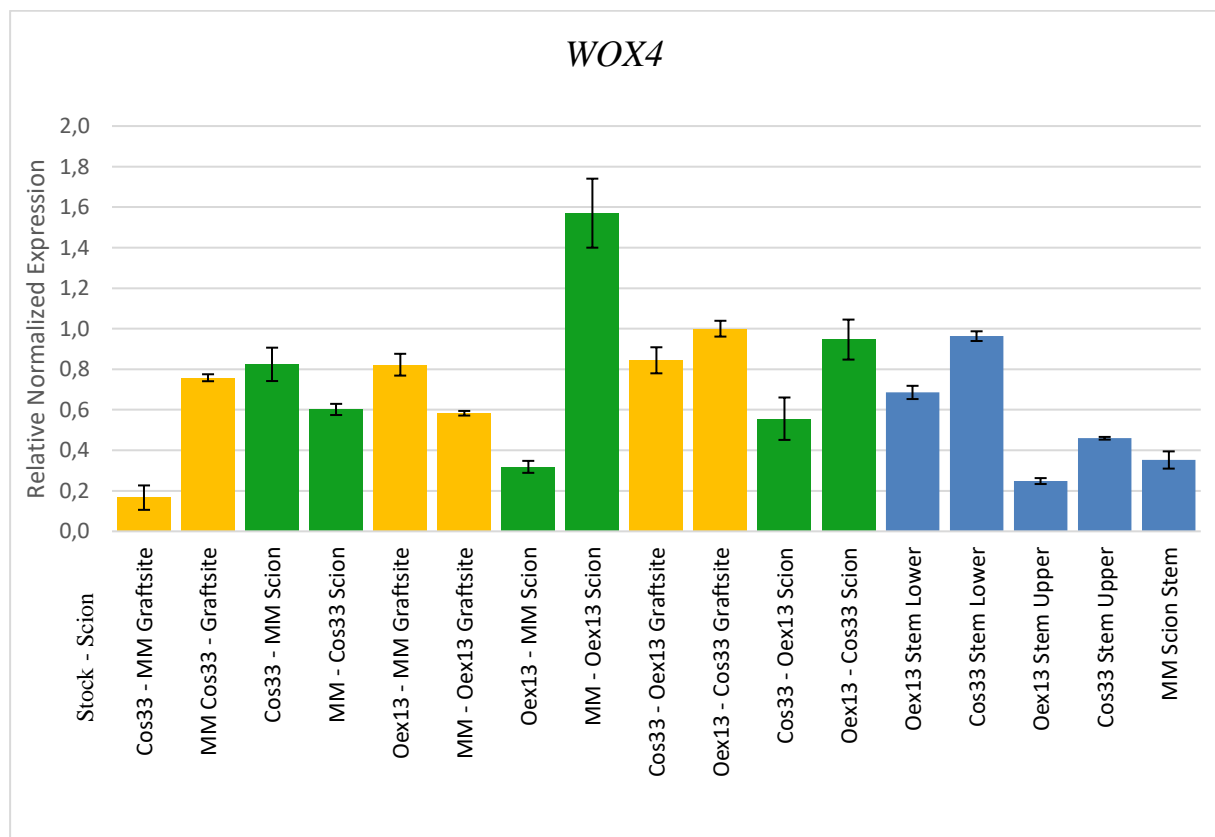


Figure 27 Relative gene expression of the cambium *WOX4* in sampled tissues. Relative normalized expression, relative to Oex13 – Cos33 Graft site = 1, normalization = $\Delta\Delta Cq$ of the target genes and reference genes GAPDH, EIF4a, and Actin. All graft sites in yellow, all Scion samples (sampled above the graft site) in green, and all un-grafted samples in blue. Error bars show standard deviation of the Cq values of the two technical replicates. Number of biological replicates was one.

4 Discussion

4.1 *S. pennellii*'s low graft success

S. pennellii was found to have a lower success rate for grafting compared to the cultivated tomato lines, especially when being the stock in the graft. Although, a more fitting grafting clip seemed to even out the differences, the wild tomato was more difficult to graft due its fragility. Additionally, the *S. pennellii* stock induced dwarfing when grafted with M82 (Krause *et al.*, 2018).

The overall graft success seemed to be somewhat linked to the grafting clip used, where a bigger clip which held the scion and stock tighter together than the first clip, greatly increased the success rate (Figure 12, Figure 13, Figure 15). This is in agreement with the theory that the two parts in a graft must have a tight physical contact (Pina and Errea, 2005; Crang, Lyons-Sobaski and Wise p.500, 2018). *S. pennellii* proved to be less successful, an issue observed in all *S. pennellii* graft combinations (MM, M82, Cos33 and Oex13), something that has been observed before in *S. pennellii* – *S. lycopersicum* M82 tube grafts (Krause *et al.*, 2018). While the specific reason(s) for the un-successful grafts with *S. pennellii* are unknown, one reason could be that the plant itself is fragile in comparison with *S. lycopersicum*. The wild type tomato has also been observed having poor root growth (Egea *et al.*, 2018), which could be one explanation for the dwarfing effect when grafted with M82 (Figure 14), and failure in general. This corroborates the knowledge that vigorous stocks do have an effect in grafts, and therefore the less vigorous stock of *S. pennellii* can negatively affect the graft (see subsections: Importance of grafting and Crop yield in the introduction). The average time for graft vascular development seems to be around a week after grafting, but sometimes more than that (Melnik, 2017). However, it has been observed to occur at around 15 days after grafting in *S. pennellii* autografts (Moore, 1984b), which acts as one possible explanation for the unsuccessfulness in the *S. pennellii* heterografts, as the *S. pennellii* rootstock simply was a too slow growing component of the chimeric plant. Due to its slow growth, the wild tomato was sown one week before the cultivated tomato lines, to compensate for stem diameter. Although, spite the one-week advantage, the wild tomato still might be too slow growing.

The dwarfing effect observed in all three biological replicates of the M82 – *S. pennellii* grafts (incl. reciprocal counterparts), as well as the scrappy leaf growth for the M82 scion, was the only observation of this characteristic among the measured plants that was strong enough to withstand a statistical test. As shown in Figure 14, the height difference between the

homografts ($M = 39.33$; $SD = 7.71$) and the heterografts grouped ($M = 38.22$; $SD = 9.04$), was insignificant $t = (0.22)$, $p = 0.42$. The dwarfing effect proved to be statistically significant $t = (5.56)$, $p = 0.015$, which further supports the impression that *S. pennellii* serves as a poor stock, as the wild tomato had a higher success when serving as a scion, than a stock.

4.2 Correlation between graft success and XET activity (or lack thereof)

According to the initial hypothesis, XET activity differences could potentially influence the graft success rate variations between *S. pennellii* and *S. lycopersicum*. However, from the XET assays done in this thesis there was no immediate indication that *S. pennellii* had weaker levels of XET activity, as compared to the other tomato lines. Fluorescence was observed in the cell walls of MM cortex and *S. pennellii* parenchyma-like cells along the graft interface of the scion and stock.

In Figure 19C, F, and I it is clearly shown that there is XET activity in the cell wall of *S. pennellii* parenchyma-like cells. The activity visible in the cell walls can be related to cell growth caused by wounding, as this would require loosening and tightening of the cell wall through XET activity. Such an activity would be expected as the pith cells in a cleft graft would be cells wounded during initial cutting of the plant tissue (the used technique, cleft graft, is illustrated Figure 1A).

In the graft union of the stock and scion in Figure 19F and I there also seems to be some connection between the MM cortex cells with the parenchymal-like cells of *S. pennellii*. A similar pattern can be seen between Oex13 and M82 (Supplemental XET activity images page X in the appendix), but in contrast, as Figure 19I shows, the cells of two different species interact and connect, something that could reveal important knowledge about how different plant tissues or even different plant species connect.

The XET activity between pith and cortex of the two grafts was not as clearly observed in the reciprocal graft to *S. pennellii* - MM (Figure 19 G - L). However, it is possible that the position of the cross-section in the vertical plane of graft junctions that were tested for XET activity can play a role here. The cross-sections could reveal more information based on the vertical location in the 3-dimensional graft site. This is a parameter that has not been tested rigorously in this thesis and is advised for potential future studies. What was observed in the reciprocal graft (MM – *S. pennellii*), was a high XET activity in the vascular bundle of the

stock (best visible in Figure 19 J and L), as well as intimate relations between the vascular tissue of both scion and stock, which is expected in a successful graft as the vascular tissue are, as specified in subchapter 1.1, an important growing factor in grafts. High fluorescence in the vascular regions was seen in several of the labeled samples (Figure 20 - Figure 23, (also Supplemental XET activity images p. X in the appendix)). However, to know if this activity was graft specific or induced by other factors cannot be concluded merely on the results in this thesis.

The fact that *S. pennellii* grafts showed little difference from the other tomato lines may indicate that XET activity alone does not control graft success, and that other factors that were not investigated here are relevant for the formation of the graft junction. For the other tomato lines grafted for the duration of this thesis, there was not enough data on graft success to correlate safely with XET activity. Thus, this same experiment should be repeated with non-successful grafts, and in homo- or autografts to be able to safer conclude on this matter. Additionally, gene expression analysis of *XTHs* in *S. pennellii* and M82 should be included, and possibly extended to other gene families, which due to time limitations was not done during this thesis.

4.3 XET activity in grafts compared to *Cuscuta*

It is known that parasitic plants, such as *Cuscuta* can penetrate host cells, and form interfamilial plasmodesmatal connections in its search through the host tissue for the vascular tissue (Heide-Jørgensen, 2008). This is, as explained in section 1.2.3, with stark similarities to grafting. The XET activity results from this thesis do draw some similarities to XET activity in the *Cuscuta*-host interface. Olsen and Krause (2017) found that XET activity was pronounced at the interface between *Cuscuta* and its host during the early phases of haustoriogenesis, a similarity to the XET activity at the graft union presented in this thesis. However Olsen and Krause (2017) also reported that the fluorescence from XET activity was not present in the later stages of haustoriogenesis. This is in contrast to the XET activity results in this thesis as the ~20-day old grafts analyzed would be considered well established-, or at least late stage -grafts which the author of this thesis would compare to fully developed haustorium time-wise, due to the established vascular connections. Since no experiments on transport through xylem or phloem was conducted for this thesis, the evaluation of vascular connection is merely based on the morphology observed during microscopy, which leaves

room for error. Regardless of this, the results provided in this thesis do provide an interesting finding of XET activity which should be further investigated alongside parasitic plants.

4.4 *SIXTH1* plays a minor role in grafting

The fluorescence shown in the XET activity assay (presented in subsection 3.2 in the results) showed little difference in the co-suppression line with regards to *SIXTH1* compared to the over-expresser and the other tomato lines (M82, MM, *S. pennellii*).

Figure 17 shows the longitudinal sections of representative samples of the different combinations, and as observed with the naked eye there seemed to be a higher level of fluorescence in the Oex13 tissue while Cos33 showed lower activity. However, after using the ImageJ Fiji software to measure pixel intensity, the difference between the two lines was, in fact, minor (data not shown). It is important to remember that the Oex13 and Cos33 lines only affect expression of the *SIXTH1* gene and that other *XTH* genes had the same expression as *S. lycopersicum* cv. MM (Figure 25A). The observation that the same pattern of fluorescence was shown between Cos33 – MM and Oex13 – Cos33 in Figure 17 could indicate only a minor role of *SIXTH1* in the graft union and may suggest that one of the other 24 tomato *XTHs* may rather be more important. Nevertheless, the results presented in this thesis are inadequate to answer this question. Cos33 also show little to no difference visually in level of fluorescence compared to the other tomato lines when grafted with M82 (Figure 22), further strengthening that *SIXTH1* may not be the only (or even the main) *XTH* present in the graft tissue, and that one or more additional *XTHs* perform XET activity. The same case was found at the parasite-host interface of tomato and *Cuscuta* (Olsen, 2017). The gene expression results showed that *SIXTH1* did have a higher fold change between samples than the two other *XTHs*, but many more *XTHs* remain to be tested.

Figure 25 shows that *SIXTH4* and *SIXTH12* have a different pattern of expression in the samples compared to *SIXTH1* in the Cos33 and Oex13 stem tissue. This indicates that *SIXTH4* and *SIXTH12* could play a slightly different role than *SIXTH1* in the graft sites analyzed, which strengthens the claim that other *XTHs* than *SIXTH1* (not necessarily *SIXTH4* and *SIXTH12*) are at play in the grafts. The same trend can be seen in the graft samples shown in Figure 26. There was also a clearly dominant level of expression in the Oex13 – Cos33 graft site sample for *SIXTH12* (Figure 26). This can be a possible explanation for why there still was a high level of fluorescence in the XET activity assay for the Cos33 line.

The gene expression data presented in this thesis are based on only one biological replicate and a statistical test would require at least three replicates, hence none of the expression data are statistically validated and serve only as an indication. To further investigate this matter, more tomato *XTHs* should be included in the gene expression analysis and the number of replicates should be increased. Knowing the amino acid sequence DEIDFEFLG being special for *XTHs* can be used to design a gene expression study with *XTHs* as targets, something that could support an *in vivo* XET activity assay like the one used in this thesis.

4.5 The effect of the Scion

It has been shown that there can be an asymmetry between stock and scion in contributing factors for graft success (Melnyk *et al.*, 2018). Therefore, investigating the role of the scion could reveal interesting information in the grafts.

Although the MM - Cos33 grafts (including reciprocal grafts) did seem to yield lower graft success rates than the other lines of tomatoes (Figure 13 and Figure 15), there was no apparent statistical difference between the combinations ($F=[5,54]=0.63$, $p=0.67$). The Cos33 line had a slightly shorter average height (Figure 14) in homografts compared to the other homografts, although the experiment should be redone with an increased number of replicates. These results, however, might be an indication that *SIXTH1* is influencing plant growth, as the Cos33 homograft was shorter than the MM homograft. Observations were made that Cos33 grafts yielded plants of less quality than the other grafts (personal observation), although they were graftable. In contrast, the Oex13 line did seem to grow taller before developing true leaves, which might be a result of the overexpression of *SIXTH1*, as *XTHs* has been shown to be involved in cell elongation processes (Vissenberg *et al.*, 2005).

Another interesting observation was that of adventitious rooting from the scion (Figure 11D). This seemed to occur most rapidly where the initial cut was in the hypocotyl region close to the cotyledons, such as the third set of grafts. For the first and second set of grafts some cuts were in the epicotyl region, which did not result in as much adventitious rooting, although for these two sets of grafts the sample size was only three biological replicates compared to the 10 replicates in the last set of grafts. Therefore, it is hard to conclude on the matter of adventitious rooting. Adventitious rooting from the scion can potentially lead to increased contact with soil pathogens (Lee *et al.*, 2010), and the adventitious rooting from scion can negatively affect the formation of the graft union (Turnbull, 2010), and even negatively affect the function and growth of the rootstock (Meyer *et al.*, 2017).

All the three *XTHs* seem to be more expressed in scion tissue than in graft tissue, with exception of *SIXTH1* and *SIXTH12* in the Oex13 - Cos33 graftsite sample (Figure 26). That the gene expression was higher in scion tissue might support the earlier claim that these three *XTHs* are not necessarily important for grafting, at least not at the time when the tissue was harvested (~20 Days after grafting (DAG)).

Further, Figure 26 shows that *SIXTH4* was expressed most when the MM and Oex13 lines serves as scions. Maybe these two scions could salvage the Cos33 stock. Previous research have shown that there can be an asymmetry in the scion and rootstock with regards to auxin (Melnik *et al.*, 2015), and this might be the case for *XTHs* as well, due to some *XTHs* being auxin regulated (Pitaksaringkarn *et al.*, 2014). Looking at the graft success presented in this thesis (Results, subsection 3.1) the possible effect of the scion on the stock show no clear connection however, and further experiments with the Cos33 line as a stock would be needed to conclude on this matter. A new study with more biological replicates, homografts controls, and the inclusion of stock tissue could shed more light in general on the effect of the scion in regard to *SIXTH1*, *SIXTH4* and *SIXTH12* and grafting. Including unsuccessful grafts to the analysis could reveal factors that influence the success and compatibility of grafting, which could be useful knowledge in the quest for the optimal graft union.

4.6 Increased gene expression in younger cells

Figure 25A shows that the transgenic lines express *SIXTH1* as expected, with Cos33 having little to no expression of *SIXTH1*, while Oex13 have a relative high expression as compared to Cos33. Unfortunately, there was no un-grafted control plant other than the Oex13 and Cos33 lines. In lack of such a proper control, MM Scion Stem was chosen as being closest to a proper control. The gene expression of *SIXTH1* in the MM scion stem tissue (Figure 34 in appendix p. X) was higher than in the Oex13 mutant. This could be due to the nature of the scion sample consisting of younger cells since the scion tissue for gene expression analysis was harvested several centimeters away from the graftsite (see Figure 10, sample harvested in the upper stem mark), closer to the apical shoot tip. These cells might go through increased levels of growth as compared to the well-established graft site. This would explain higher expression levels of *XTHs* due to loosening and tightening of the cell walls. There was a relative high expression in the upper stem tissue compared to lower stem tissue of both Cos33 and Oex13 for all three *XTHs* which further supports this claim. Additionally, this

corroborates with the theory of XTHs and cell walls in relation with cell growth (Scheller and Ulvskov, 2010; Höfte and Voxeur, 2017).

As mentioned in subchapter 4.5, the scion tissue had a higher expression than the graft tissue, an asymmetry that might be explained by the younger tissue in the scions, although, as the experimental design of this thesis did not focus on cell age and gene expression, this matter cannot be safely concluded on. With inclusion of the gene expression in the stock tissue, the difference in gene expression between stock, graftsite and scion could be better investigated. This was not done in this thesis due to the nature of the stock tissue below the graft junction being mostly covered with soil. A micrograft setup as the one described by Melnyk *et al.* (2015) would be ideal for this purpose and could reveal interesting knowledge on this matter.

4.7 XET activity in specific to the graft union

A trend indicating high XET activity at the graft interface was observed for all samples. This points towards XET being important for the formation of grafts. Figure 23 shows a distinct line of fluorescence at the graft site, and similar patterns can clearly be seen in Figure 20 J - R, Figure 21, and Cos33 – M82 grafts shown in Figure 22. While displaying high fluorescence at the graft union, the longitudinal samples (Figure 17 and Figure 20) also show high levels of fluorescence along the xylem vessels from the graft union and along into the scion and stock tissue. This is an indication that the XET activity was not just located at the graft union, but also works along the vascular tissue in the close proximity of the graft union, which is in conjunction with XET activity being involved in cell growth and cell wall adjustments (Fry *et al.*, 1992; Miedes *et al.*, 2011) as these regions are likely to undergo growth after grafting, as well as ordinary secondary growth in older well established grafts. With that said, this activity can be non-graft related, as the plants were around 20 DAG when the enzyme activity assay was done. Samples with lower DAGs should be investigated to reveal the dynamics of XTH activity at graft sites over time as interesting findings could be in the past.

The M82 grafts were 15 DAG when the activity assay was done, while still showing similar levels of XET activity compared with the ~20 DAG samples, spite being different genotypes, indicating there is a little difference in XET activity with a five-day difference. Although, XET activity over time was not a focus in this thesis and should be considered monitored in future studies to assess XET activity over time in grafting.

Wound responses could be interfering with the XET activity in the graft site, thus, the observed activity might not be graft specific. Analyzing the stock and scion sections (Figure 16), the XET activity remained more or less the same in the entire section, which is in contrast to the patchy fluorescence of the graft sites (Figure 18). However, drawing conclusions based on this should be done with care as there are no wounded un-grafted control plants

4.8 Relevance of cambium in grafts

Cambium regeneration is an important factor for graft success, as explained in subsection 1.1. From Figure 27 one can see that there was an increased level of expression in all graft sites as compared with the un-grafted Cos33 and Oex13 plants which makes sense due to graft sites being tissue growing together, especially the vascular regions (Cambium). Although, the scion samples show little difference in expression compared to the graft sites, which might indicate that *WOX4* is not important at this stage in the grafts. The two technical replicates used for the gene expression analysis is based on the same biological replicate however, and if this data proves to be statistically significant remains untested.

4.9 Choice of methods

The vibratome is a great tool for sectioning live tissue in plants. However, the use of a vibrating blade on the fragile grafts proved to be a disadvantage. Even though the blade itself was exchanged frequently to avoid dullness, the retrieval of intact sections proved difficult, as seen in most microscopy pictures in the results. Since fixation and embedding would abolish the XTH activity, hand sectioning with a micro dissection knife, which has been used for graft samples earlier and with great success (Melnyk *et al.*, 2015), should be considered before future studies are performed.

The plants used for the experiments in this thesis were 15-20 DAG, which was a late stage to investigate the graft union. Previous studies have been performed with micro-propagated plants, and micro-grafted plants *in vitro* (Pina, Errea and Martens, 2012; Melnyk *et al.*, 2018). This was attempted as a side project during the duration of this thesis (data not shown), which unfortunately was un-successful due to problematics with contamination and the grafting procedure itself. Future analyses should be done with the awareness that early events are not captured with the approach described in this thesis.

4.10 Conclusion

XET activity was shown with fluorescence microscopy to be located at the graft union in the interface between scion and stock, and in cells with a close proximity to the graft union. This was the case in plants 15-20DAG, in the four different genotypes of cultivated tomato: M82, MM, Cos33, Oex13, as well as *Solanum pennellii*. Further evidence could not be statistically proven significant due to lack of biological replicates, and no specific pattern in gene expression for *SIXTH1*, *SIXTH4*, and *SIXTH12* can be concluded in relation to grafting. While the data presented in this thesis are considered preliminary, XTH activity do seem to play a role in grafting, providing more common ground for the graft-parasite connection.

4.11 Outlook

In this study, XET activity was observed in ~20 DAG samples. Implementing the same assay in micro-grafts could reveal the potential role of XET at the early stages in graft development, results on which (by the knowledge of the author) has not been published earlier. Using a micro-graft setup would also make microscopy of the graftsite easier as the micro-grafts can be directly placed under the microscope. Using micro-grafts for the XET assay may provide difficulties in sectioning, although hand sectioning with a sharp microdissection knife should be a viable method. In addition to the XET assay, gene expression analysis of more *XTHs* should be considered, as only three of the 25 known tomato *XTHs* were analyzed in this thesis. This could either be done with gene specific primers for each *XTH* of interest, or by widening the target with more general primers for *XTHs*, for example targeting the DEIDFEFLG sequence common for *XTHs*.

Studying the graft interface and XET activity at different timepoints could also reveal useful information about XET activity throughout the development of grafts. Including homografts, un-grafted plants, wounded plants, and incompatible grafts would cover all needs for controls, and give a good view on the graft specificity of XET.

5 References

- Albert, M. *et al.* (2008) ‘Cuscuta spp: “Parasitic Plants in the Spotlight of Plant Physiology, Economy and Ecology”’, *Progress in Botany*, 69(January), pp. 267–277. doi: 10.1007/978-3-540-72954-9_11.
- Asante, A. K. and Barnett, J. R. (1997) ‘Graft union formation in mango (*Mangifera indica* L.)’, *Journal of Horticultural Science*, 72(5), pp. 781–790. doi: 10.1080/14620316.1997.11515571.
- Catala, C. *et al.* (2001) ‘Characterization of a tomato xyloglucan endotransglycosylase gene that is down-regulated by auxin in etiolated hypocotyls’, *Plant Physiology*, 127(3), pp. 1180–1192. doi: 10.1104/pp.010481.
- Chen, S., Chiu, Y. C. and Chang, Y. C. (2010) ‘Development of a Tubing-Grafting robotic system for fruit-bearing vegetable seedlings’, *Applied Engineering in Agriculture*, 26(4), pp. 707–714.
- Cosgrove, D. J. (2005) ‘Growth of the plant cell wall’, *Nature Reviews Molecular Cell Biology*, 6(11), pp. 850–861. doi: 10.1038/nrm1746.
- Crang, R., Lyons-Sobaski, S. and Wise, R. (2018) *Plant Anatomy A Concept-Based Approach to the Structure of Seed Plants*, Springer Nature. Cham, Switzerland: Springer Nature. doi: 10.1038/278100b0.
- Egea, I. *et al.* (2018) ‘The drought-tolerant *Solanum pennellii* regulates leaf water loss and induces genes involved in amino acid and ethylene/jasmonate metabolism under dehydration’, *Scientific Reports*, 8(2791), pp. 1–14. doi: 10.1038/s41598-018-21187-2.
- Eklöf, J. M. and Brumer, H. (2010) ‘The XTH gene family: An update on enzyme structure, function, and phylogeny in xyloglucan remodeling’, *Plant Physiology*, 153(2), pp. 456–466. doi: 10.1104/pp.110.156844.
- Estañ, M. T. *et al.* (2004) ‘Grafting raises the salt tolerance of tomato through limiting the transport of sodium and chloride to the shoot’, *Journal of Experimental Botany*, 56(412), pp. 703–712. doi: 10.1093/jxb/eri027.

Francescato, P. *et al.* (2010) 'Evaluation of Graft Compatibility between Quince Rootstocks and Pear Scions', *Acta Horticulturae*, 872, pp. 253–260. doi: 10.17660/ActaHortic.2010.872.34.

Fry, S. C. *et al.* (1992) 'Xyloglucan endotransglycosylase, a new wall-loosening enzyme activity from plants', *Biochemical Journal*, 282(3), pp. 821–828. doi: 10.1042/bj2820821.

Gale, G. D. J. (2011) *Dying on the Vine : How Phylloxera Transformed Wine*. 1st edn. Berkeley: University of California Press. Available at: <http://ebookcentral.proquest.com/lib/tromsoub-ebooks/detail.action?docID=692424>.

Granett, J. *et al.* (2001) 'Biology and Management of Grape Phylloxera', *Annual Reviews of Entomology*, 46, pp. 387–412. doi: 10.1146/annurev.ento.46.1.387.

Gulen, H. *et al.* (2002) 'Peroxidase Isozyme Profiles in Compatible and Incompatible Pear–Quince Graft Combinations', *Journal of the American Society for Horticultural Science*, 127(2), pp. 152–157. doi: 10.21273/jashs.127.2.152.

Heide-Jørgensen, H. S. (2008) *Parasitic Flowering Plants*. 1st edn. Boston: BRILL. Available at: <https://ebookcentral.proquest.com/lib/tromsoub-ebooks/detail.action?docID=593748>.

Höfte, H. and Voxeur, A. (2017) 'Plant cell walls', *Current Biology*. Elsevier, 27(17), pp. 865–870. doi: 10.1016/j.cub.2017.05.025.

Jeffree, C. E. and Yeoman, M. M. (1983) 'Development of intercellular connections between opposing cells in a graft union', *The New Phytologist*, 93(4), pp. 491–509. doi: 10.1111/j.1469-8137.1983.tb02701.x.

Juniper, B. E. and Mabberley, D. J. (2006) 'The story of the apple', in *The Story of the Apple*. Portland, OR: Timber press, pp. 91–114.

Koka, C. V. *et al.* (2000) 'A Putative Role for the Tomato Genes DUMPY and CURL-3 in Brassinosteroid Biosynthesis and Response', *Plant Physiology*, 122(1), pp. 85–98. doi: 10.1104/pp.122.1.85.

Kollmann, R. and Glockmann, C. (1985) 'Studies on graft unions. I. Plasmodesmata between cells of plants belonging to different unrelated taxa', *Protoplasma*, 124(3), pp. 224–235. doi: 10.1007/BF01290774.

Kollmann, R. and Glockmann, C. (1991) 'Studies on graft unions - III. On the mechanism of secondary formation of plasmodesmata at the graft interface', *Protoplasma*, 165(1–3), pp. 71–85. doi: 10.1007/BF01322278.

Krause, K. *et al.* (2018) 'Identification of tomato introgression lines with enhanced susceptibility or resistance to infection by parasitic giant dodder (*Cuscuta reflexa*)', *Physiologia Plantarum*, 162(2), pp. 205–218. doi: 10.1111/ppl.12660.

Lee, J.-M. (1994) 'Cultivation of grafted vegetables. I. Current status, grafting methods, and benefits', *HortScience*, 29(4), pp. 235–239. doi: 10.21273/HORTSCI.29.4.235.

Lee, J.-M. and Oda, M. (2003) 'Grafting of Herbaceous Vegetable and Ornamental Crops', *Horticultural Reviews*, 28, pp. 61–124. doi: 10.1002/9780470650851.ch2.

Lee, J. M. *et al.* (2010) 'Current status of vegetable grafting: Diffusion, grafting techniques, automation', *Scientia Horticulturae*. Elsevier B.V., 127(2), pp. 93–105. doi: 10.1016/j.scienta.2010.08.003.

Martinez-Rodriguez, M. M. *et al.* (2008) 'The effectiveness of grafting to improve salt tolerance in tomato when an "excluder" genotype is used as scion', *Environmental and Experimental Botany*, 63(1–3), pp. 392–401. doi: 10.1016/j.envexpbot.2007.12.007.

Melnyk, C. W. *et al.* (2015) 'A developmental framework for graft formation and vascular reconnection in *Arabidopsis thaliana*', *Current Biology*. Elsevier Ltd, 25(10), pp. 1306–1318. doi: 10.1016/j.cub.2015.03.032.

Melnyk, C. W. (2016) 'Connecting the plant vasculature to friend or foe', *New Phytologist*, 213(4), pp. 1611–1617. doi: 10.1111/nph.14218.

Melnyk, C. W. (2017) 'Plant grafting: insights into tissue regeneration', *Regeneration*, 4(1), pp. 3–14. doi: 10.1002/reg2.71.

- Melnyk, C. W. *et al.* (2018) 'Transcriptome dynamics at Arabidopsis graft junctions reveal an intertissue recognition mechanism that activates vascular regeneration', *Proceedings of the National Academy of Sciences of the United States of America*, 115(10), pp. E2447–E2456. doi: 10.1073/pnas.1718263115.
- Melnyk, C. W. and Meyerowitz, E. M. (2015) 'Plant grafting', *Current Biology*. Elsevier, pp. R183–R188. doi: 10.1016/j.cub.2015.01.029.
- Meyer, L. J. *et al.* (2017) 'Leaf removal reduces scion adventitious root formation and plant growth of grafted tomato', *Scientia Horticulturae*. Elsevier B.V., 214(January), pp. 147–157. doi: 10.1016/j.scienta.2016.11.019.
- Miedes, E. *et al.* (2011) 'Xyloglucan endotransglucosylase and cell wall extensibility', *Journal of Plant Physiology*. Elsevier GmbH., 168(3), pp. 196–203. doi: 10.1016/j.jplph.2010.06.029.
- Moore, R. (1984a) 'A Model for Graft Compatibility-Incompatibility in Higher Plants', *American Journal of Botany*, 71(5), pp. 752–758. doi: 10.2307/2443372.
- Moore, R. (1984b) 'Graft formation in *Solanum pennellii* (Solanaceae)', *Plant Cell Reports*, 3(5), pp. 172–175. doi: 10.1007/BF00270192.
- Moore, R. (1986) 'Graft Incompatibility between Pear and Quince: The Influence of Metabolites of *Cydonia oblonga* on Suspension Cultures of *Pyrus communis*', *American Journal of Botany*, 73(1), pp. 1–4. doi: 10.2307/2444270.
- Mudge, K. *et al.* (2009) 'A History of Grafting', in Janick, J. (ed.) *Horticultural Reviews*, pp. 437–493. doi: 10.1002/9780470593776.ch9.
- Munns, R. (2005) 'Genes and salt tolerance: bringing them together', *New Phytologist*, 167(3), pp. 645–663. doi: 10.1111/j.1469-8137.2005.01487.x.
- Nanda, A. K. and Melnyk, C. W. (2018) 'The role of plant hormones during grafting', *Journal of Plant Research*. Springer Japan, 131(1), pp. 49–58. doi: 10.1007/s10265-017-0994-5.

- Olsen, S. *et al.* (2016) ‘Getting ready for host invasion: Elevated expression and action of xyloglucan endotransglucosylases/hydrolases in developing haustoria of the holoparasitic angiosperm *Cuscuta*’, *Journal of Experimental Botany*, 67(3), pp. 695–708. doi: 10.1093/jxb/erv482.
- Olsen, S. (2017) *Mechanisms of Host Plant Infection by the Parasitic Angiosperm Cuscuta*. University of Tromsø. Available at: <https://hdl.handle.net/10037/10958>.
- Olsen, S. and Krause, K. (2017) ‘Activity of xyloglucan endotransglucosylases/hydrolases suggests a role during host invasion by the parasitic plant *Cuscuta reflexa*’, *PLoS ONE*, 12(4), p. e0176754. doi: 10.1371/journal.pone.0176754.
- Olsen, S., Popper, Z. A. and Krause, K. (2016) ‘Two sides of the same coin: Xyloglucan endotransglucosylases/hydrolases in host infection by the parasitic plant *Cuscuta*’, *Plant signaling & behavior*. Taylor & Francis, 11(3), p. e1145336. doi: 10.1080/15592324.2016.1145336.
- Park, J. *et al.* (2017) ‘Plant hormone transporters: What we know and what we would like to know’, *BMC Biology*. BMC Biology, 15(93), pp. 1–15. doi: 10.1186/s12915-017-0443-x.
- Pauly, M. *et al.* (1999) ‘Molecular domains of the cellulose/xyloglucan network in the cell walls of higher plants’, *The Plant Journal*, 20(6), pp. 629–639. doi: 10.1046/j.1365-313X.1999.00630.x.
- Pessarkli, M. and Szabolcs, I. (1999) ‘Soil Salinity and Sodicity as Particular Plant/Crop Stress Factors’, in Mohammad Pessarakli (ed.) *Handbook of Plant and Crop Stress*. 2nd edn. Marcel Dekker, inc., pp. 1–16. doi: 10.1201/9780824746728.ch10.
- Pina, A. and Errea, P. (2005) ‘A review of new advances in mechanism of graft compatibility-incompatibility’, *Scientia Horticulturae*, 106(1), pp. 1–11. doi: 10.1016/j.scienta.2005.04.003.
- Pina, A., Errea, P. and Martens, H. J. (2012) ‘Graft union formation and cell-to-cell communication via plasmodesmata in compatible and incompatible stem unions of *Prunus* spp.’, *Scientia Horticulturae*. Elsevier B.V., 143, pp. 144–150. doi: 10.1016/j.scienta.2012.06.017.

Pitaksaringkarn, W. *et al.* (2014) 'XTH20 and XTH19 regulated by ANAC071 under auxin flow are involved in cell proliferation in incised Arabidopsis inflorescence stems', *The Plant Journal*, 80(4), pp. 604–614. doi: 10.1111/tpj.12654.

Rivero, R., Ruiz, J. and Romero, L. (2003) 'Role of grafting in horticultural plants under stress conditions', *Journal of Food, Agriculture & Environment*, 1(1), pp. 70–74.

Rose, J. K. C. *et al.* (2002) 'The XTH Family of Enzymes Involved in Xyloglucan Endotransglucosylation and Endohydrolysis: Current Perspectives and a New Unifying Nomenclature', *Plant and Cell Physiology*, 43(12), pp. 1421–1435. doi: 10.1093/pcp/pcf171.

Ruiz, J. M. *et al.* (1997) 'Leaf-macronutrient content and yield in grafted, melon plants. A model to evaluate the influence of rootstock genotype', *Scientia Horticulturae*, 71(3–4), pp. 227–234. doi: 10.1016/S0304-4238(97)00106-4.

Saladié, M. *et al.* (2006) 'Characterization of a new xyloglucan endotransglucosylase/hydrolase (XTH) from ripening tomato fruit and implications for the diverse modes of enzymic action', *Plant Journal*, 47(2), pp. 282–295. doi: 10.1111/j.1365-313X.2006.02784.x.

Scheller, H. V. and Ulvskov, P. (2010) 'Hemicelluloses', *Annual Review of Plant Biology*, 61(1), pp. 263–289. doi: 10.1146/annurev-arplant-042809-112315.

Schneider, J. H. M., S'Jacob, J. J. and van de Pol, P. A. (1995) 'Rosa multiflora "Ludiek", a rootstock with resistant features to the root lesion nematode *Pratylenchus vulnus*', *Scientia Horticulturae*, 63(1–2), pp. 37–45. doi: 10.1016/0304-4238(95)00794-T.

Solanke, A. U. *et al.* (2009) 'Characterization and phylogenetic analysis of environmental stress-responsive SAP gene family encoding A20/AN1 zinc finger proteins in tomato', *Molecular Genetics and Genomics*, 282(2), pp. 153–164. doi: 10.1007/s00438-009-0455-5.

Suchoff, D. H., Louws, F. J. and Gunter, C. C. (2019) 'Yield and Disease Resistance for Three Bacterial Wilt-resistant Tomato Rootstocks', *HortTechnology*, 29(3), pp. 330–337. doi: 10.21273/HORTTECH04318-19.

Suzuki, H. *et al.* (2012) 'Effects of Elevated Peroxidase Levels and Corn Earworm Feeding on Gene Expression in Tomato', *Journal of Chemical Ecology*, 38(10), pp. 1247–1263. doi: 10.1007/s10886-012-0205-8.

Turnbull, C. G. N. (2010) 'Grafting as a Research Tool. Methods in molecular biology (Clifton, N.J.)', *Plant Developmental Biology*. Humana Press, Totowa, NJ, 655(June 2010), pp. 11–26. doi: 10.1007/978-1-60761-765-5.

Vissenberg, K. *et al.* (2000) 'In Vivo Colocalization of Xyloglucan Endotransglycosylase Activity and Its Donor Substrate in the Elongation Zone of Arabidopsis Roots', *The Plant Cell*, 12(7), pp. 1229–1237. doi: 10.1105/tpc.12.7.1229.

Vissenberg, K. *et al.* (2005) 'XTH acts at the microfibril-matrix interface during cell elongation', *Journal of Experimental Botany*, 56(412), pp. 673–683. doi: 10.1093/jxb/eri048.

Zarrouk, O. *et al.* (2010) 'Changes in Cell/Tissue Organization and Peroxidase Activity as Markers for Early Detection of Graft Incompatibility in Peach/Plum Combinations', *Journal of the American Society for Horticultural Science*, 135(1), pp. 9–17. doi: 10.21273/jashs.135.1.9.

Appendix

Grafting

Grafting clips

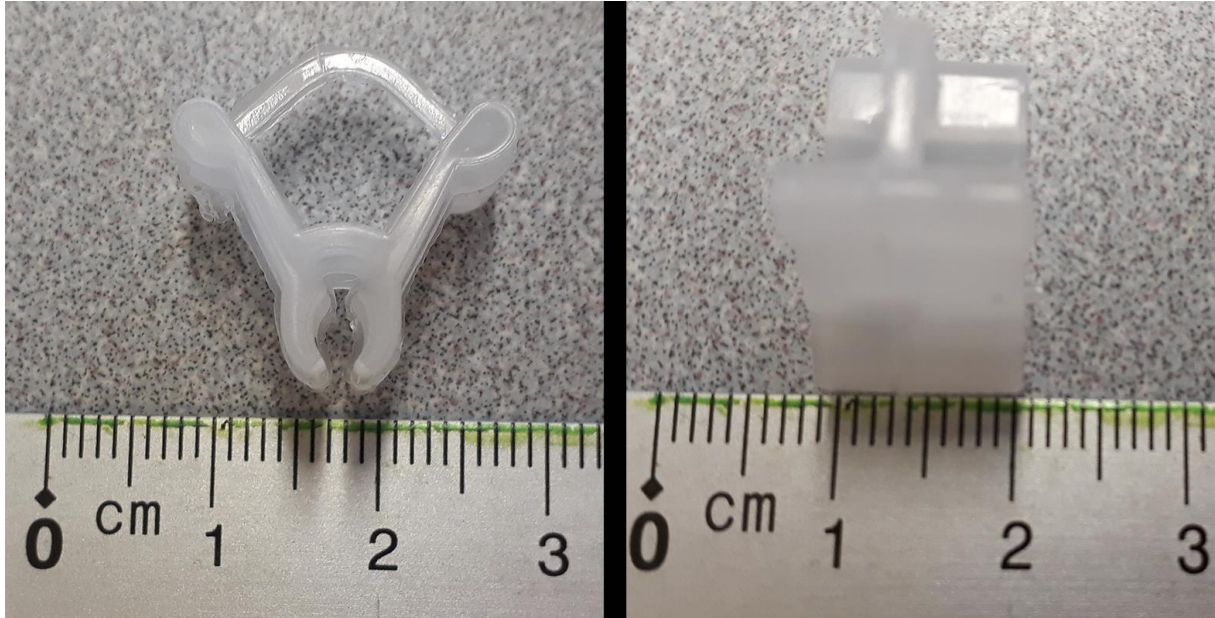


Figure 28 Grafting clips used for the first set of grafts. This was later changed out with new ones due to low graft success as a result of the clip not holding the plants together properly.

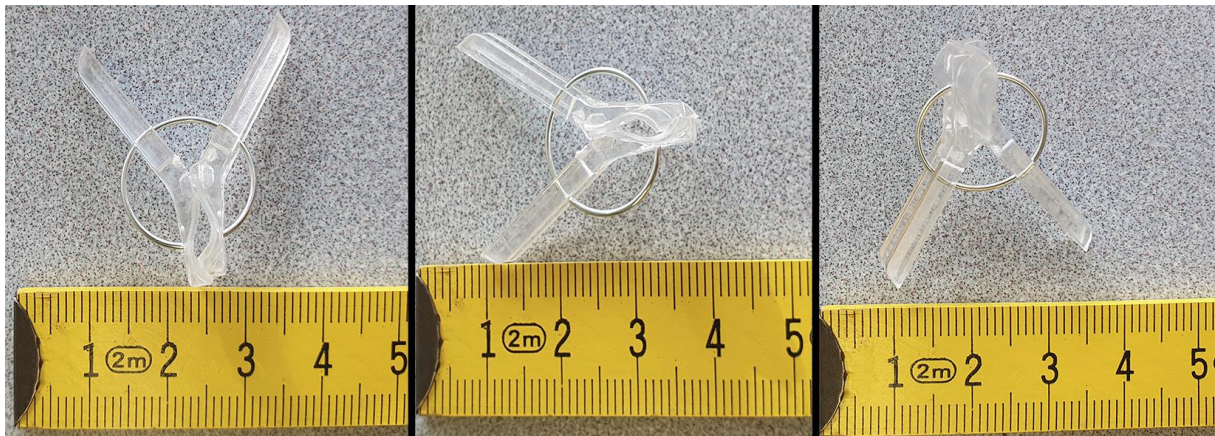
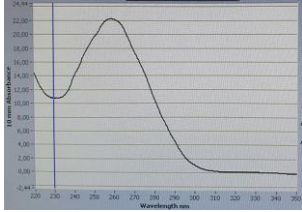
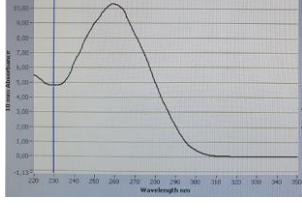
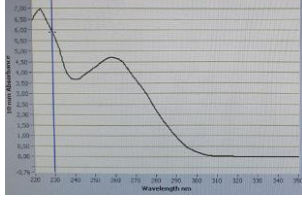
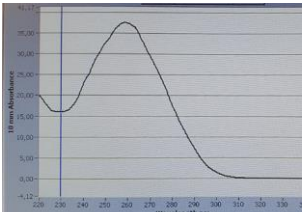
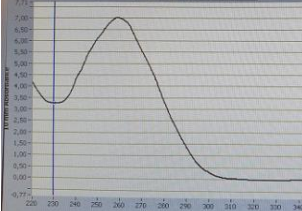
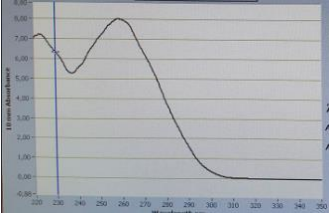
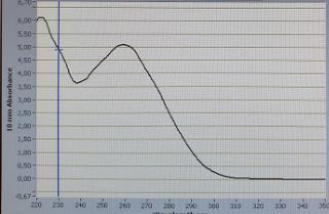
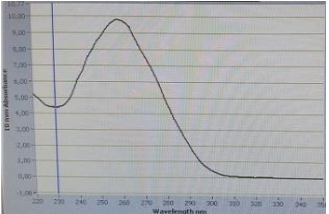

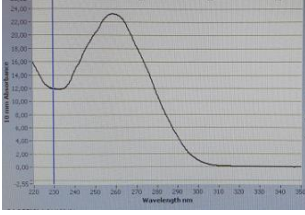
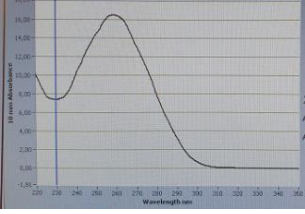
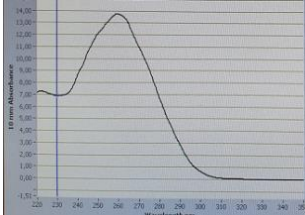


Figure 29 The grafting clips used for all but the first set of grafts. These clips were bigger than the previous and yielded easier and more successful grafts. All scales are in centimeters.

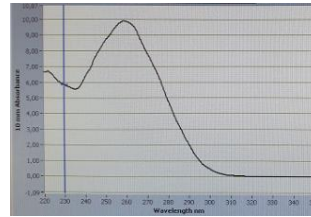
NanoDrop measurements

Tabell 1 NanoDrop 1000 spectrophotometry OD 260 – 280, and an illustration of the spectrophotometry curve showing absorption between 220 – 350 nm.

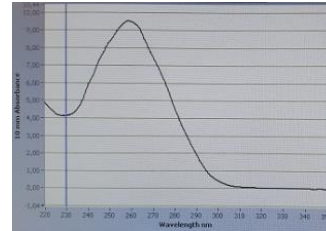
sample	OD 260/23	OD 260/280	ng/ μ l	Illustration of the spectrophotometry curve
MM Scion Leaf	2.05	2.13	884.5	
MM Scion Stem	2.14	2.11	410.3	
Oex13 MM Scion	0.79	2.11	186.8	
Oex13 Leaf	2.3	2.14	954.3	
Cos33 Leaf	2.33	2.15	1491.8	
Cos MM Scion	2.14	2.12	279.1	

Cos33 Oex13 Scion	1.26	2.12	318.5	
MM Oex13 Scion	1.03	2.07	202.2	
Oex13 Cos33 Graftsite	2.22	2.1	389.9	
Oex13 Cos33 Scion	2.27	2.11	344.4	
Cos33 Stem Upper	1.94	2.15	924.8	
Cos33 MM Graftsite	2.21	2.16	655.4	
Cos33 Stem Lower	1.98	2.09	547.8	

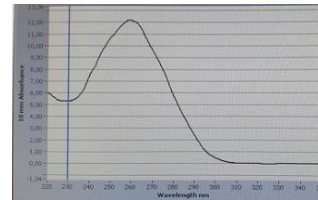
Oex13 Stem Upper 1.69 2.11 393.5



MM Cos33 Graftsite 2.29 2.11 378.1

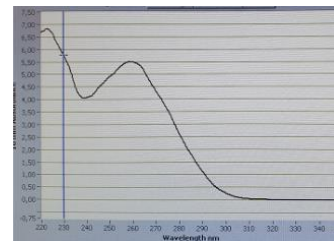


Oex13 MM Graftsite 2.29 2.14 484.6

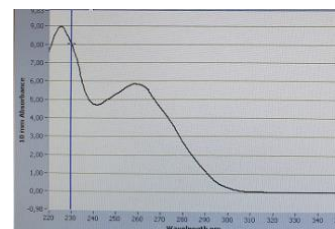


MM Oex13 graftsite 2.25 2.08 587.4

MM Cos33 Scion 0.95 2.11 219.2



Cos33 Oex13 Graftsite 0.73 2.14 232.4

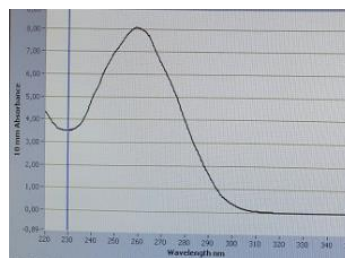


**Oex13 Stem
Lower**

2.28

2.1

320.3

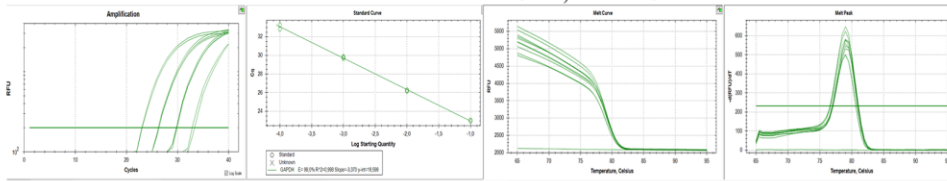


Primer melt data and standard curves from qPCR

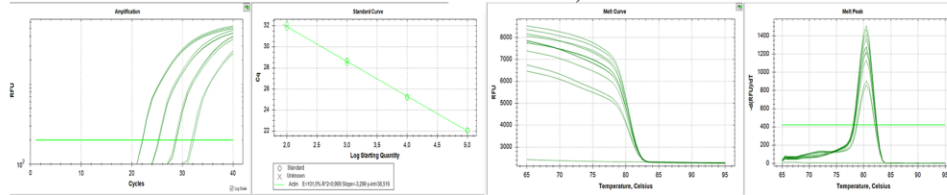
Amplification and standard curve

Melt curve and peak

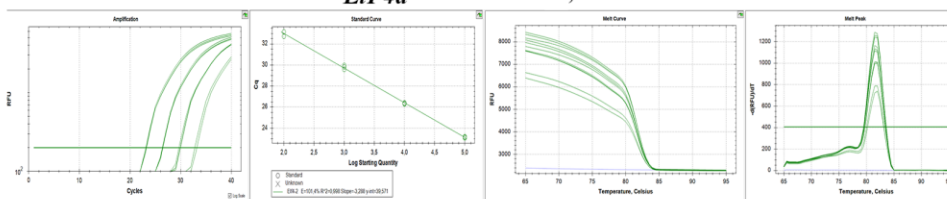
***GAPDH* E = 98.0%, R² = 0.998**



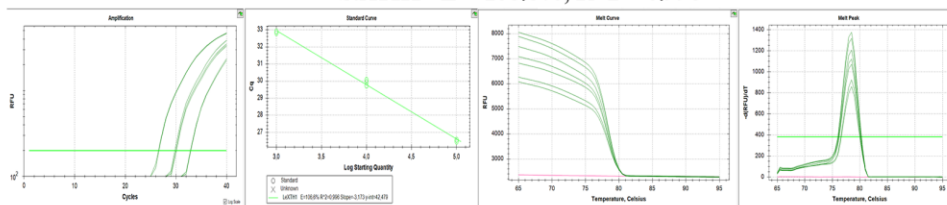
***Actin* E = 101.0%, R² = 0.999**



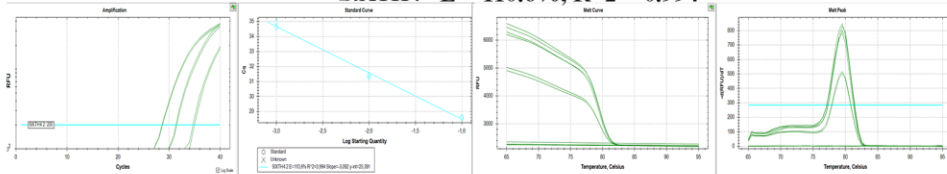
***EIF4a* E = 101.4%, R² = 0.998**



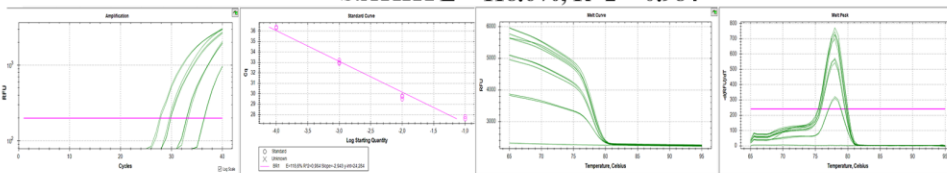
***SIXTH1* E = 106.6%, R² = 0.996**



***SIXTH4* E = 110.6%, R² = 0.994**



***SIXTH12E* E = 118.6%, R² = 0.984**



***WOX4* E = 102.3%, R² = 0.995**

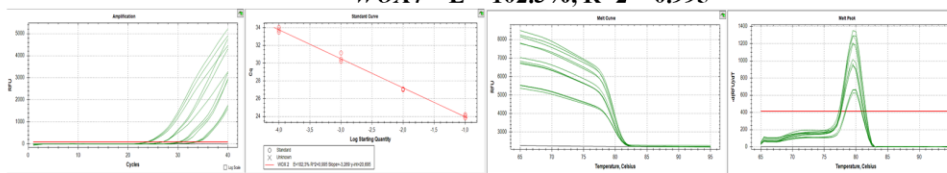


Figure 30 Left, Standard curves for all genes. Right, melt curves and melt peaks for all tested genes. No unwanted amplicons appeared on the melt curves / peaks.

qPCR product amplification and melt data

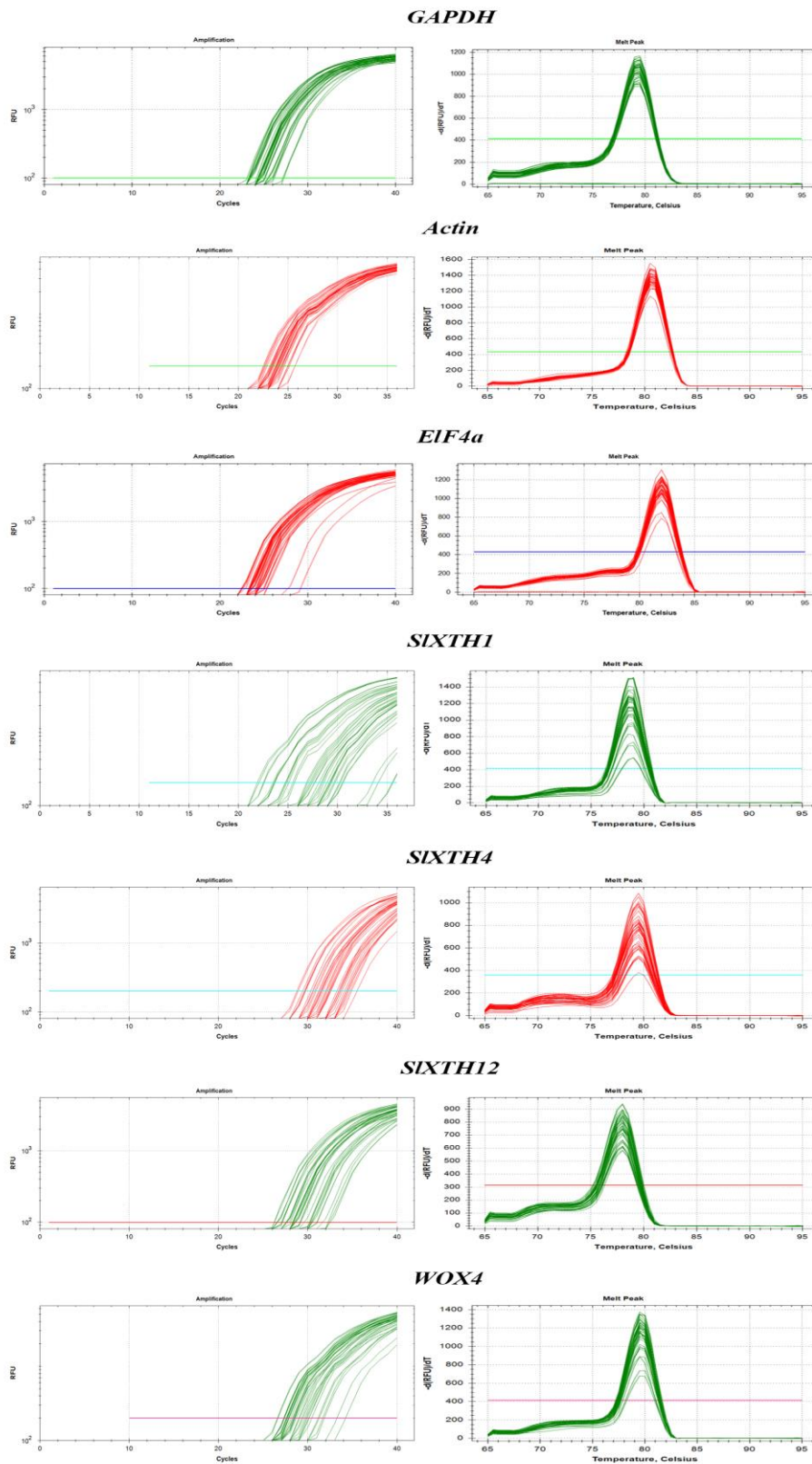


Figure 31 qPCR product amplification curves and melt peaks. Amplification curves shows that most of the sample duplicates amplified at the same time. From the melt peak there seem to be no unwanted amplicons in the mix due to no early peaks on the curve.

Gel electrophoresis

DNase treated RNA

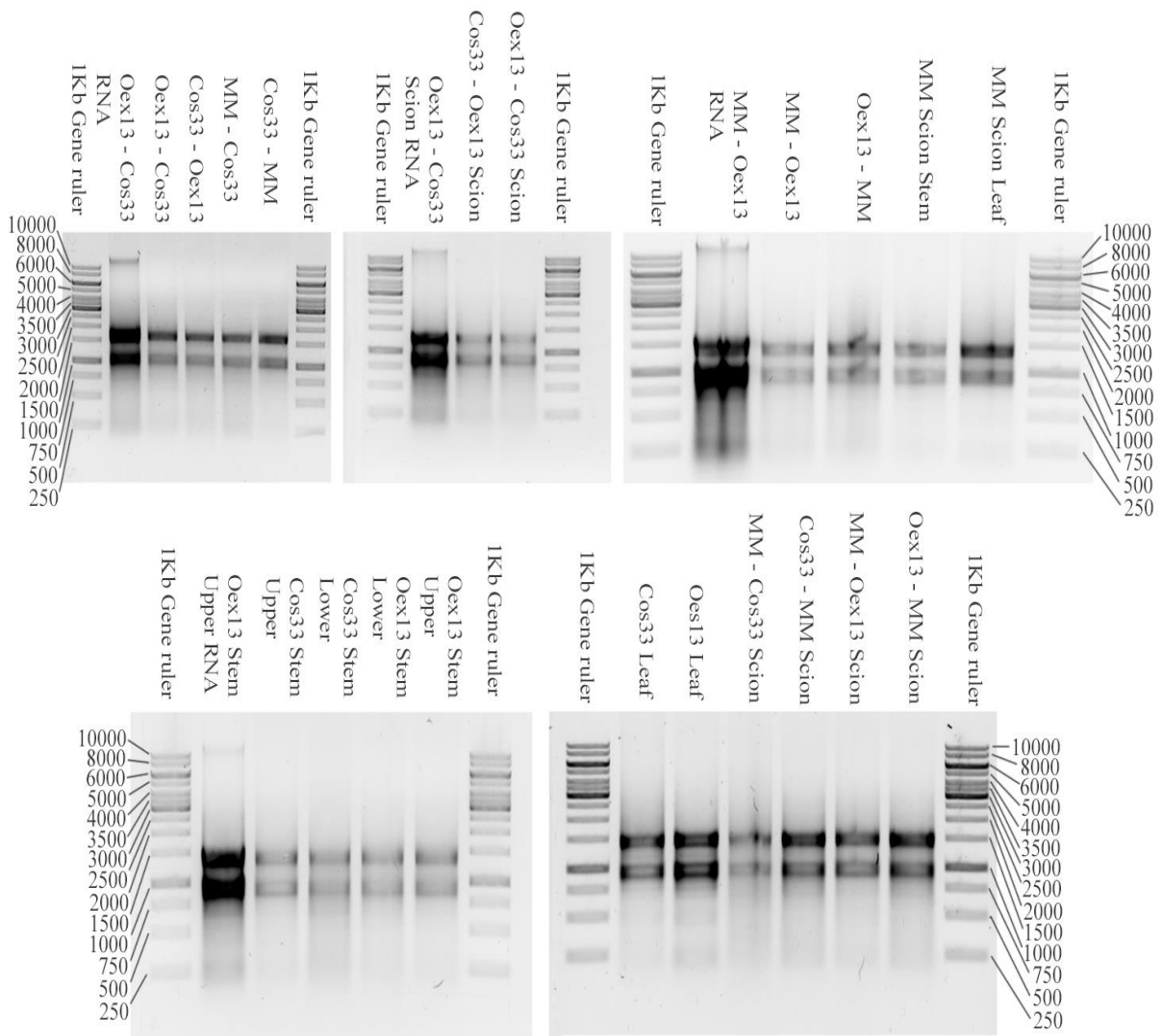


Figure 32 Gel-electrophoresis from DNase treatments. Samples named RNA are samples that have not been treated with DNase and serves as controls to see the difference in the treated samples and untreated samples, and to make sure all DNA and DNase enzyme was removed from the samples. All other samples are treated with DNase as described in the DNase treatment section in methods at p. 20. 1kb Gene Ruler as ladder, displayed on the sides of the gels. Numbers indicate base pairs

PCR products

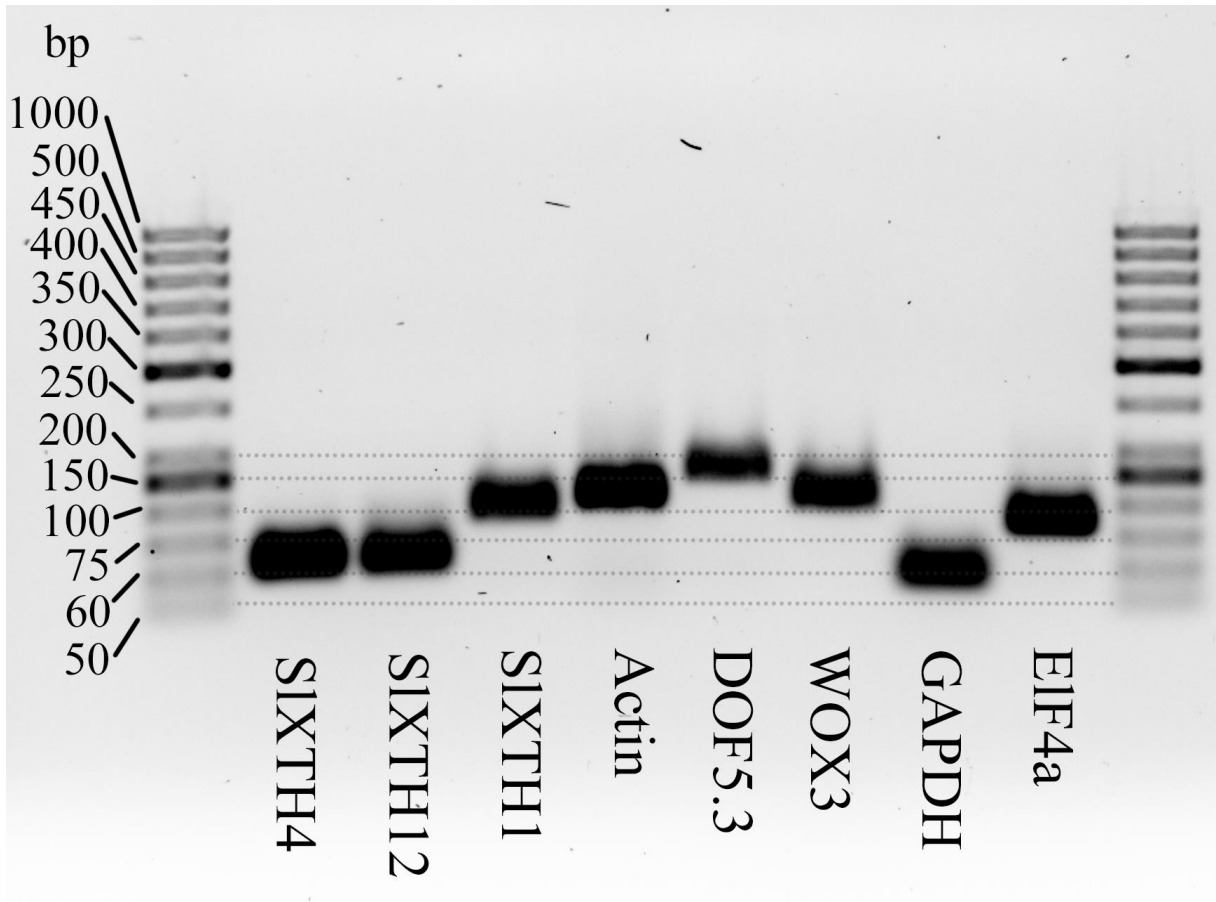


Figure 33 Gel-electrophoresis run of the PCR products after RT-qPCR. The ladder is displayed on the left (Gene Ruler 50bp). Ladder numbers indicate number base pairs (bp).

Gene expression included Moneymaker Scion Stem

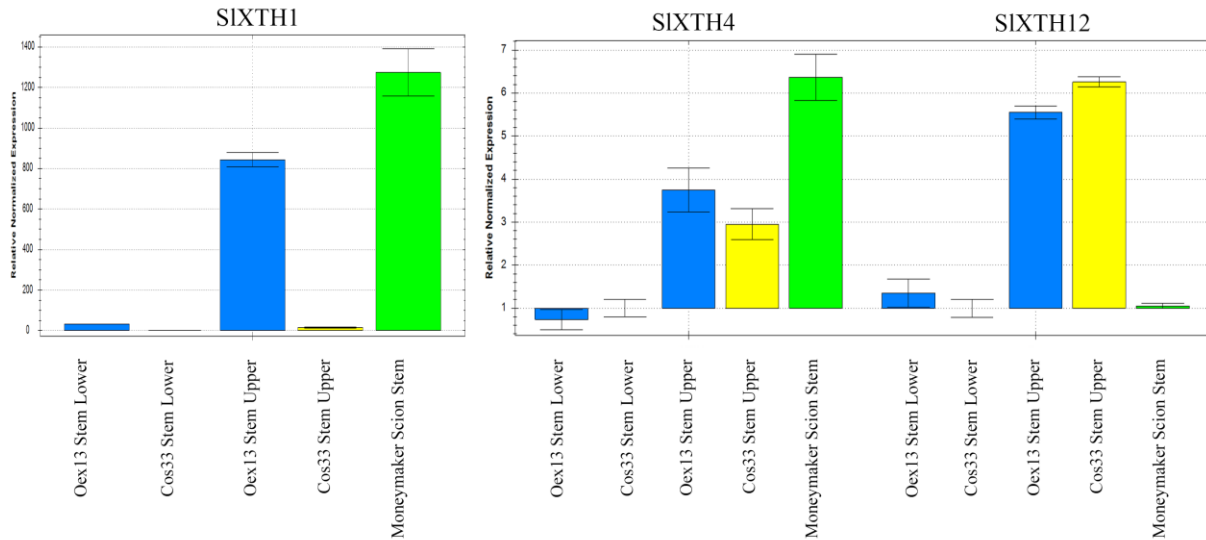


Figure 34 Expression of the three *XTHs* in un-grafted stem tissue of the mutant lines, with the Moneymaker (MM) Scion Stem included in the data to serve as a control.

Supplemental XET activity images

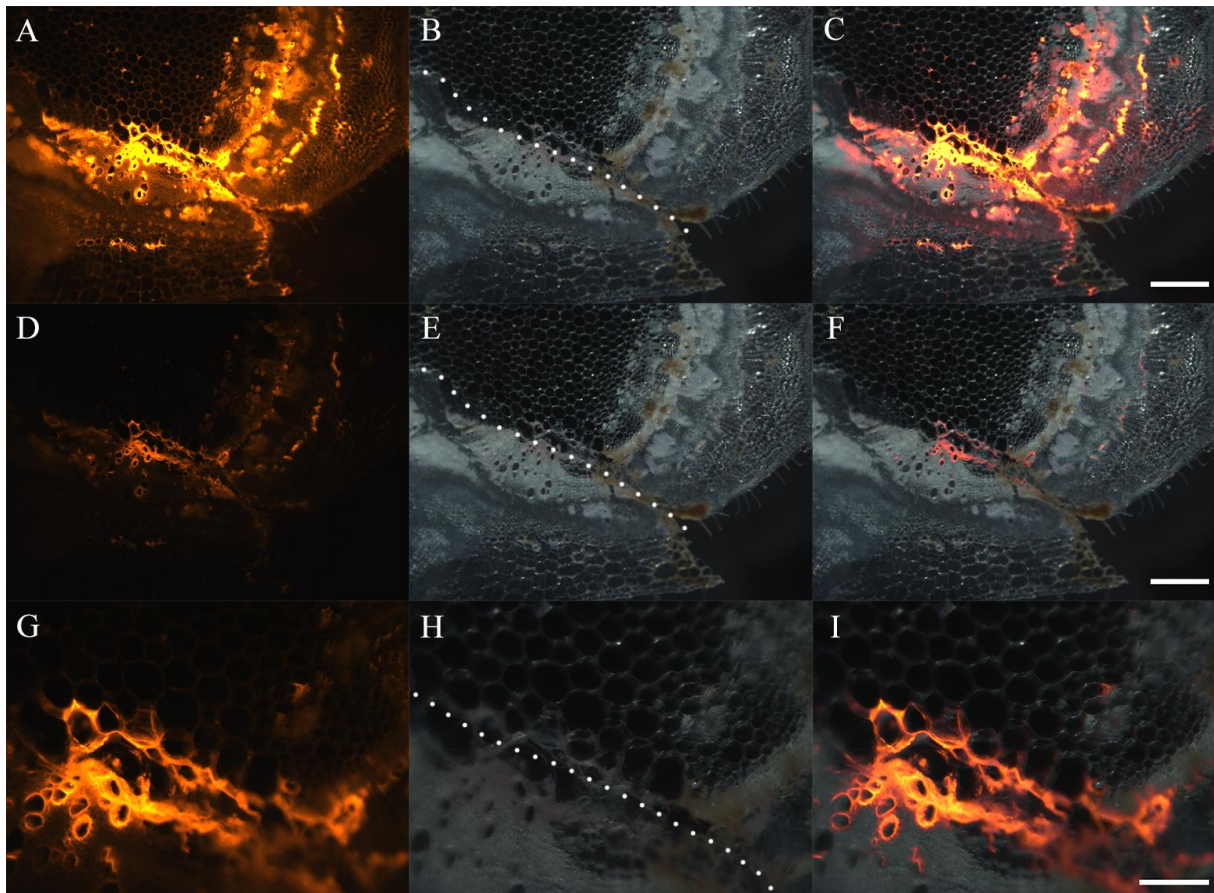


Figure 35 Oex13 (Stock) – M82 (Scion) graft site crosssections labeled with fluorescing XyGO-SRs fluorescing red where XET activity has occurred. Images display (from left to right) CY3 filter images, darkfield images, and a merged image of the two latter. Exposure time in A = 800ms, B = 50ms, C = 200ms. Scalebars showing C and F = 500 μ m, I = 200 μ m. Stippled line marks the graft union where the stock and scion has grown together. Images A – F are the same, but with two different exposure times, as specified.

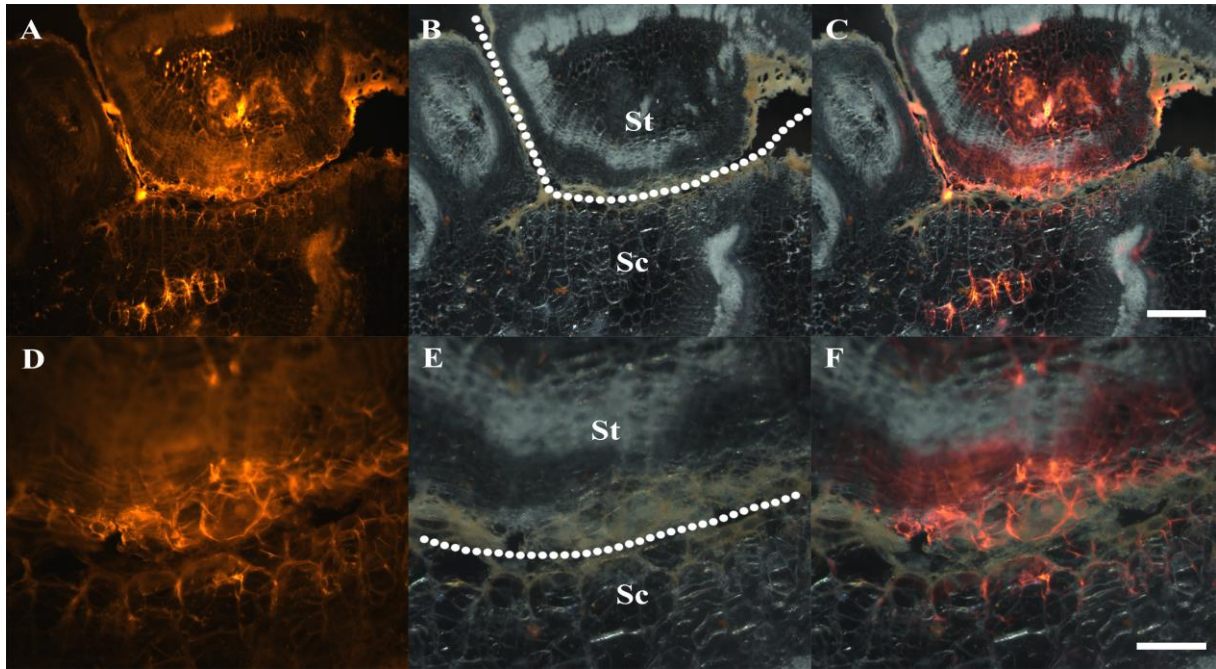


Figure 36 Oex13 (stock) – Cos33 (scion) graft site cross-sections. Images display (from left to right) CY3 filter images, darkfield images, and a merged image of the two latter. St = Stock, Sc = Scion. Stippled lines mark the graft union, where the two plants have grown together. C scalebar = 500 μ m, F scalebar = 200 μ m. Exposure times = 800ms

ImageJ Fiji script

Following is an example macro-script from ImageJ Fiji for merging of the color channels, as well as adding the scalebars. All scalebars were added with ImageJ Fiji, which was calibrated with a Carl Zeiss Zen Lite Blue Edition .zvi file with a scalebar converted to .tif format using the Zen Lite software. All microscopy images processed with ImageJ Fiji was processed as .tif files.

```
run("Merge Channels...", "c1=[M82Cos33 Graftsite XY c CY3.tif]
c4=[M82Cos33 Graftsite XY c DF.tif] create");

selectWindow("M82Cos33 Graftsite XY c CY3 scalebar calib.tif");

//setTool("line");

run("Focus Search Bar");

run("Set Scale...", "distance=142 known=1000 pixel=1 unit=um global");

selectWindow("Composite");

makeLine(454, 282, 453, 281);

run("Focus Search Bar");

run("Scale Bar...", "width=1000 height=12 font=30 color=White
background=None location=[Lower Right] bold overlay");
```

RNA extraction protocol

Protocol: Purification of Total RNA from Plant Cells and Tissues and Filamentous Fungi

This protocol requires the RNeasy Plant Mini Kit.

Determining the correct amount of starting material

It is essential to use the correct amount of starting material in order to obtain optimal RNA yield and purity. A maximum amount of 100 mg plant material or 1×10^7 cells can generally be processed. For most plant materials, the RNA binding capacity of the RNeasy spin column and the lysing capacity of Buffer RLT will not be exceeded by these amounts. Average RNA yields from various plant materials are given in Table 2 (page 19).

If there is no information about the nature of your starting material, we recommend starting with no more than 50 mg plant material or $3\text{--}4 \times 10^6$ cells. Depending on RNA yield and purity, it may be possible to use up to 100 mg plant material or up to 1×10^7 cells in subsequent preparations.

Do not overload the RNeasy spin column, as this will significantly reduce RNA yield and quality.

Counting cells or weighing tissue is the most accurate way to quantitate the amount of starting material. As a guide, a 1.5 cm diameter leaf disc weighs 25–75 mg.

Important points before starting

- If using the RNeasy Plant Mini Kit for the first time, read “Important Notes” (page 18).
- If working with RNA for the first time, read Appendix A (page 63).
- Fresh or frozen tissues can be used. Tissues can be stored at -70°C for several months. Flash-freeze tissues in liquid nitrogen, and immediately transfer to -70°C . Do not allow tissues to thaw during weighing or handling prior to disruption in Buffer RLT. Homogenized tissue lysates from step 4 can also be stored at -70°C for several months. Incubate frozen lysates at 37°C in a water bath until completely thawed and salts are dissolved before continuing with step 5. Avoid prolonged incubation, which may compromise RNA integrity.
- The RNeasy Plant Mini Kit provides a choice of lysis buffers: Buffer RLT and Buffer RLC, which contain guanidine thiocyanate and guanidine hydrochloride, respectively. In most cases, Buffer RLT is the lysis buffer of choice due to the greater cell disruption and denaturation properties of guanidine thiocyanate. However, depending on the amount and type of secondary metabolites in some tissues (such as milky endosperm of maize or mycelia of filamentous fungi), guanidine thiocyanate can cause solidification of the sample, making extraction of RNA impossible. In these cases, Buffer RLC should be used.

- Buffer RLT may form a precipitate upon storage. If necessary, redissolve by warming, and then place at room temperature (15–25°C).
- Buffer RLT, Buffer RLC, and Buffer RW1 contain a guanidine salt and are therefore not compatible with disinfecting reagents containing bleach. See page 8 for safety information.
- Perform all steps of the procedure at room temperature. During the procedure, work quickly.
- Perform all centrifugation steps at 20–25°C in a standard microcentrifuge. Ensure that the centrifuge does not cool below 20°C.

Things to do before starting

- β -Mercaptoethanol (β -ME) must be added to Buffer RLT or Buffer RLC before use. Add 10 μ l β -ME per 1 ml Buffer RLT or Buffer RLC. Dispense in a fume hood and wear appropriate protective clothing. Buffer RLT or Buffer RLC containing β -ME can be stored at room temperature for up to 1 month.
- Buffer RPE is supplied as a concentrate. Before using for the first time, add 4 volumes of ethanol (96–100%) as indicated on the bottle to obtain a working solution.
- If performing optional on-column DNase digestion, prepare DNase I stock solution as described in Appendix D (page 69).

Procedure

1. **Determine the amount of plant material. Do not use more than 100 mg.**

Weighing tissue is the most accurate way to determine the amount.

2. **Immediately place the weighed tissue in liquid nitrogen, and grind thoroughly with a mortar and pestle. Decant tissue powder and liquid nitrogen into an RNase-free, liquid-nitrogen-cooled, 2 ml microcentrifuge tube (not supplied). Allow the liquid nitrogen to evaporate, but do not allow the tissue to thaw. Proceed immediately to step 3.**

RNA in plant tissues is not protected until the tissues are flash-frozen in liquid nitrogen. Frozen tissues should not be allowed to thaw during handling. The relevant procedures should be carried out as quickly as possible.

3. **Add 450 μ l Buffer RLT or Buffer RLC (see “Important points before starting”) to a maximum of 100 mg tissue powder. Vortex vigorously.**

A short 1–3 min incubation at 56°C may help to disrupt the tissue. However, do not incubate samples with a high starch content at elevated temperatures, otherwise swelling of the sample will occur.

Note: Ensure that β -ME is added to Buffer RLT or Buffer RLC before use (see “Things to do before starting”).

- 4. Transfer the lysate to a QIAshredder spin column (lilac) placed in a 2 ml collection tube, and centrifuge for 2 min at full speed. Carefully transfer the supernatant of the flow-through to a new microcentrifuge tube (not supplied) without disturbing the cell-debris pellet in the collection tube. Use only this supernatant in subsequent steps.**

It may be necessary to cut off the end of the pipet tip to facilitate pipetting of the lysate into the QIAshredder spin column. Centrifugation through the QIAshredder spin column removes cell debris and simultaneously homogenizes the lysate. While most of the cell debris is retained on the QIAshredder spin column, a very small amount of cell debris will pass through and form a pellet in the collection tube. Be careful not to disturb this pellet when transferring the lysate to the new microcentrifuge tube.

- 5. Add 0.5 volume of ethanol (96–100%) to the cleared lysate, and mix immediately by pipetting. Do not centrifuge. Proceed immediately to step 6.**

Note: The volume of lysate may be less than 450 μ l due to loss during homogenization.

Note: Precipitates may be visible after addition of ethanol. This does not affect the procedure.

- 6. Transfer the sample (usually 650 μ l), including any precipitate that may have formed, to an RNeasy spin column (pink) placed in a 2 ml collection tube (supplied). Close the lid gently, and centrifuge for 15 s at $\geq 8000 \times g$ ($\geq 10,000$ rpm). Discard the flow-through.***

Reuse the collection tube in step 7.

If the sample volume exceeds 700 μ l, centrifuge successive aliquots in the same RNeasy spin column. Discard the flow-through after each centrifugation.*

Optional: If performing optional on-column DNase digestion (see “Eliminating genomic DNA contamination”, page 23), follow steps D1–D4 (page 69) after performing this step.

- 7. Add 700 μ l Buffer RW1 to the RNeasy spin column. Close the lid gently, and centrifuge for 15 s at $\geq 8000 \times g$ ($\geq 10,000$ rpm) to wash the spin column membrane. Discard the flow-through.***

Reuse the collection tube in step 8.

Note: After centrifugation, carefully remove the RNeasy spin column from the collection tube so that the column does not contact the flow-through. Be sure to empty the collection tube completely.

Skip this step if performing optional on-column DNase digestion (page 69).

- 8. Add 500 μ l Buffer RPE to the RNeasy spin column. Close the lid gently, and centrifuge for 15 s at $\geq 8000 \times g$ ($\geq 10,000$ rpm) to wash the spin column membrane. Discard the flow-through.**

Reuse the collection tube in step 9.

Note: Buffer RPE is supplied as a concentrate. Ensure that ethanol is added to Buffer RPE before use (see “Things to do before starting”).

- 9. Add 500 μ l Buffer RPE to the RNeasy spin column. Close the lid gently, and centrifuge for 2 min at $\geq 8000 \times g$ ($\geq 10,000$ rpm) to wash the spin column membrane.**

The long centrifugation dries the spin column membrane, ensuring that no ethanol is carried over during RNA elution. Residual ethanol may interfere with downstream reactions.

Note: After centrifugation, carefully remove the RNeasy spin column from the collection tube so that the column does not contact the flow-through. Otherwise, carryover of ethanol will occur.

- 10. Optional: Place the RNeasy spin column in a new 2 ml collection tube (supplied), and discard the old collection tube with the flow-through. Close the lid gently, and centrifuge at full speed for 1 min.**

Perform this step to eliminate any possible carryover of Buffer RPE, or if residual flow-through remains on the outside of the RNeasy spin column after step 9.

- 11. Place the RNeasy spin column in a new 1.5 ml collection tube (supplied). Add 30–50 μ l RNase-free water directly to the spin column membrane. Close the lid gently, and centrifuge for 1 min at $\geq 8000 \times g$ ($\geq 10,000$ rpm) to elute the RNA.**

- 12. If the expected RNA yield is $>30 \mu\text{g}$, repeat step 11 using another 30–50 μ l RNase-free water, or using the eluate from step 11 (if high RNA concentration is required). Reuse the collection tube from step 11.**

If using the eluate from step 11, the RNA yield will be 15–30% less than that obtained using a second volume of RNase-free water, but the final RNA concentration will be higher.

* Flow-through contains Buffer RLT, Buffer RLC, or Buffer RW1 and is therefore not compatible with bleach. See page 8 for safety information.

